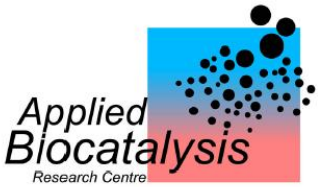

ENGINEERING *PICHIA PASTORIS FOR WHOLE CELL BIOTRANSFORMATIONS EMPLOYING OXIDOREDUCTASES*

DIPLOMA THESIS

KLAUS P. LUEF

RESEARCH CENTRE APPLIED BIOCATALYSIS

GRAZ, AUSTRIA

Supervisor: Ao.Univ.-Prof. Mag. Dr.rer.nat. Anton Glieder

Graz, 2012

Statutory declaration

I declare that I have authored this thesis independently, that I have not used other than the declared sources / resources, and that I have explicitly marked all material which has been quoted either literally or by content from the used sources.

…… ……..

(date) (signature)

Danksagung

“Never gonna give you up;
Never gonna let you down;
Never gonna run around and desert you.”

-- Rick Astley

Ich möchte die Gelegenheit an dieser Stelle ein wenig nutzen, um ein paar ganz besondere Menschen zu erwähnen, die mir während meines ganzen Studiums mit Rat und Tat zur Seite gestanden sind, und mir damit geholfen haben, meine Ziele zu erreichen.

Allen voran geht mein Dank an meine Familie, die stets mit absolutem Verständnis, unerschütterlichen Vertrauen und grenzenlosen Umsicht hinter mir gestanden sind, um mir damit stets große Lasten von den Schultern zu nehmen.

Dann möchte ich mich bei meinen Freunden bedanken, die für die wichtige moralische Unterstützung, aber auch die notwendige Ablenkung während meines Studiums gesorgt haben und mich damit wohl irgendwie auf den mittleren oder gemittelten Weg meines Lebens (mit-)geführt haben, den ich nun bestreite. Auch wenn es vielleicht ein wenig unfair anderen gegenüber erscheint, möchte ich gewisse Personen hierbei auch namentlich erwähnen. (Liste in alphabetischer Reihung)
Alexander Albrecher, Carola Duschl, Claus Flaig, Dr. Stephanie Flaig, Laura Gräbener, Sonja Luef, Simon Lux, Michael Malderle, Dr. Andreas Marn, Annemarie Marold, Ákos Palotási, Christine Pfarrmaier, Oliver Pimas, Christian Schäfer, Bernhard Sihler, Eva-Maria Tahedl, Eva Trotscha.
Danke für die wunderschöne Zeit, die war, das wunderbare Leben, das ich führe und all die tollen Jahre, die noch kommen mögen.

Besonderer Dank geht auch an meinen Diplomarbeitsbetreuer Prof. Glieder, der mir viel Freiraum bei der Arbeit an einem faszinierenden Themengebiet ermöglichte sowie Beate Pscheidt und Sandra Abad, die stets offene Ohren für die diversesten Fragen hatten und nicht eher ruhten, bis diese geklärt waren. Auch die restlichen Kollegen der Glieder Group – allen voran Alexander Gutmann und Gabi Bergler – möchte ich nicht unerwähnt lassen, ohne die es nicht dieses unglaublich positive Arbeitsklima gegeben hätte, das ohne Zweifel seinesgleichen sucht.

Last but not least geht mein Dank auch an alle Mitglieder des Styrian Bears American Football Clubs, die mein Leben mit einer Würze bereichert haben, die ich mir mittlerweile nicht mehr wegdenken könnte.

Abstract

The methylotrophic yeast *Pichia pastoris* is known as efficient host system for the production of recombinant proteins and to grow to very high cell densities. However, only a few examples of its application as whole cell biocatalyst have been reported. Compared to the use of isolated enzymes, whole cell biocatalysts provide endogenous pathways for the regeneration of redox-cofactors, an advantage for reactions catalyzed by oxidoreductases which require cofactors in stoichiometric amounts.

We recently succeeded in engineering *Pichia pastoris* for more efficient whole-cell bioreductions exploiting the methanol pathway for cofactor regeneration. Employing *Saccharomyces cerevisiae* butanediol dehydrogenase (*Sc*BDH) and *Candida tenuis* xylose reductase (*Ct*XR) as model oxidoreductases, it was possible to establish a highly efficient *P. pastoris* platform for potential large-scale biotransformations.

Kurzfassung

Die methylotrophe Hefe *Pichia pastoris* ist bekannt für ihre Leistungsfähigkeit im Rahmen der Produktion rekombinanter Proteine sowie ihrer Möglichkeit, zu sehr großen Zelldichten heranzuwachsen.
Trotz ihrer häufigen Anwendung sind bisher nur wenige Beispiele für ihre Verwendung in der Ganzzellbiokatalyse publiziert. Im Vergleich zu dem Einsatz isolierter Enzyme bietet die Ganzzellbiokatalyse durch die Nutzung endogener Stoffwechselwege die Möglichkeiten einer effizienten Cofaktorregenerierung. Dies wiederum stellt einen deutlichen Vorteil für von Oxidoreduktasen katalysierte Reaktionen dar, die stöchiometrische Mengen der Redox-Cofaktoren NADH bzw. NADPH benötigen.

Es gelang die Herstellung rekombinanter *P. pastoris* mit verbesserten Eigenschaften seitens der Cofaktorregenerierung durch das Überexprimieren der Enzyme des endogenen Methanolabbaus. Unter der Verwendung der Butandiol Dehydrogenase von *Saccharomyces cerevisiae* und der Xylose Reduktase von *Candida tenuis* als Modelle für Oxidoreduktasen war es möglich eine sehr effizient arbeitende *P. pastoris* Plattform für eine etwaige Anwendung in der industriellen Synthese zu schaffen.

Contents

1 Introduction 1

1.1 The role of biocatalysis in industrial processes 1

***1.2 Pichia pastoris* 1**

1.2.1 Historical facts about P. pastoris 1

1.2.2 The P. pastoris methanol utilizing pathway 2

Alcohol oxidase (*AOX*) 3

Formaldehyde dehydrogenase (*FLD*) 4

Formate dehydrogenase (*FDH*) 5

Dihydroxyacetone synthase (*DAS*) 6

1.2.3 P. pastoris as a tool for recombinant protein production 6

1.2.4 Whole-cell biotransformations 7

1.3 Cofactor recycling 8

1.3.1 The role of NADH and NADPH 8

1.3.2 Cofactor dependency in industrial synthesis 9

1.3.3 Engineering aspects (on FDH) 10

1.4 Model enzymes for *P. pastoris* whole-cell biocatalysis 10

1.4.1 Butanediol dehydrogenase (BDH) 10

1.4.2 Xylose reductase (XR) 11

2 Objectives 13

3 Materials and methods 14

3.1 Instruments and Devices 14

3.1.1 Centrifuges 14

3.1.2 Thermocycler 14

3.1.3 Instruments/Devices 14

3.1.4 Shaker 14

3.1.5 Homogenisator 15

3.1.6 Pipettes 15

3.1.7 Platereader 15

3.1.8 96-well plates 15

3.2 Media 16

3.2.1 E. coli media 16

3.2.2 P. pastoris media 16

3.2.3 Buffers and solutions 17
3.3 Enzymes 18
3.3.1 Restriction enzymes (Fermentas Inc., Glen Burnie, MA, USA) 18
3.3.2 Polymerases 18
3.3.3 Other enzymes 19
3.4 Software 19
3.5 Kits and protocols 19
3.6 Plasmid 20
3.6.1 pJET 1.2/blunt 20
3.6.2 Kan 3,2-8 E. coli / P. pastoris Shuttle Vector 21
3.6.3 T2 E. coli / P. pastoris Shuttle Vector 22
3.7 Strains 22
3.7.1 E. coli strains 22
3.7.2 P. pastoris strains 23
3.8 Methods 23
3.8.1 Plasmid isolation and DNA purification 23
3.8.2 GeneJet™ ligations 23
3.8.3 Standard ligations 23
3.8.4 PCR 24
3.8.5 Site-directed mutagenesis 24
3.8.6 DNA gel electrophoresis 24
3.8.7 E. coli transformation 24
3.8.8 Pichia pastoris transformation 25
3.8.9 Genomic DNA Extraction using Y-Per® 25
3.8.10 Cultivation and Screening 26
3.9 Activity screening 26
3.9.1 AOX1 photometric assay 26
3.9.2 FDH photometric assay 27
3.9.3 FLD photometric assay 27
3.9.4 XR and XR-M photometric assay 27
3.10 Primers 28
4 BDH strains 30
4.1 Strategy description 30
4.2 Experimental 31

4.2.1 Identification of genes of interest 31
4.2.2 Construction of Pichia pastoris strains for enhanced cofactor recycling 33
4.2.3 Amplification of expressions cassette 34
Standard PCR 34
Overlap Extension PCR (OE-PCR) 35
Ligation into shuttle vector 39
4.2.4 P. pastoris transformation 39
4.2.5 Cultivation and induced protein expression 40
4.3 Results and discussion 40
4.3.1 P. pastoris CBS 7435 MUT over-expression strains 40
***AOX1* over-expression 41**
***FLD* over-expression 42**
***FDH* over-expression 43**
Over-expression of FDH + FLD 44
Re-screen results 45
4.3.2 P. pastoris Δdas1das2 MUT over-expression strains 46
Over-expression of AOX1 46
Over-expression of FLD 46
Over-expression of FDH 47
Over-expression of FLD + FDH 47
Re-screen results 49
4.3.3 Final discussion 49
AOX1 screening 49
***P. pastoris* CBS 7435 as host strain 50**
P. pastoris Δdas1das2 as host strain 51
Comparison CBS 7435 ↔ *Δdas1das2* 52
Future perspectives 52
5 Xylose reductase strains 54
5.1 Strategy description 54
5.2 Experimental 55
5.2.1 Identification of genes of interest 55
5.2.2 Construction of Pichia pastoris strains for enhanced cofactor recycling 55
5.2.3 Amplification of expression cassettes 56
5.2.4 P. pastoris transformation 60
5.2.5 Cultivation and induced protein expression 60

5.3 Results and discussion 61
5.3.1 P. pastoris CBS 7435 MUT + XR over-expression strains 61
5.3.2 P. pastoris CBS 7435 MUT + XR-M over-expression strains 68
5.3.3 P. pastoris Δdas1das2 MUT + XR over-expression strains 72
5.3.4 P. pastoris Δdas1das2 MUT + XR-M over-expression strains 77
5.3.5 Final discussion 82
6 Cofactor dependency of FDH 85
6.1 Strategy description 85
6.2 Experimental 87
6.2.1 Identification of genes of interest 87
6.2.2 Construction of P. pastoris strains with enhanced NADPH acceptance 87
6.2.3 Generation of expression cassettes 87
6.2.4 Transformation into P. pastoris 91
6.2.5 Cultivation and induced protein expression 92
6.3 Results and discussion 93
6.3.1 FDH double mutant 93
6.3.2 Site-saturated mutagenesis of FDH 95
6.3.3 Final discussion 100
7 Conclusion 102
7.1 BDH strains 102
7.2 XR and XR-M strains 102
7.3 Cofactor dependency 102
8 Outlook 104
9 Appendix 105
9.1 Sequence of genes 105
9.1.1 E. coli / P. pastoris shuttle vector 3,2-8 Kan 105
9.1.2 E. coli / P. pastoris shuttle vector T2 106
9.1.3 S. cerevisiae BDH 107
9.1.4 C. tenuis xylose reductase 107
9.1.5 P. pastoris AOX1 107
9.1.6 P. pastoris FLD 108
9.1.7 P. pastoris FDH 108
9.1.8 P. pastoris FLD+FDH cassette 109

9.2 Strains generated during this thesis 110
9.3 Index of tables 111
9.4 Index of figures 112
10 Literature 118

Abbreviations

Amp, A	Ampicillin™
AOX	Alcohol oxidase gene
AP	Acetophenone
B	Biotin
BDH	Butanediol dehydrogenase
Bidest	Bidestilled
BMD	Buffered minimal medium with dextrose
BMM	Buffered minimal medium
Candida m., *C.m.*	*Candida magnoliae*
C. tenuis, C.t.	*Candida tenuis*
CAP	2-Chloro-1-phenyl-ethanone
CDS	Coding sequence
CIAP	Calf intestine alkaline phosphatase
D	Dextrose
Da	Dalton
ddH_2O	Double destilled water "Fresenius"
DMSO	Dimethylsulfoxide
DNA	Deoxyribonucleic acid
dNTP	Deoxyribonucleotide triphosphate
E. coli	Escherichia coli
Ee	Enantiomeric excess
EtOH	Ethanol
FDH	Formate dehydrogenase gene
FLD	Formaldehyde dehydrogenase gene
fw, fwd.	Forward
GC	Gas chromatography
Gen, G	Geneticin™
GFP	Green fluorescent protein gene
Gly	Glycerol
h	Hour
His	Histidine
HPLC	High performance liquid chromatography

Kan, K	Kanamycin™
LB	Luria bertani
M	Molar
MD	Minimalmedia with Glucose
DiCAP, DiCAP	2-Chloro-1-(3-chlorophenyl)-ethanone
MeOH	Methanol
Min	Minute
MM	Minimal media with methanol
mM	Milimolar
µM	Micromolar
Mr	Moleculare mass
NAD^+	Nicotinamide adenine dinucleotide, oxidised form
NADH	Nicotinamide adenine dinucleotide, reduced form
$NADP^+$	Nicotinamide adenine dinucleotide phosphate, oxidised form
NADPH	Nicotinamide adenine dinucleotide phosohate, reduced form
nm	Nanometer
Nr.	Number
OD	Optical density
OE	Overlap extension
Oligos	Oligonucleotide
P(AOX1) or P_{AOX1}	Promoter of the *AOX1* gene of *Pichia pastoris*
P.pastoris	*Pichia pastoris*
PAGE	Polyacrylamide gel electrophoresis
PCR	polymerase chain reaction
Poly.	Polymerase
Pos.	Position
PPB	Potassium phosphate buffer
RFU	Relative fluorescence units
RNA	Ribonucleic acid
Rpm	Rounds per minute
RT	Real Time
rv, rev	Reverse
SDS	Sodium dodecyl sulfate
SDS-PAGE	Sodium dodecyl sulphate polyacrylamide gel electrophoresis

sec	Second
St.,Std.	Standard
T, Temp.	Temperature
Trafo	Transformation
TH	Transhydrogenase
TT	Transcription termination
WT	Wild type
XR	Xylose reductase
XR-M	Xylose reductase (mutant)
YNB	Yeast nitrogen base
YPD	Yeast extract/peptone/dextrose- media
Zeo, Z	Zeocin™

1 Introduction

1.1 The role of biocatalysis in industrial processes

The recent years brought an acceptance and a new view on biocatalysis as a useful tool for chemical synthesis on an industrial scale. While in the late nineties, the idea of enzymes or whole-cells as catalysts in high-throughput processes was not the main stream, the situation in the last decade changed with the production of industrial key compounds via biotransformations [1-3].

The industrial use of biocatalysts is directly connected with a number of benefits, ranging from the high selectivities (e.g. regio-, chemo- and enantio selectivity) to the shorter preparation times in comparison to chemical processes [4].

Especially the advancements on the topic of biotransformations employing living cells, or products of eukaryotic recombinant protein expression brought up a huge spectrum of new possibilities and resources for more efficient industrial applications. This new interest in whole-cell biocatalysis and our expertise in the field of recombinant protein production resulted in testing the methlyotrophic yeast *Pichia pastoris* as a host system [5-7].

The yeast *P. pastoris* showed excellent features concerning protein expression and cell growth. Hence, this yeast had become one of the most prominent tools in the field of enzyme production and whole-cell catalysis.

The following chapter concentrates on *P. pastoris* and the methanol utilizing pathway, one of its central metabolic pathways, which is in the focus of this thesis.

1.2 Pichia pastoris

1.2.1 Historical facts about *P. pastoris*

Since the discovery of methylotrophic yeasts, forty years ago, by Koichi Ogata, this microorganism became immediately interesting as a potential source of single-cell protein (SCP), and the associated applications in the animal feeding industry [5]. Therefore the development of media and cultivation protocols for its high density growing on methanol at >130 $g \cdot L^{-1}$ cell dry weight, developed by Phillips Petroleum Company in the 1970s was the first step [8].

Due to the economical and industrial impact of the 1973 oil crisis, this field of application was rather short-termed for *P. pastoris*.

In the following decades, Phillips Petroleum in cooperation with SIBIA, Inc developed *P. pastoris* as an organism for heterologous protein expression. During this work, the gene and promoter of the alcohol oxidase 1 (AOX1) was isolated and analyzed.

Since 1993, the patent holder for this expression system is Research Corporation Technologies, who have an ongoing license agreement with Invitrogen concerning the use of the system [9].

Further milestones that contributed to the popularity of *P. pastoris* are the FDA classification as GRAS (generally regarded as safe) and the availability of experiments.

The full genome of *P. pastoris* was published first in May 2009 by De Schutter and Lin [10].

1.2.2The *P. pastoris* methanol utilizing pathway

The methanol utilizing pathway of *P. pastoris* is a central metabolic pathway which allows the yeast to use MeOH as sole carbon and energy source. In combination with the availability of a strong and tight regulated promoter like P_{AOX1} from the alcohol oxidase 1 (*AOX1*) gene or the promoter of the 3-phosphate dehydrogenase (*GAP*) gene, *P. pastoris* is an interesting platform for recombinant protein expression.

The methanol utilizing pathway consists of three main enzymes responsible for the degradation of MeOH to CO_2 whilst generating two equivalents of cofactor NADH.

The first step of utilizing MeOH is its oxidation to formaldehyde, which is catalyzed by alcohol oxidase (*AOX*) in the peroxisome. Formaldehyde is further oxidized to formate via formaldhedyde dehydrogenase (*FLD*) and generates within this reaction the first equivalent of NADH. The second equivalent is generated in the last step of the degradation catalyzed by formate dehydrogenase (*FDH*), converting formate to CO_2 in an irreversible reaction.

Parallel to the cofactor regeneration, the peroxisome enzyme catalase directly converts the byproduct of step one, the toxic H_2O_2, to O_2 and the enzyme dihydroxyacetone synthase (*DAS*) is capable of utilizing formaldehyde to dihydroxyacetone and glyceraldehyde 3-phosphate, which are further metabolized to generate biomass [11] as depicted in figure 1.

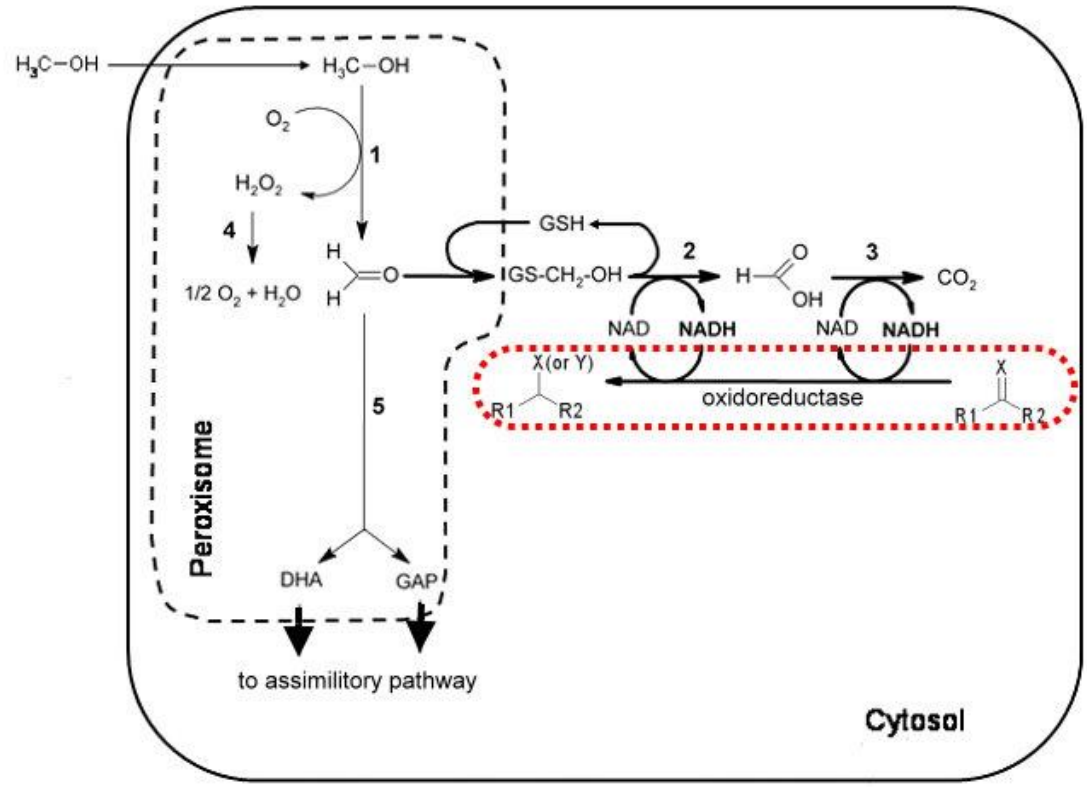

Figure 1: Detail of the *P. pastoris* MeOH utilization pathway (MUT). 1: alcohol oxidase 1 and 2 (AOX1/2). 2: formaldehyde dehydrogenase (FLD). 3: formate dehydrogenase (FDH). 4: catalase. 5: dihydroxyacetone synthase 1 and 2 (DAS1/2). GSH: glutahion, DHA: dihydroxyacetone, GAP: glyceraldehydes 3-phosphate. The reaction marked by the dotted red line shows the general conversion of an oxidoreductase. Figure adapted from Kirsten Schroer [35].

The enzymes of the methanol utilizing pathway are further described in detail as following.

Alcohol oxidase (*AOX*)

All four of the well-known methylotrophic yeasts (genera *Hansenula, Pichia, Candida* and *Torulopsis*) possess an alcohol oxidase activity (EC 1.1.3.13) which allows them to consume MeOH [12-14].

In *P. pastoris*, there are two homologous proteins, alcohol oxidase 1 *(AOX1)* and 2 *(AOX2)*, which are responsible for the first step in MeOH degradation as depicted in following figure 2.

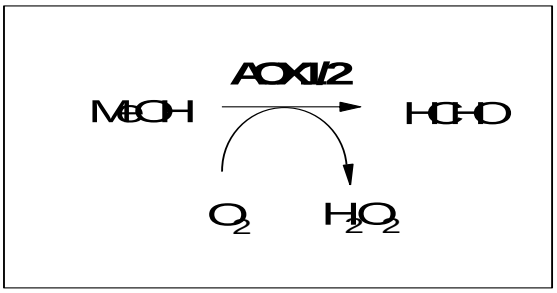

Figure 2: Reaction catalyzed by *P. pastoris* AOX1/2. Methanol is oxidized to formaldehyde under the production of toxic compound H_2O_2.

This reaction is located in the peroxisome due to the production of the toxic byproduct H_2O_2.

Both proteins are homologous and display more than 90% identity of DNA as well as amino acid level [8]. However, *AOX1* is expressed 10-20 times higher than *AOX2*. [12].

The promoters of the *AOX1* and *AOX2* genes became important tools in recombinant protein expression. P_{AOX1} is known as one of the strongest promoters within the *P. pastoris* genome and widely accepted in eukaryotic gene expression [11].

Previous studies on this topic showed, that a deletion of *AOX1* in *P. pastoris* ended in a Mut^S strain, still capable of growing on methanol, but at a significant reduced rate, while deletion of both genes resulted in the Mut^- strain, which lost the ability to convert MeOH as carbon and energy source at all [15].

Table 1: *P. pastoris* phenotypes concerning the Mut pathway

Mut^+ (wildtype)	*AOX1 + AOX2*	Normal growth rate on MeOH
Mut^S	*AOX2*	Slower growth rate on MeOH
Mut^-	none	No growth on MeOH

Formaldehyde dehydrogenase (*FLD*)

P. pastoris FLD (EC 1.2.1.1) is a glutathione dependent enzyme with a length of 379 amino acids and an approx. protein size of 40 kDa. At the very 5'-end of the *FLD* gene, 18 nucleotides downstream of the start codon, is an intron present with a length of 114 nucleotides.

Endogenous *P. pastoris FLD* is regulated on a transcriptional basis [16-18] by the promoter P_{FLD}, which has a comparable strength to the AOX promoters and therefore became an attractive tool for recombinant protein expression [19].

It catalyzes the conversion of formaldehyde to formate while generating one equivalent of NADH in the process as depicted in figure 3.

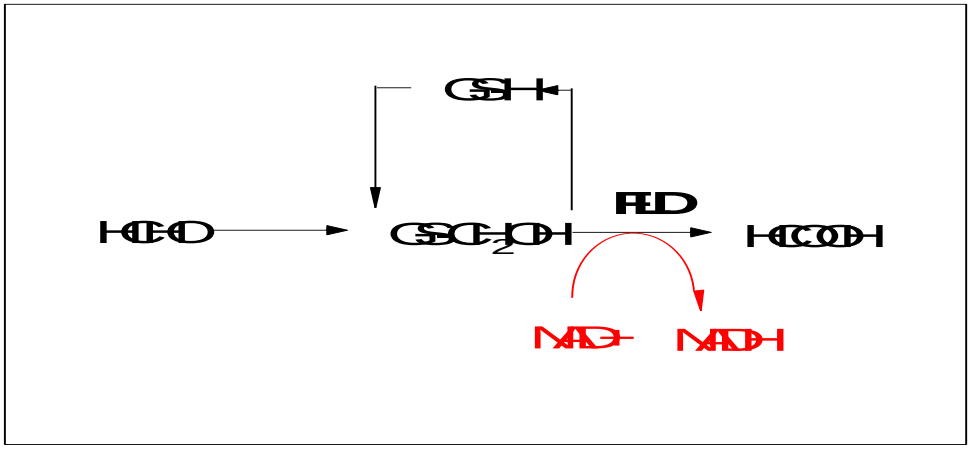

Figure 3: Reaction catalyzed by *P. pastoris FLD.* After separation of the glutathione intermediate, formaldehyde is oxidized to formate and consumes one equivalent of cofactor NAD^+.

As seen in figure 3, the conversion of formaldehyde is not only dependent on the presence of the enzyme, but also on the presence of reduced glutathione for transporting formaldehyde out of the peroxisome into the cytosol.

FLD is the enzyme leading from the branch point of the intermediate formaldehyde towards the cofactor regeneration pathway or alternatively to the synthesis of new cell compounds.

Formate dehydrogenase (*FDH*)

P. pastoris FDH (EC 1.2.1.2) is 365 amino acids long and has an approximate molecular mass of 40 kDa.

It is the last enzyme in the degradation of MeOH to CO_2 within the *P. pastoris* cell and catalyzes the conversion of formate to CO_2 at expense of another equivalent of NAD^+ as seen in figure 4.

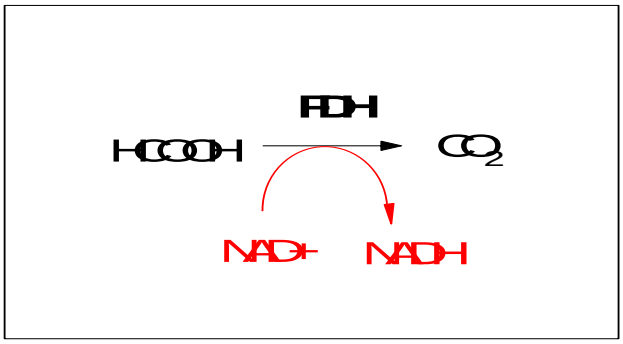

Figure 4: Reaction catalyzed by *P. pastoris FDH.* Formate is irreversible converted to CO_2 and consumes one equivalent of NAD^+ in the process.

The very nature of this last step in methanol utilization resulting in CO_2 promises the theoretical 100% yield marker without disturbing by-product formation, which makes this conversion quite desirable. Including a number of additional positive aspects (which are explained in detail later in chapter 1.3.2) these properties made *FDH* to one of the most common model enzymes on the topic of cofactor regeneration.
A significant number of studies and publications concerning cofactor regeneration in whole-cell biocatalysis center around the possibilities of recombinant *FDH* co-expression. [20-23]

Dihydroxyacetone synthase (*DAS*)

DAS converts intermediate formaldehyde towards the other side of the previous mentioned branching point in degradation, resulting in GAP and therefore as carbon source for cell growth. [24]
Studies on this topic revealed that in contrast to other methylotrophic yeasts there are actually two different genes encoding the *DAS1* and *DAS2* proteins in *P. pastoris*. [11]
Further research also showed that the deletion of these genes resulted in a slowed growth rate on MeOH, but enhanced cofactor regeneration abilities due to the shift in the metabolic flux [11,35].

1.2.3*P. pastoris* as a tool for recombinant protein production

The most important tool for the creation of recombinant *P. pastoris* strains is the existence of adequate expression constructs. While there is a study of a linear

expression system [25] using only PCR to achieve the necessary amounts of DNA for transformation into yeast, the classical system employs an *E. coli* / *P. pastoris* shuttle vector system, which is constructed via classical cloning technique.

1.2.4Whole-cell biotransformations

The biotransformation with whole-cells has a number of advantages compared to the conversions catalyzed with (immobilized-) enzymes. Whole-cell biotransformations are cheaper and faster due to the lack of further purification (and immobilization) of the employing enzymes.

Historically, the use of whole-cells was nearly limited to *Saccharomyces cerevisiae* or *E. coli* [9] but within the last decades, *P. pastoris* has become an alternative platform with high potential.

By growing on MeOH the methylotrophic yeast combines the benefits of having a solvent capable of handling various organic compounds present with the benefits of having a C-source present. Furthermore, by inducing the recombinant protein expression with the P_{AOX1}, the enzymes of the NADH consuming as well as the NADH recycling system are induced simultaneously. These facts are depicted in figure 5.

Due to the GRAS status of wildtype *P. pastoris*, no special biological safety measurements are necessary while working with whole cells.

The purification of the product became a straightforward task done by low-g centrifugation and utilization of the supernatant.

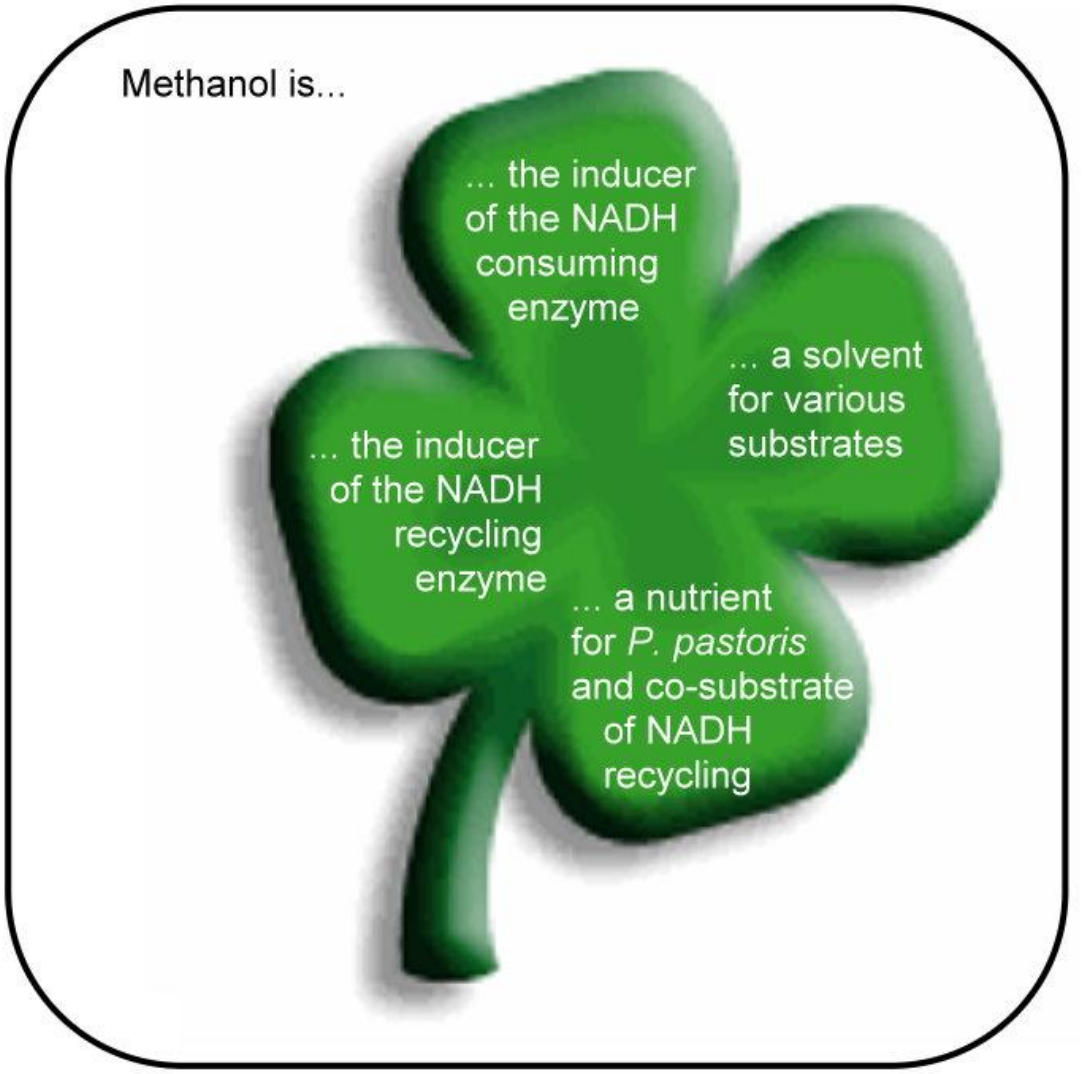

Figure 5: The Lucky Four Facts of the methylotrophic yeast *P. Pastoris* as a platform for whole-cell biocatalysis. Figure adopted from A. Glieder.

1.3 Cofactor recycling

1.3.1 The role of NADH and NADPH

In biological redox reactions within living systems, the roles of NAD(H) and NADP(H) are very specific and distinctive. In the presence of the relevant enzyme and substrate they formally transfer a hydride ion from or to the carbon atom at position 4 of the nicotine ring. Despite their structural similarities, only differing by the additional phosphate group, they differ quite substantially in their biochemistry. NAD(H) is used majorly in the oxidative degredations yielding ATP, while NADP(H) is used mostly as a reductant [26].

1.3.2 Cofactor dependency in industrial synthesis

Leaping from nature into industrial production, the cost for pure cofactor addition becomes too severe. Therefore, efficient cofactor regeneration is necessary for scaling up the production. This includes not only a system ready for high throughput, but one with cheap and simple substrates as well. The costs of the recycling system play a major role in the process and the substrates cannot trigger unwanted side reactions.

Considering all this facts, various eukaryotic FDHs became the solution for this problem. FDH has a wide pH-optimum for catalytic activity ranging between pH 5.5 and 11.0, making not only an ideal enzyme in whole-cell environment, but also in purified form. Sodium and Ammonium formate are very cheap and seldom inhibit the activity of the employed production enzymes. On the downside, due to the high acidic nature, of these substrates high concentrations could be considered as toxic for the cell. On the other hand their occurrences in the biosynthesis of methylotrophic yeasts made these the ideal candidates for recombinant protein expression [27].

Also, when using FDH not in the whole-cell environment, but as purified enzyme, the cheap sources for enzyme production as well as the high stability during processing are two important factors speaking for the use of this system.

The major drawback of using this system for cofactor recycling is the fact that there are no NADP+ dependent or highly accepting FDHs known [28]. Therefore, this system is only capable of efficiently working in combination with NADH consuming reactions.

Compared to already established solutions in NADH regeneration, the recent years brought a few approaches in NADPH regeneration, all of them with one or more major flaws, majorly in the topic of the chosen substrates. Although some published systems showed promising results, the substrates used are undesirable for industrial production due to their nature [29].

Due to these complications, an easy and simple system would not only be interesting, but economically desirable.

1.3.3 Engineering aspects (on FDH)

Due to reasons mentioned above and the lack of an attractive alternative, there were numerous studies on different engineering approaches designing a FDH with higher acceptance of NADP+ [20, 30-32].

The focus of this published work concentrates on small point mutations within the structural motif of the Rossman fold within the protein. This structural motif consisting of three to four beta strands and two alpha helices is the NAD(H) and NADP(H) cofactor recognition and docking site. A semi-rational design concerning the shape and size of the binding pocket hypotheses an exchange of certain amino acids within the motif could lead to a different size and therefore a higher acceptance to NADPH.

1.4 Model enzymes for *P. pastoris* whole-cell biocatalysis

As described before in chapter 1.2.2, the driving force of the catalyzed conversion would be employed by an oxidoreductase consuming NADH and/or NADPH. The requirements for these oxidoreductases are straightforward. An enzyme with a well-known and fast reaction, an established screening system and an interesting product for industrial synthesis is needed.

In this thesis, the oxidoreductases *S. cerevisiae* butanediol dehydrogenase and *C. tenuis* xylose reductase were chosen and described in detail as followed.

1.4.1 Butanediol dehydrogenase (BDH)

S. cerevisiae BDH is an already well-established model enzyme for recombinant protein expression in *P. pastoris* [33, 34].

Its common use is the asymmetric reduction of ketones to chiral secondary alcohols providing important precursors in pharmaceutical synthesis as depicted in following figure [35].

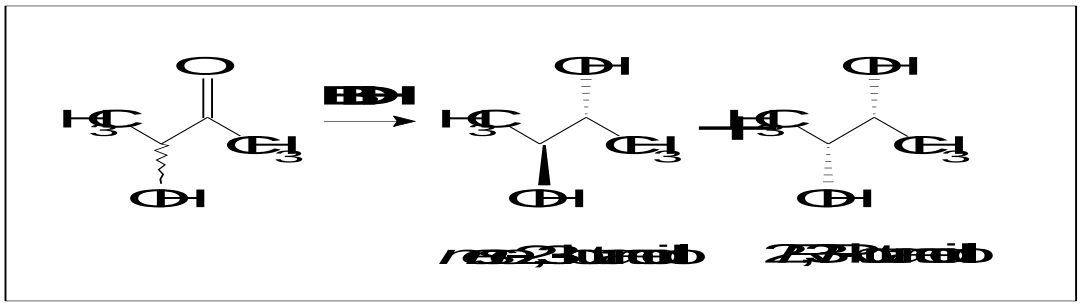

Figure 6: The reaction catalyzed by *S. cerevisiae* BDH. Butanone is converted via BDH to a mix of *meso*-2,3-butanediol and *2R,3R*-butanediol.

In the recent years, a number of applications for isolated BDH [36] and whole-cells employing a over-expressed BDH [35, 37] were published and BDH also shows a high k_{cat} for many substrats.

1.4.2Xylose reductase (XR)

Xylose is one of the most abundant sugar monomers in lignocellulosic biomass known [38]. Hence, there is great economical interest in using this monosugar in industrial-scale processes, for instance in the production of green fuel.

C. tenuis XR catalyzes the first degradation step towards easier accessible C-compounds as depicted as followed.

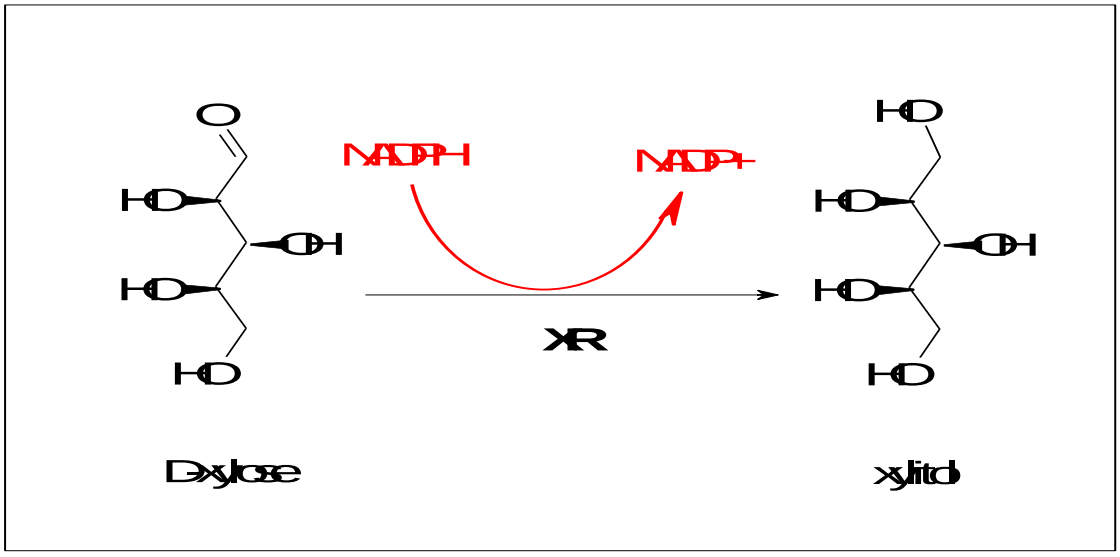

Figure 7: The reaction catalyzed by *C. tenius* XR. D-xylose is converted to xylitol and consumes one equivalent of NADPH in the process.

In the recent years, the main developments for XR in industrial processes focused on the conversion of xylose into fuel ethanol employing a recombinant *S. cerevisiae* as host strain [39-41].

Additionally, studies concerning a mutation of *C. tenuis* XR targeting the NADH acceptance of said enzyme were done in the recent years and brought an engineered strain capable of using NADH and NADPH equally [42-44].

2 Objectives

In terms of recombinant protein expression the methylotrophic yeast *Pichia pastoris* has become an increasingly popular alternative to hosts like *Saccheromyces cerevisiae* or *Escherichia coli*. The recent years brought a significant number of applications in the field of industrial synthesis and whole-cell biotransformations. In this context, the need of an efficient cofactor regeneration system had become very important.

The main objective of this diploma thesis was the construction and screening of *P. pastoris* strains employing the oxidoreductase butanediol dehydrogenase (BDH) with enhanced NADH regeneration by over-expression of the endogenous methanol utilization (MUT) pathway enzymes.

Secondly, the employment of the NADPH dependent oxidoreductase Xylose reductase, as well as a mutant of said enzyme with enhanced acceptance of cofactor NADH was targeted.

The final topic of this work was the construction of *P. pastoris* strains containing an engineered FDH with enhanced acceptance of NADP+ with perspective on a flexible *P. pastoris* platform for future implementations of new oxidoreductases.

3 Materials and methods

3.1 Instruments and Devices

3.1.1 Centrifuges

Eppendorf Centrifuge 5415R: Eppendorf AG, Hamburg, Germany
Eppendorf Centrifuge 5810R: Eppendorf AG, Hamburg, Germany

3.1.2 Thermocycler

GeneAmp® PCR System 2700: Applied Biosystems, Foster City, CA, USA
Mastercycler® personal: Eppendorf AG, Hamburg, Germany
Mastercycler® gradient: Eppendorf AG, Hamburg, Germany

3.1.3 Instruments/Devices

Gene Pulser: Bio-Rad Laboratories, Vienna, Austria
Electroporation cuvettes 2mm, blue cap: Cell Projects, Kent, UK
DU 800 Spectrophotometer: Beckman Coulter Inc, Fullerton, CA, USA
Half-micro cuvettes: Greiner Bio-One GmbH, Frickenhausen, Germany
Vortex-Genie 2: Scientific Industrie Inc, Bohemia, NY, USA

3.1.4 Shaker

Titramax 1000: Heidolph Instruments, Schwabach, Germany (1.5 mm)
Thermomixer comfort: Eppendorf AG, Hamburg, Germany (3 mm)
Multitron II: Infors AG, Bottmingen-Basel, Switzerland (25 mm)
RS 306: Infors AG, Bottmingen-Basel, Switzerland (50 mm)

3.1.5Homogenisator

Precellys 24-Dual: PEQLAB Biotechnologie GMBH, Erlangen, Germany

3.1.6 Pipettes

Denville XL 3000i™ (0.1-2 µL, 2-20 µL, 20-200 µL, 100-1000 µL)**:** Denville Scientific, Metuchen, NJ, USA
Pipetman P20/200/1000 (2-20 µL, 50-200 µL, 200-1000 µL)**:** Gilson S.A.S, F-95400, Villiers le Bel, France
Biohit Proline® multi-channel mechanical pipettor (8ch 50-1200 µL)**:** Biohit Plc., Helsinki, Finland
Biohit Proline® single-channel electronic pipettor (0.2 - 10 µL)**:** Biohit Plc., Helsinki, Finland
Biohit Proline® multi-channel electronic pipettor (8ch 5-100 µL, 8ch 50-1200µL)**:** Biohit Plc., Helsinki, Finland

3.1.7Platereader

Spectramax Plus 384: Molecular Devices, Ismanig/München, Germany

3.1.8 96-well plates

PS-Microplate 96-well, flat bottom: Greiner Bio.One GmbH, Frickenhausen Germany
96-well footprint deep well plate: Bel-Art Products, Pequannock, NJ, USA
Cover for deep well plate: Bel-Art Products, Pequannock, NJ, USA

3.2 Media

All media were stored after autoclaving at + 4° C.

3.2.1 *E. coli* media

LB (Low Salt Luria Bertani):

10 g/L Tryptone, 5 g/L Yeast Extract, 5 g/l NaCl, autoclaved.

Antibiotics if needed where added after autoclaving to a final concentration of: Ampicillin 100 µg/mL, Zeocin 25 µg/mL and Kanamycin 50 µg/mL

LB agar plates:

LB medium was made as described above and 15 g Oxoid agar per litre were added before autoclaving. Antibiotics were again added after autoclaving to a final concentration as described above.

Alternatively, an Bacto™ instant mix of LB agar was available, which was prepared as described in the according manual on the container.

SOC:

20 g/L Bacto^{TM} Tryptone, 0.58 g/L NaCl, 5 g/L Bacto^{TM} Yeast Extract, 2 g/L $MgCl_2$, 0.18 g/L KCl, 2.46 g/L $MgSO_4$, 3.81 g/L α-D(+)-Glucose monohydrate

3.2.2 *P. pastoris* media

Table 2 *P. pastoris* media. Stock solutions for *P. pastoris* media; all solutions except 500xB were autoclaved at 121°C for 20 minutes (500x B was filter sterilised)

Medium	Ingredients
500xB	0.02% d-Biotin, filter sterilized
10xYNB	134 g/L Difco^{TM} Yeast Nitrogen Base w/o Amino Acids
10xD	220 g/L a-D(+)-Glucose monohydrate
10xS	200 g/L D-Sorbitol

10xPPB (1 M PPB, pH 6.0)	30.13 g/L K_2HPO_4, 118.13 g/L KH_2PO_4; if needed pH was adjusted to 6.0

YPD (Yeast Extract Peptone Dextrose Medium)

10 g Bacto™ Yeast Extract and 20 g Bacto™ Peptone were dissolved in 900 mL dH_2O and autoclaved for 20 minutes at 121°C. 100 mL 10xD were added below 50°C. Store at +4°C.

If needed, Zeocin was added after autoclaving to a final concentration of 100 µg/mL

Alternatively, Genetecin was added to a final concentration of 300 µg/mL

YPD agar plates

YPD medium was made as described above and 15 g Bacto™ agar per litre were added before autoclaving.

BMD1 (1% D-Glucose)

50 mL 10xD, 100 mL 10xYNB, 2 ml 500xB, 200 mL 10xPPB, 650 ml dH_2O

BMM2 (1% MeOH)

200 mL 10xPPB, 100 mL 10xYNB, 10mL Methanol, 2mL 500xB, 700mL dH_2O

BMM10 (5% MeOH)

200 mL 10xPPB, 100 mL 10xYNB, 50 mL Methanol, 2 mL 500xB, 640 mL dH_2O

3.2.3 Buffers and solutions

1M DTT: 1.54 g Dithiothreitol/10 mL ddH_2O, filter sterilised

BEDS solution: 10 mM Bicine-NaOH, pH 8.3, 3% (v/v) ethylene glycol, 5% (v/v) DMSO, 1 M Sorbitol

dATP: 100 mM, Fermentas Inc, Glen Burnie, MA, USA

dCTP: 100 mM, Fermentas Inc, Glen Burnie, MA, USA

dTTP: 100 mM, Fermentas Inc, Glen Burnie, MA, USA

dGTP: 100 mM, Fermentas Inc, Glen Burnie, MA, USA

Y-Per®: Yeast Protein Extraction Reagent #78990; Pierce Biotechnology Inc.,

Rockford IL, USA

Ampicillin stock [100 mg/ml]: 5 g Ampicillin/50 mL ddH_2O**,** filter sterilized

Zeocin stock [100 mg/ml]: 1 g Zeocin/10 mL ddH_2O**,** filter sterilized

Geneticin stock [100 mg/mL]: 1 g Geneticin/10mL ddH_2O**,** filter sterilized

DNA Ladder Mix: ready-to-use, Fermentas Inc, Glen Burnie, MA, USA

Lambda DNA/*Hind*III Marker: Fermentas Inc, Glen Burnie, MA, USA

3.3 Enzymes

3.3.1 Restriction enzymes (Fermentas Inc., Glen Burnie, MA, USA)

Restriction enzymes were purchased from MBI Fermentas. Restriction with conventional enzymes was performed as recommended by the producer (www.fermentas.com) using the suggested buffer combination.

Table 3: **Restriction enzymes (Fermentas)**

Enzyme	Concentration	Buffer
*Eco*RI	10 U/µL	10x Buffer *Eco*RI
*Not*I	10 U/µL	10x Buffer orange
*Bgl*II	10 U/µL	10x Buffer orange
*Dpn*I	10 U/µL	10x Buffer Tango™
SpeI	10 U/µL	10x Buffer Tango™
SacI	10 U/µL	10x Buffer *Sac*I
*Bam*HI	10 U/µL	10x Buffer *Bam*HI

Definition U: One unit (U) is defined as the amount of enzyme required to digest 1 µg of lamdba DNA in 1 hour at 37°C in 50 µL of recommended reaction buffer.

3.3.2 Polymerases

The following polymerases were used according to the producer's manuals:

***Phusion™* Polymerase:** 2 U/µL, Finnzymes Oy, Espoo, Finland
***PfuUltra™*:** 2.5 U/µL, Stratagene Corperation, La Jolla, CA, USA

3.3.3 Other enzymes

T4 DNA Ligase: 3 U/µL, Promega Corperation, Madison, WI, USA
Calf Intestine Alkaline Phosphatase (CIAP): 1 U/µL, Fermentas Inc, Glen Burnie, MA, USA

3.4 Software

VectorNTI® 10.3: Invitrogen Corporation, Carlsbad, CA, USA
SoftMax Pro 4.8: Molecular Devices, Ismaning/München, Germany
Lasergene 7.0: DNAStar Inc., Madison, WI, USA
DNA 2.0: DNA2.0, Mento Park, CA, USA
Microsoft® Office 2003: Microsoft Corporation, USA

3.5 Kits and protocols

DNA purification kits were used as described in the supplied manuals. The amount of ddH_2O for elution of the purified product from the column varied from 20 µL to 50 µL according to the end volume needed.

GeneJet™ PCR Cloning Kit #K1222: Fermentas Inc, Glen Burnie, MA, USA
GeneJet™ Plasmid Miniprep Kit, Fermentas Inc, Glen Burnie, MA, USA
QIAquick PCR Purification Kit: Qiagen Inc., Valencia, CA, USA
QIAquick Gel Extraction Kit: Qiagen Inc., Valencia, CA, USA
QuikChange: Stratagene Inc., La Jolla, CA, USA

3.6 Plasmid

3.6.1 pJET 1.2/blunt

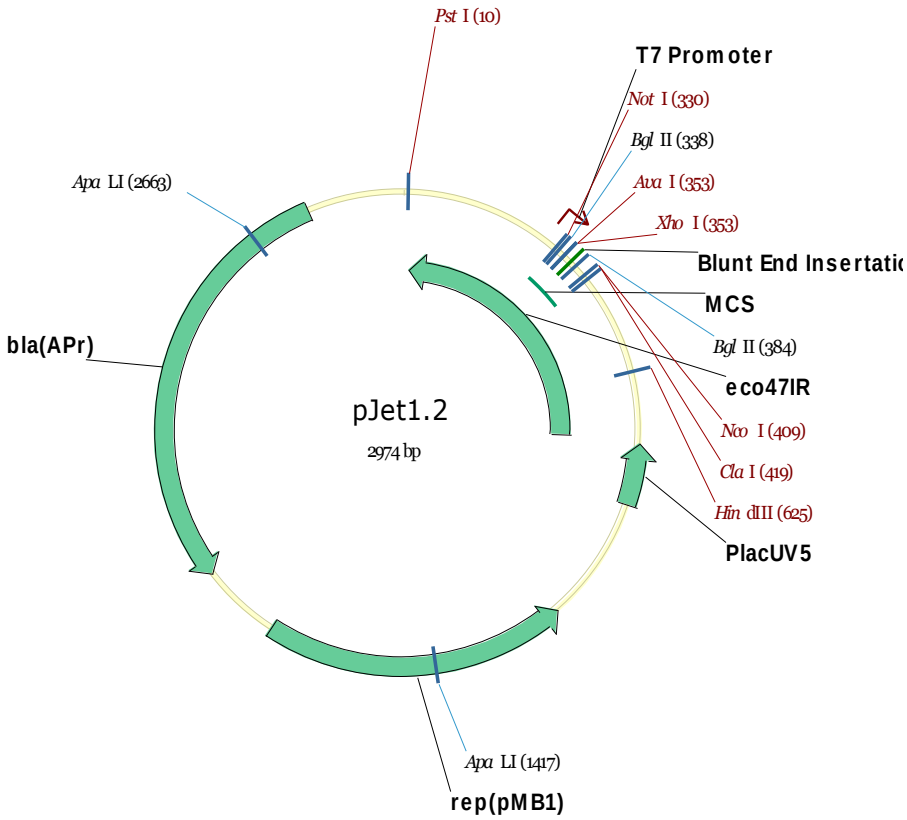

Figure 8 pJET 1.2/blunt vector: *bla*: β-lactamase gene conferring Ampicillin resistance; rep (pMB1): replicon for plasmid replication in *E. coli*; PlacUV5: modified Lac promoter for IPTG independent *eco47IR* gene expression; *eco47IR*: lethal gene for positive selection of transformants bearing an insert; MCS: multiple cloning site containing different restriction sites; T7 Promoter: T7 RNA polymerase promoter for *in vitro* transcription of the cloned insert (GeneJet™ PCR cloning Kit, Fermentas Inc., Glen Burnie MA, USA).

3.6.2 Kan 3,2-8 *E. coli / P. pastoris* Shuttle Vector

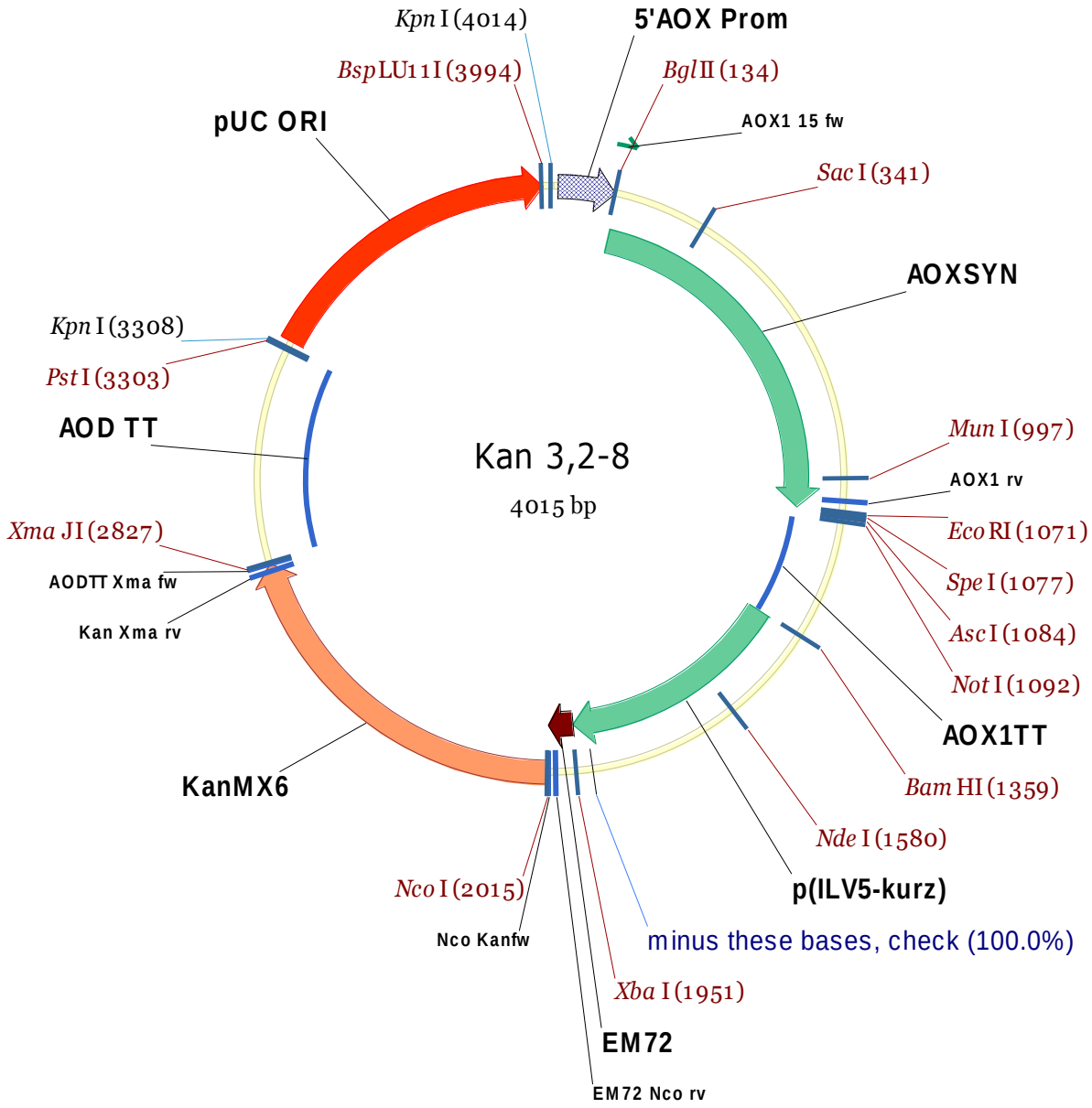

Figure 9 Kan 3,2-8 Shuttle Vector: pUC ORI: origin of replication for *E. coli*; 5'AOX Prom: 5' extension of the standard *AOX1* promoter; AOX SYN: synthetic *AOX1* promoter region; AOX1 TT: synthetic *AOX1* transcription termination sequenze; p(ILV5-kurz): *P. pastoris* IL5V (acetohydroxyacid reductoisomerase) promoter; EM72: synthetic bacterial promoter EM72; KanMX6: gene for Kanamycin/Geneticin resistance; AOD TT: *P. pastoris* AOD (alternative oxidase) transcription terminaton site; Vector provided by Beate Pscheidt.

3.6.3 T2 *E. coli / P. pastoris* Shuttle Vector

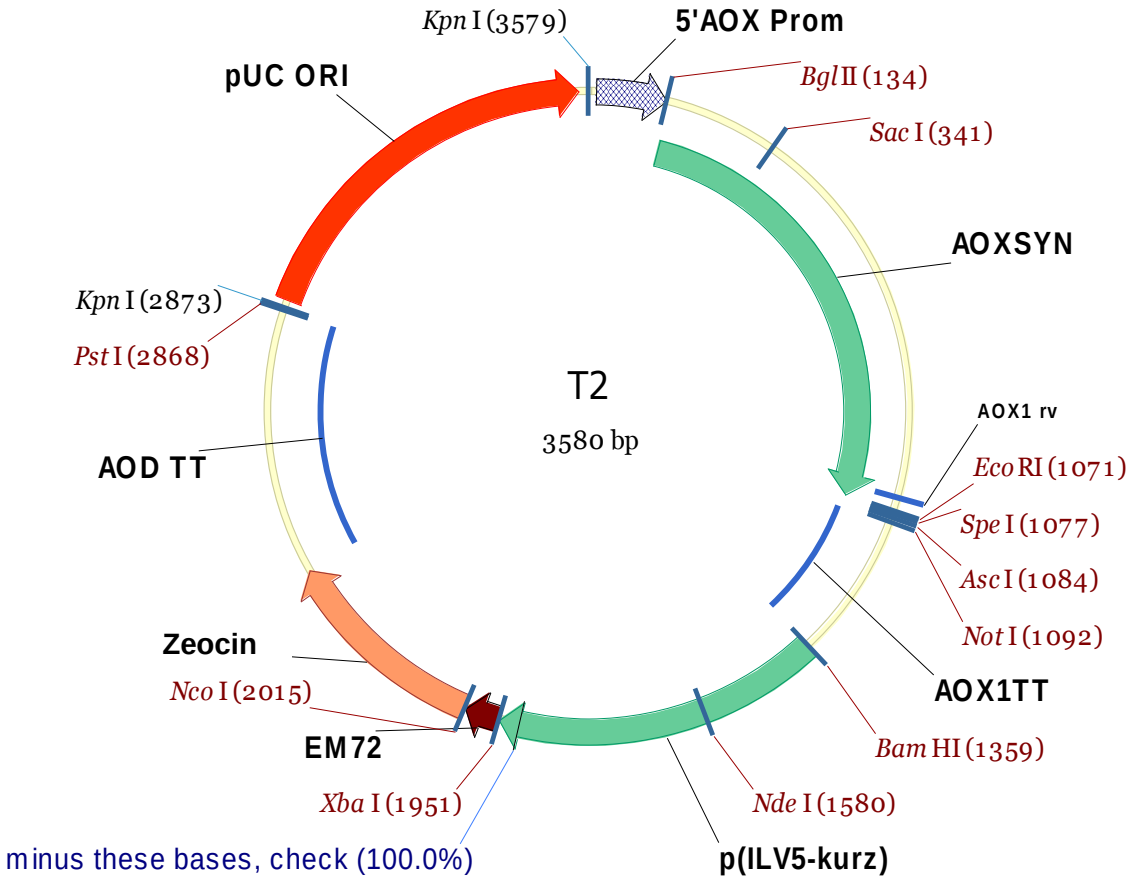

Figure 10 T2 shuttle vector: pUC ORI: origin of replication for *E. coli*; 5'AOX Prom: 5' extension of the standard *AOX1* promoter; AOX SYN: synthetic *AOX1* promoter region; AOX1 TT: synthetic *AOX1* transcription termination sequenze; p(ILV5-kurz): *P. pastoris* IL5V (acetohydroxyacid reductoisomerase) promoter; EM72: synthetic bacterial promoter EM72; Zeocin: gene for Zeocin™ resistance; AOD TT: *P. pastoris* AOD (alternative oxidase) transcription terminaton site; Vector provided by Beate Pscheidt

3.7 Strains

3.7.1 *E. coli* strains

***E. coli* DH5α-T1^{R}**: F- φ80*lac*ZΔM15 Δ(*lac*ZYA-*arg*F)U169 *rec*A1 *end*A1 *hsd*R17(r_k-, m_k+) *pho*A *sup*E44 *thi*-1 *gyr*A96 *rel*A1 *ton*A, Invitrogen Corporation, Carlsbad, CA, USA

3.7.2 *P. pastoris* strains

CBS 7435: Genotype: wild type, Centraalbureau voor Schimmelcultures, Utrecht, The Netherlands, BT3132

P. pastoris* D12-B1H: *das1Δ das2Δ, Franz Hartner, PhD thesis, 2007, BT3425

***P. pastoris* BDH 742D4: CBS 7435 + BDH**, BT3441

***P. pastoris* BDH 764D10: *das1Δ das2Δ* + BDH**

Strains generated during this thesis are listed in the appendix.

3.8 Methods

3.8.1 Plasmid isolation and DNA purification

QIAquick Kits for both applications were used according to the supplied manuals with minimal modifications: For gel extraction, Buffer QG was used, for the melted gel fragment displaying a violet color due to a pH ≤ 7.5, more of buffer QG was added, until the color disappeared.

3.8.2 GeneJet™ ligations

The supplied manual of the GeneJET^{TM} PCR Cloning Kit was followed carefully with following exceptions: 3 µL of PCR product (if possible not purified) and half of the other prescribed amounts were used for ligation (total amount of 10 µL instead of 20 µL).

3.8.3 Standard ligations

For standard ligations of an insert into a vector, the plasmid was digested, dephosphorylated and gel purified (e.g. Kan 3,2-8 *E. coli* / *P. pastoris* shuttle vector, *Eco*RI / *Not*I). Ligation was done with T4 DNA ligase for two hours at room temperature or over night at 16°C without shaking. A molar ratio of 1:3 for insert and vector was used for ligation.

3.8.4 PCR

For all PCR reactions the final dNTP concentrations were 200 µM and 0.2 µM for each primer, respectively. Primer melting temperature was determined using the VectorNTI™ software. Reaction and cycling conditions were chosen according to the polymerase manual. The number of cycles was 30-35. Overlap PCRs and standard PCRs were performed with Phusion^{TM} Polymerase as described in the user's manual. 10 ng of plasmid or chromosomal DNA was used as template.

3.8.5 Site-directed mutagenesis

Site-directed mutagenesis was performed with *Pfu*Ultra^{TM} DNA polymerase by following the SOP for Two Step PCR Protocol for Site Directed Mutagenesis (AA.04). First two single PCR reactions were performed with the forward and reverse primers. After amplification of the single strands these components were combined in another PCR and the desired plasmid was amplified. Before transformation of *E. coli*, 10 µL of the PCR reaction were taken and the native methylated *E. coli* DNA was digested for 2-3 hours with 1 µL of the enzyme *Dpn*I at 37°C.

3.8.6DNA gel electrophoresis

For a 1% agarose gel, 2 g of agarose were added in 200 mL ddH_2O and dissolved through heating up in the lab microwave for 45-60 sec. After cooling down in cold water stream to roughly 60°C, a drop of ethidium bromide solution was added, resulting in an end concentration of about 0.5 µg/mL. Gel was stored at room temperature with negatives of desired chamber volume till solidification. Afterwards, DNA samples, as well as lamda or GeneRuler™ standards were filled into gel chambers at dilution with loading dye at ratio 1:6. 200 mL gels ran at a constant voltage of 90-100 V and for about 40-60 min, following UV detection.

3.8.7 *E. coli* transformation

Transformation of *E. coli* was done using chemical competent *E.coli* DH5α-T1^{R} cells by heat shock. Therefore 100 µL competent cells were incubated with 1-5 µL ligation mixture on ice for approx. 30 min. Afterwards cells were heat shocked for 40 sec at 42°C. Immediately, cells were regenerated in 500 µL SOC media at 37°C and 700

rpm for 60 min and then plated on LB plates containing the appropriate antibiotic. Plates were incubated for 24 hours at 37°C.

3.8.8 *Pichia pastoris* transformation

Competent cell preparation and transformation of *P. pastoris* was done as described in the condensed protocol of Lin-Cereghino *et al* [45].

The amount of DNA used varied from 2-8 µg. Plasmid DNA was linearized prior to transformation. DNA was purified for transformation by GeneJet™ Plasmid Miniprep DNA Purification Kit.

For the preparation of competent cells one single colony was inoculated in 50 mL YPD media and grown over night in a 250 or 300 mL baffled wide-mouthed flask at 30°C, 110 rpm and 60% humidity (RS 306, 50mm/ Infors AG).

Cells were harvested at an OD_{600} of 0.8-2 and the condensed protocol was followed exactly. Finally, 80 µL aliquots of competent cells were made.

For transformation, linearized DNA was mixed with one aliquot of electro competent cells and incubated on ice for 2 min. After electroporation at 1.5 kV, 200 Ω, 25 µF, the cells were regenerated for 2 h at 30°C with light shaking (120 rpm) in a sterile 12 mL PP-tube (Greiner, Frickenhausen, Germany, #184261).

If a Zeocin™ resistance cassette was transformed, cells were regenerated for 1 h in 500 µL 1 M ice-cold Sorbitol, then 500 µL YPD were added and incubated further for 1 h before aliquots were spread on selective agar plates. For the transformation of a geneticin resistance cassette 500 µL 1 M sorbitol and 500 µL YPD were added simultaneously after electroporation and after incubation of 2 h at 30°C aliquots were plated immediately on selective plates. Plates were incubated for 48 hours at 30°C.

3.8.9 Genomic DNA Extraction using Y-Per®

For the isolation of the genomic DNA a *P. pastoris* single colony was resuspended in 50 µl Y-PER® and incubated at 60°C for 10 minutes as described in the producer's manual. After a short cooling period on ice and addition of 50 µL ddH_2O, the DNA was extracted with 100 µL of a C/P/I (chloroform/propanol/isoamylalcohol) 25:24:1 mixture and the upper (aqueous) phase was separated. Isolated DNA was purified by ethanol precipitation. 2.5 volume abs. EtOH and 1/10 volume 3 M NaOAc were

added to the DNA solution and incubated at -20°C for 60 min. The pellet was washed with 1 volume ice-cold EtOH 70% with an incubation step at -20°C for 20 min. The pellet was dried well at room temperature and resuspended in 60 µL water.

3.8.10 Cultivation and Screening

Transformants were cultivated in 96 deep well plates on 1%- glucose minimal media according to Weis *et al* [46]. Whole cell biotransformations were started by the addition of MeOH.

After cultivation the transformants were centrifuged at 4000 rpm for 10 minutes, the supernatant was disposed and the cell pellet was resuspended in 50 µL Y-PER®. After incubation at room temperature for 20 min with light shaking, the 96 deep well plates were centrifuged again under the same conditions and the supernatant was used for further analysis.

Analysis of transformants was done by photometric detection on specific activity assays.

3.9 Activity screening

3.9.1 *AOX1* photometric assay

Detection of AOX1 activity was done according to the already published method from Jungo *et al*. [47] After 10 min incubation at room temperature, a color change to pink should occur, followed by a photometric measurement at 500 nm.

Table 4: Composition of *AOX1* activity assay

400µM	AAP
25 mM	PSA
2 U/mL	HRP
50 mM	PPB pH 7.5
10 µL	crude cell extrect
25 µL	MeOH*

* The addition of MeOH starts the reaction

3.9.2*FDH* photometric assay

Detection of FDH was done under analysis of photometric absorption at 340 nm as described in [48] with following modifications:

Table 5: Composition of FDH photometric assay

50 mM	phosphate buffer pH 7.5
300 mM	sodium formate
200 µM	NAD(P)+*
10 µL	crude extract of cell lysis

* The addition of NAD(P)+ was used to start the reaction

3.9.3*FLD* photometric assay

A second photometric detection of NADH absorption at 340 nm was performed as described in [49] and was used as follows:

Table 6: Composition of FLD photometric assay

150 mM	phosphate buffer pH 7.5
3 mM	formaldehyde
9 mM	glutathione (reduced form)
200 µM	NAD(P)+*
10 µL	crude extract of cell lysis

* The addition of NAD(P)+ was used to start the reaction

3.9.4XR and XR-M photometric assay

In contrast to previous established assays, the detection of XR and XR-M activity goes directly after the depletion of NADH during the reaction. Hence, a negative gradient would be the desired outcome of the experiments.
Assays originate from literature [38, 44] and uses following components:

For detection with NADPH (XR wildtype and XR mutant):

Table 7: Assay for NADPH screening of xylose reductase

800 mM	Xylose
50 mM	PPB pH 7.0
30 µM	NADPH*
10 µL	crude extract of cell lysis

*The addition of NADPH was used to start the reaction

For detection with NADH (XR mutant only):

Table 8: Assay for NADH screening of xylose reductase mutant

800 mM	Xylose
50 mM	PPB pH 7.0
400 µM	NADH*
10 µL	crude extract of cell lysis

*The Addition of NADH was used tom start the reaction

Measurement on plate reader in 96-microtiter scale.

3.10 Primers

All Primers for PCR Reactions were designed in VectorNTI™ and afterwards ordered at Invitrogen Corp.

Table 9: Primeres used

Nummer	Name	Sequenz (5' → 3')
08-759	primer1_rv	CTTGACCTTCGGTAGACATGTTGAATAATAACTGTGTATTTTTCAGTGTT
08-760	primer2_fw	TTCGTGCTGTGATTACTATGCACTAATCAAGAGGATGTCAGAATGCCA
08-761	PpFdh_fw	AACGAATTCATGAAAATCGTTCTCGTTTTG
08-762	PpFdh_rv	AACGCGGCCGCTTTATGCGACCTTTTTG
08-771	sense_prm	AACCGGATCCAATTCCCGCTTTGAACTGC
08-772	antisense_prm	AACGGATCCGCACAAACGAAGGTCTCA
08-773	PpFLD_not_rv	AACGCGGCCGCTTAGTGCATAGTAATCAC
08-774	PpFLD_spe_fw	AACACTAGTATGTCTACCGAAGGTCAA
08-775	FDH_seq2_rv	GGACAGAAGCTCCTTGTTAA
08-776	FDH_seq1_fw	GCTCACGAGCAAATTGTTAA
08-777	primer1_fw	TATTATTCAACATGTCTACCGAAGGTCAAG
08-778	primer2_rv	TTAGTGCATAGTAATCACAGCACG
08-779	HI-zeo-1-r	GAAGCTATGGTGTGTGGGCCTTAGAAACGTCAATTTTGC
08-780	HI-zeo-2-f	GGAGACCAACATGTGAGCAAAAGGCCTCCTCACAAGAAATTG
08-781	UR-zeo-1-r	GAAGCTATGGTGTGTGGGCCTTGATATTGATGCTTGACAG

08-782	UR-zeo-2-f	GGAGACCAACATGTGAGCAAAAGGAGGTGTCTACAAGATTGCAC
08-791	FDH_spe_fw	ACCACTAGTATGAAAATCGTTCTCGTTTTG
08-792	OeFDHtt_fw	TCAAGAGGATGTCAGAATGCCATTT
08-793	Oettaox_fw	AACATCCAAAGACGAAAGGTTGAAT
08-794	OeaoxFLD_fw	ATGTCTACCGAAGGTCAAGTAAGTT
08-795	MutFLD_rv	TTAGCAGTGTTGATAGCAGCACCGT
08-796	AOX_bam_fw	ACCGGATCCAACATCCAAAGACGAAAG
08-797	OeFDHtt_rv	AAATGGCATTCTGACATCCTCTTGATTTATGCGACCTTTTGTCATTACC
08-798	Oettaox_rv	ATTCAACCTTTCGCTTTTGGATGTTGCACAAACGAAGGTCTCACTTAATC
08-799	OeaoxFLD_rv	AACTTACTTGACCTTCGGTAGACATTTTCAATAATTAGTTGTTTTTTGAT
08-800	MutFLD_fw	ACGGTGCTGCTATCAACACTGCTAAAATCTCTAAGGGTGACAAGATCGGT
08-801	FDHdMut_rv	CGGCCTCTTTTGGAAGACCTTGTCTGGCGTAGTACAACAATTCCTTAGGG
08-802	FDHdMut_fw	CCCTAAGGAATTGTTGTACTACGCCAGACAAGGTCTTCCAAAAGAGGCCG
08-803	TH_spe_fw	ACCACTAGTATGCCACATTCCTACGATTAC
08-804	TH_not_rv	ACCGCGGCCGCTTAAAACAGGCGGTTTAA
08-805	TH_seq_fw	CTCGATCAAGAGATGTCAGATTCTCTCTCC
08-806	TH_seq_rv	CCGGTGCGACCGTTGGCATAGAGCAGGCAG
08-807	OeAoxPOx_fw	ATCAAAAAACAACTAATTATTGAAAATGGCTATCCCCGAAGAGTTTGATA
08-808	OeOxMut_fw	GAACCCAAAGAAGCCAAGTCACAAAATCTACCGTGCTAGAAAGCAAATCG
08-809	OeOxTT_rv	AAATGGCATTCTGACATCCTCTTGATTAGAATCTAGCAAGACCGGTCTTC
08-810	OeAoxP_rv	TTTCAATAATTAGTTGTTTTTTGAT
08-811	OeOxMut_rv	TTGTGACTTGGCTTCTTTGGGTTC
08-812	OeTT_fw	TCAAGAGGATGTCAGAATGCCATTT
08-813	AOXdMut_fw	CTAGTTCTAGGTGGTGGTTCCAGTGGTTCCTGTATTGCCGGAAGATTGGC
08-814	AOXdMut_rv	GCCAATCTTCCGGCAATACAGGAACCACTGGAACCACCACCTAGAACTAG
08-815	BamCseqA_rv	GAGCATTCGTCAATCAATACCAAACAAG
08-816	BamCseqB_fw	GATTTGTTTCACTATATGGGATGTTCTTCC
08-817	BamCseqC_rv	CCAAACCCCTACCACAAGATATTCATCTGC
08-818	BamCseqD_fw	GCTGGAAACTGTATTCGTGCTGTGATTAC
08-819	seq0_aox_fw	GAGGGCTTTCTGAGTGTGG
08-820	FDHrd56_rv	GTAGTACAACAATTCCTTAGGGTTG
08-821	FDHrd56_fw	CAACCCTAAGGAATTGTTGTACTACNNKNNKCAAGGTCTTCCAAAAGAGG
08-822	FDHm195_fw	CAACCCTAAGGAATTGTTGTACTACGCCTACCAAGGTCTTCCAAAAGAGG
08-823	Eco_AOX1_fw	ACCGAATTCATGGCTATCCCCGAAGAG
08-824	Not_AOX1_rv	ACCGCGGCCGCTTAGAATCTAGCAAGACC
08-825	BDH_RT_fwd	CTATGTTGTCGAAGCCTTCGAA
08-826	BDH_RT_rev	CCGTTGTGGATGGCACGAACAACTT
*	XR-Eco_f	ATAGAATTCCGAAACGATGAGCGCAAGTATCCC
*	XR-Not-r	AATGCGGCCGCTTAAACGAAGATTGGAATGTT
*	Bgl_remo_r	TCTCTTCTCTCTTGACAAGACC
*	Bgl_remo_f	GGTCTTGTCAAGAGAGAAGAGATTTTCCTCACCTCCAAGTTGTGG
03-041	AOX1forw	GATCTAACATCCAAAGACGAAAGG
08-063	behAODTT_rev	TAACTACGGCTACACTAGAAGG

* Primer number not available

4 BDH strains

4.1 Strategy description

Pichia pastoris as a methylotrophic yeast is able to use MeOH as sole carbon source. Therefore MeOH, besides being substrate, also acts as an inducer for the enzymes involved in the MUT pathway. (See chapter 1.2.2) Only three enzyme activities are responsible for degradation of MeOH to CO_2, namely alcohol oxidase 1 and 2 (*AOX 1/2*), formaldehyde dehydrogenase (*FLD*) and formate dehydrogenase (*FDH*). The last two activities are NAD-Cofactor dependent. (See Figure 11)

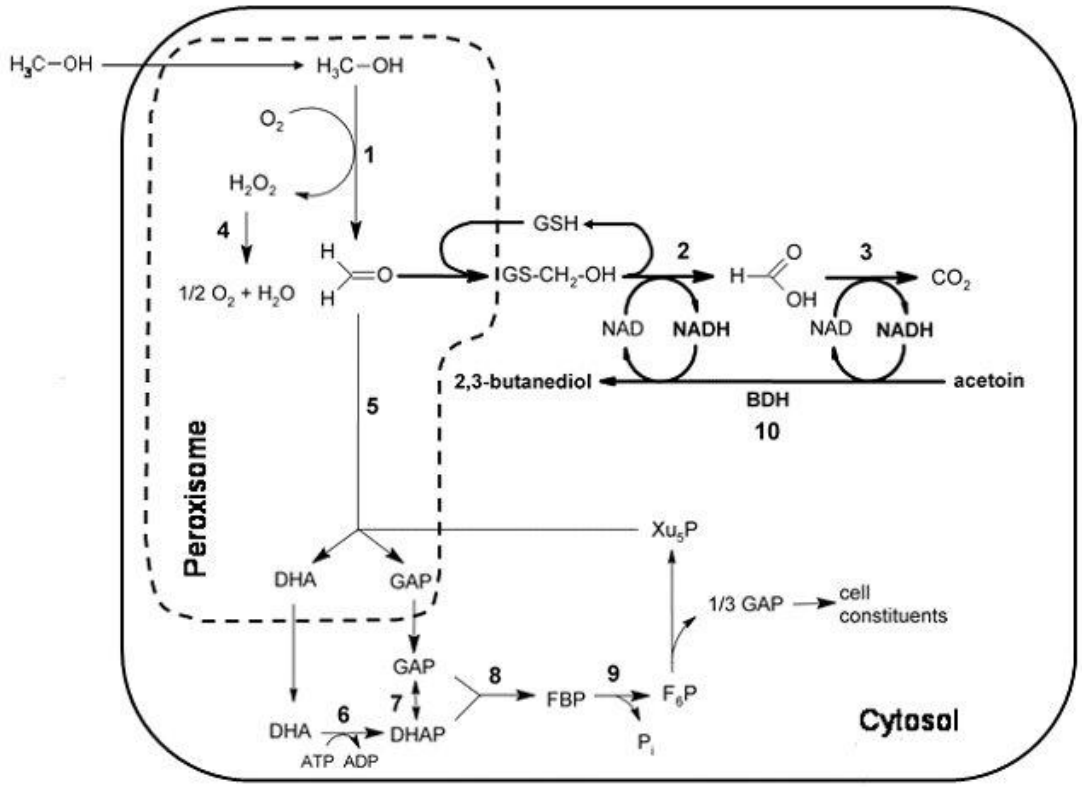

Figure 11: Schematic view of *P. pastoris* methanol utilization pathway adapted from Kirsten Schroer [35]. 1: alcohol oxidase 1 and 2 (AOX1/2). 2: formaldehyde dehydrogenase (FLD). 3: formate dehydrogenase (FDH). 4: catalase. 5: dihydroxyacetone synthase 1 and 2 (DAS 1/2). 6: dihydroxyacetone kinase. 7: triosphosphate isomerase. 8: fructose 1,6-biphosphate aldolase. 9: fructose 1,6-biphosphatase. 10: butanediol dehydrogenase. Deletion of dihydroxyacetone synthase, the methanol dissimilation pathway leads to a reinforced NADH formation

Enhancing this biochemical pathway would result in an enhanced NAD→NADH conversion which can be beneficial for NADH-dependent enzymes like e.g. the oxidoreductase *Saccheromyces cerevisae* butanediol dehydrogenase (*BDH*) (see Figure 11).

Consequently, the topic of this diploma thesis was the systematic generation of different *P. pastoris* strains that over-express enzymes of the methanol pathway as well as the characterization of these engineered strains with especial focus on improved NADH cofactor regeneration. Enhanced strains were directly handed over to Kirsten Schroer for further studies on the effects of the over-expression to the overall biotransformation rate of the oxidoreductase *BDH* for a joint publication [35].

Genes of interest were amplified from genomic DNA (gDNA) isolated from *P. pastoris* CBS 7435 and cloned into an in house available pKan 3,2-8 *E. coli* / *P. pastoris* shuttle vector, under the control of the *P. pastoris* endogenous promoter *AOX1*. Herein, the *P. pastoris* wildtype CBS 7435, as well as the previously described (see 3.7.2) Δ*das1das2* knockout strain was used as starting strain for this metabolic engineering approach.

4.2 Experimental

4.2.1 Identification of genes of interest

The genes of interest are the three *P. pastoris* endogenous enzymes of the MUT pathway, *AOX1*, *FLD* and *FDH*. Over-expression of these is assumed to lead to an enhanced degradation of MeOH and therefore to an enhanced NADH regeneration.

The DNA sequence of *P. pastoris FLD* and *AOX1* was online available in the NCBI GeneBank [50] (*Pp*AOX1 Acc. Nr.: U96967; *Pp*FLD Acc. Nr.: AF066054) as well as described in literature. The DNA sequence of *PpFDH* was found in patent application of US Patent No. 7087418 by Goldberg, *et al* and depicted in Figure 12.

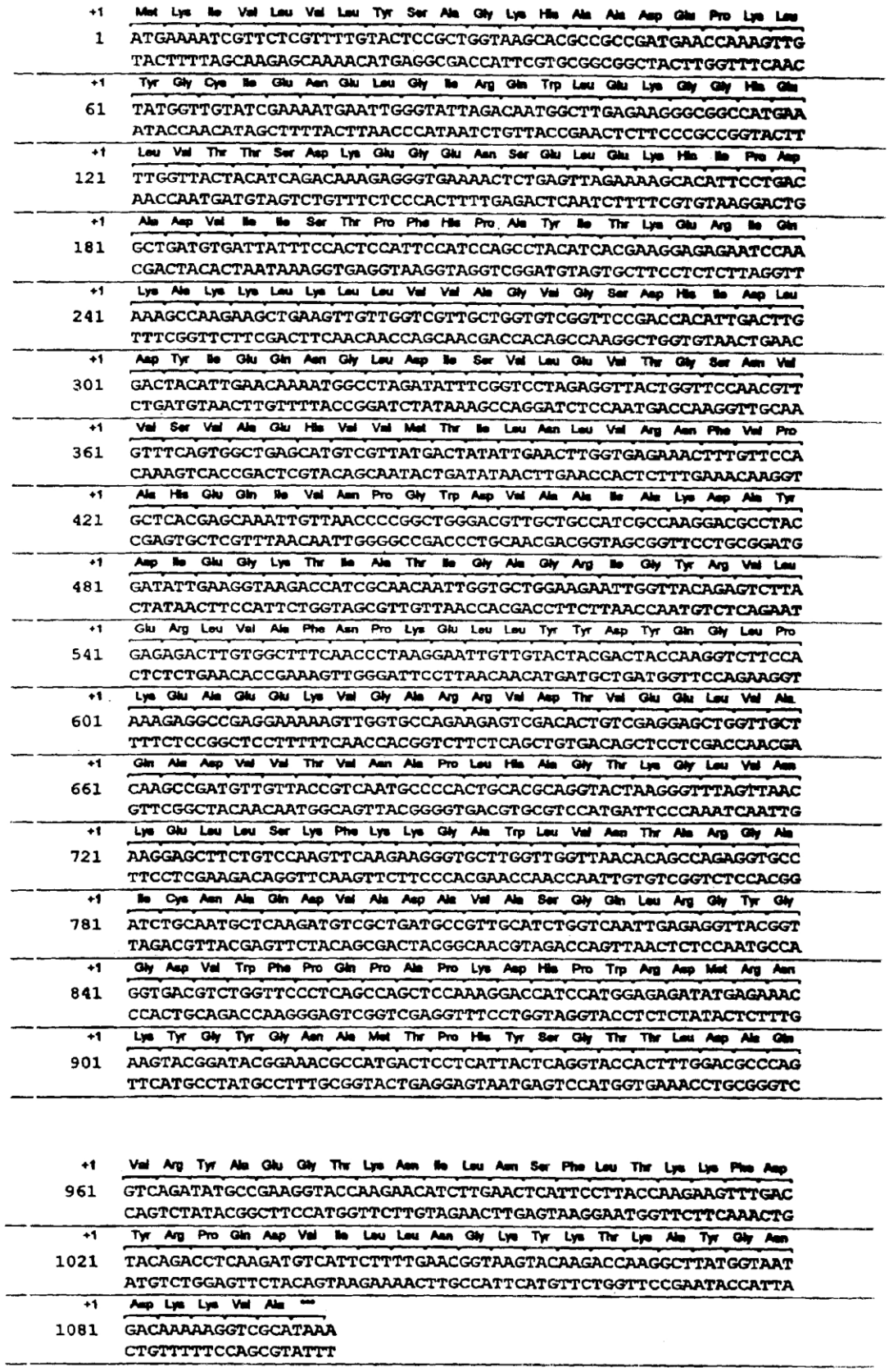

Figure 12: Gene sequence of *P. pastoris* FDH found in **US 7087418**

4.2.2 Construction of *Pichia pastoris* strains for enhanced cofactor recycling

To study, the effect of over-expression of different genes from the MUT pathway in terms of cofactor regeneration, in total eight *P. pastoris* strains were targeted. The host strains *P. pastoris* CBS 7435 as well as the *Δdas1das2* double knock-out strain, harbouring one copy of a BDH expression cassette kindly provided by Bettina Janesch were used as starting strains. The three enzymes of the MUT pathway should be over-expressed, as well as a combination of *FLD* and *FDH* as shown in Table 10:

Table 10: Construction of *P. pastoris* strains for a enhanced NADH cofactor regeneration

P. pastoris strain	Over-expression of
CBS 7435 + BDH (BT 3441: BDH 742D4)	AOX1
	FLD
	FDH
	FLD + FDH
Δdas1das2 + BDH (BDH 764D10)	AOX1
	FLD
	FDH
	FLD + FDH

These eight combinations out of 12 alternatives were chosen mainly due to time constraints and the consideration of the central role of *AOX1* in the *Pichia pastoris* MUT pathway and the assumption that under MeOH induction condition alcohol oxidase is present in high quantity. Therefore, additional over-expression of *AOX1* was thought to have little effect on enhancing the pathway.

4.2.3Amplification of expressions cassette

Standard PCR

For over-expression of a single enzyme of the MUT pathway, the genes of interest were amplified via PCR. All PCRs were done under the same standard conditions. Template of the PCR was the gDNA of *Pichia pastoris* CBS 7435, kindly provided by Beate Pscheidt. Details about the PCR can be seen in Table 11 and 11.

Table 11: Standard composition of PCR using the example of FLD

	Name	Concentration	Volume
Template	*P. pastoris* gDNA	10 ng/µL	3 µL
Primer (fw and rv)	P08-773	10 pmol/µL	2 µL
	P08-774	10 pmol/µL	2 µL
Buffer	HF-Buffer 5x	1x	10 µL
dNTPs	dNTP Mix	10 mM	1 µL
Polymerase	Phusion™	2 U/µL	0,3 µL
ddH_2O			31,7 µL
Σ			50 µL

For all standard PCRs, the same program was in use, as described in Table 12

Table 12: Standard temperature program used for PCR

Temperature	Time	
98°C	30 sec	
98°C	10 sec	30 cycles
60°C	20 sec	
72°C	1 min 20 sec	
72°C	7 min	
4°C	∞	

The PCR product was purified with QIAquick Kit, and diluted with 30 µL of ddH_2O. Purified DNA was further digested with *Eco*RI / *Not*I and *Spe*I / *Not*I for FDH and

FLD, respectively for later ligation in an equally digested E*. coli* / *P. pastoris* pKan 3,2-8 shuttle vector.

Overlap Extension PCR (OE-PCR)

For combined over-expression of FLD and FDH, a larger expression plasmid was constructed, harboring both genes. This was necessary because of the limitations in available selection markers. Zeocin™ was already used for the over-expression of BDH, therefore only Geneticin (G418) resistance was still available.
The first step in the construction of this larger plasmid was the assembling of the insert via OE-PCR. The insert, containing the genes of *FLD* and *FDH*, as well as the specific *AOX1* promoter and terminator is depicted in Figure 13. The resulting fragment was digested with SpeI/NotI for ligation into an equally prepared pKan 3,2-8 plasmid.

For integration into *P. pastoris* genome, the plasmid is usually linearized by digestion of restriction sites *Bgl*II or *Sac*I (both on the *AOX1* promoter region). Unfortunately, both restriction sites were present twice on the generated plasmid.
To solve this problem, a silent mutation in the *FLD* sequence (at the nucleotide position 570: g→a) was introduced in order to eliminate the *Bgl*II restriction site. This engineering step was performed during the fragment construction with the OE-PCR designed primers.

The further construction of the DNA insert for the expression plasmid is described in detail on following Figure 13 and Table 13.

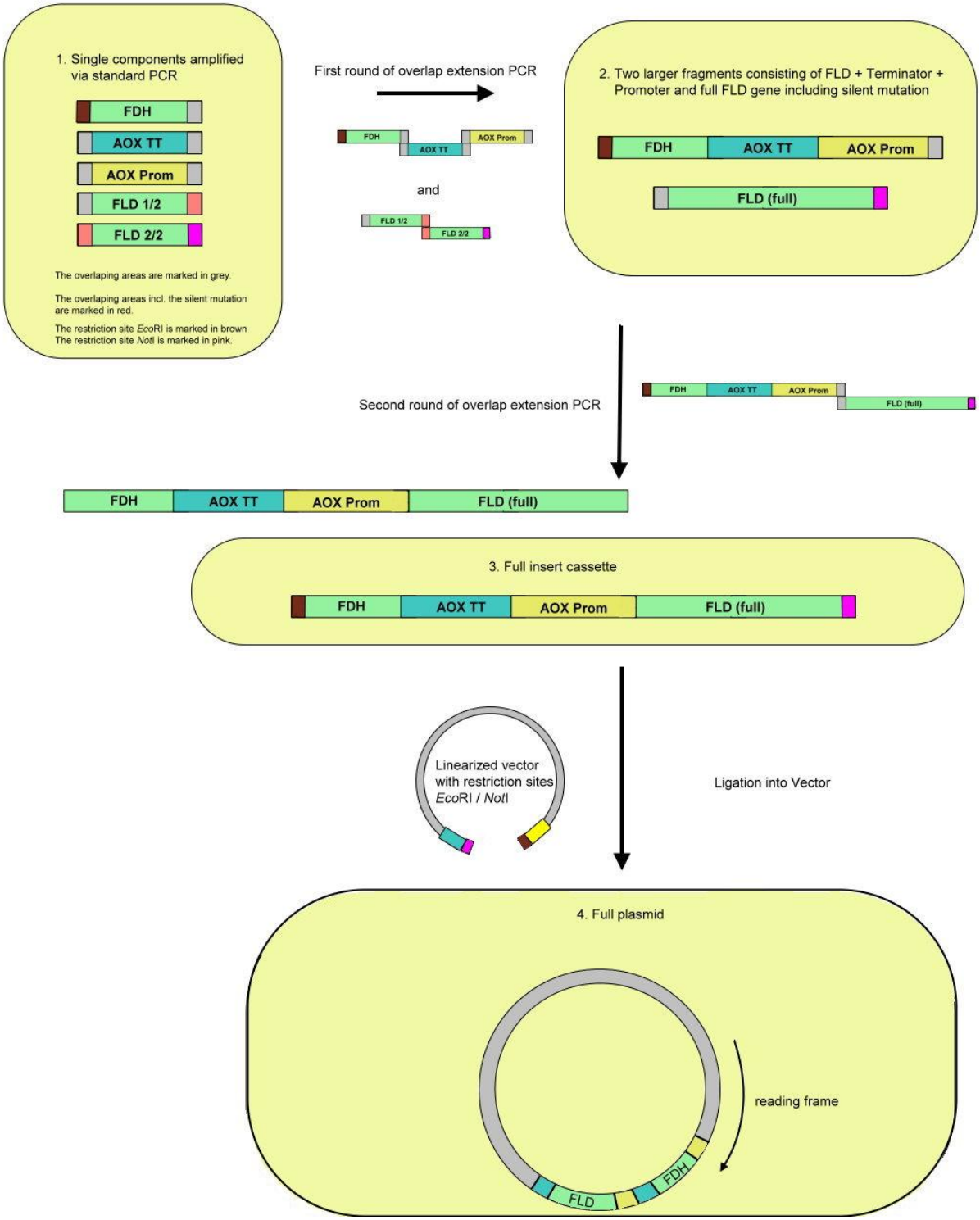

Figure 13: Schematic view of the working steps leading to a complete *FLD* and *FDH* plasmid

Table 13: Used templates and primers in OE-PCR

Name	Template	Primer	Description
FDH	*P. pastoris* gDNA	P08-791 P08-797	*P. pastoris* FDH gene
AOX TT	linearized vector T2*	P08-792 P08-798	AOX Terminator
AOX Prom	linearized vector T2*	P08-793 P08-799	AOX Promoter
FLD 1/2	*P. pastoris* gDNA	P08-794 P08-795	First half of *P. pastoris* FLD gene including silent mutation at overlap region
FLD 2/2	*P. pastoris* gDNA	P08-800 P08-773	Second half of *P. pastoris* FLD gene including silent mutation at overlap region
FDH+TT+Prom	Fragments FDH, AOX TT and AOX Prom	P08-791 P08-799	First three fragments
FLD (full)	Fragments FLD 1/2 and 2/2	P08-794 P08-773	Second two fragments
Full cassette	FDH+TT+Prom and FLD (full)	P08-791 P08-773	Complete cassette

*The linearized vector T2, as mentioned in Table 13 above, was a *Eco*RI / *Not*I digested plasmid handed out by Beate Pscheidt.

All mentioned overlap extension PCRs were done with the same procedure. Briefly, the single components were assembled by standard PCR, purified and their concentrations were determined by gel electrophoresis. Afterwards, approximately 5 ng of two or three correspondent fragments were used as template for OE-PCR. With exception of the primers, the amounts of polymerase, dNTPs and buffer were identical as described in the standard protocol (see 3.8.4) and H_2O was added to a final volume of 50 µL.

Table 14: Standard composition of OE-PCR (1st step)

	Name	Concentration	Volume
Template	fragments (1-3 / 4+5)	5 ng/µL	1 µL
Buffer	HF-Buffer 5x	1x	10 µL
dNTPs	dNTP Mix	10 mM	1 µL
Polymerase	Phusion	2 U/µL	0,3 µL
H2O			37,7 µL
Σ			50 µL

Thereafter followed a shortened PCR program:

Table 15: Standard program used for OE-PCR in thermocyclers

Temperature	Time	
98°C	30 sec	
98°C	10 sec	15 cycles
60°C	20 sec	
72°C	1 min 20 sec	
72°C	7 min	
4°C	∞	

After cooling down of samples, a 50 µL mixture of H_2O, buffer, primers and polymerase to an end volume of 100 µL were added and the same, shortened PCR program with 15 cycles was used again.

Table 16: Standard composition of OE-PCR (2nd step)

	Name	Concentration	Volume
Primer (fw and rv)	fragment1_fw	10 pmol/µL	2 µL
	fragment3_rv	10 pmol/µL	2 µL
	respectively		
	fragment4_fw	10 pmol/µL	2 µL
	fragment5_rv	10 pmol/µL	2 µL
Buffer	HF-Buffer 5x	1x	10 µL
dNTPs	dNTP Mix	10 mM	1 µL
Polymerase	Phusion	2 U/L	0,3 µL
H_2O			34,7 µL
Σ			50 µL

All DNA purification steps were done via QIAquik Kits according to the standard protocol and eluted into 30 µL ddH_2O.

Ligation into shuttle vector

After purification and determination of the concentration via gel electrophoresis, the PCR products were digested with the help of restriction enzymes *Eco*RI, *Not*I and *Spe*I according to the producer´s manual. The ligation into the *E. coli / P. pastoris* shuttle vector was performed according to previously described method. (See 3.8.3)

4.2.4*P. pastoris* transformation

The vectors containing the FLD and FDH sequence, as well as the co-expression cassette, were linearized with *Bgl*II and used for *P. pastoris* transformation according to Lin-Cereghino *et al*. [45] For each transformation, about 1 µg of linearized vector DNA was used, which resulted in an average number of about 300 transformants. The transformants were selected on YPD/Geneticin (300 µg/mL)-agar plates.
Resulting transformants were cultivated in 96-well deep well plates as described before in 3.8.8 and assayed for increased FDH and FLD activity.

4.2.5Cultivation and induced protein expression

The cultivation of *P. pastoris* transformants in 96-well deep well plates and the subsequent cell lysis with Y-Per® were performed as described in 3.8.9. For each construct, 88 transformants were cultivated, along with the wild type and host strains as depicted in Figure 14.

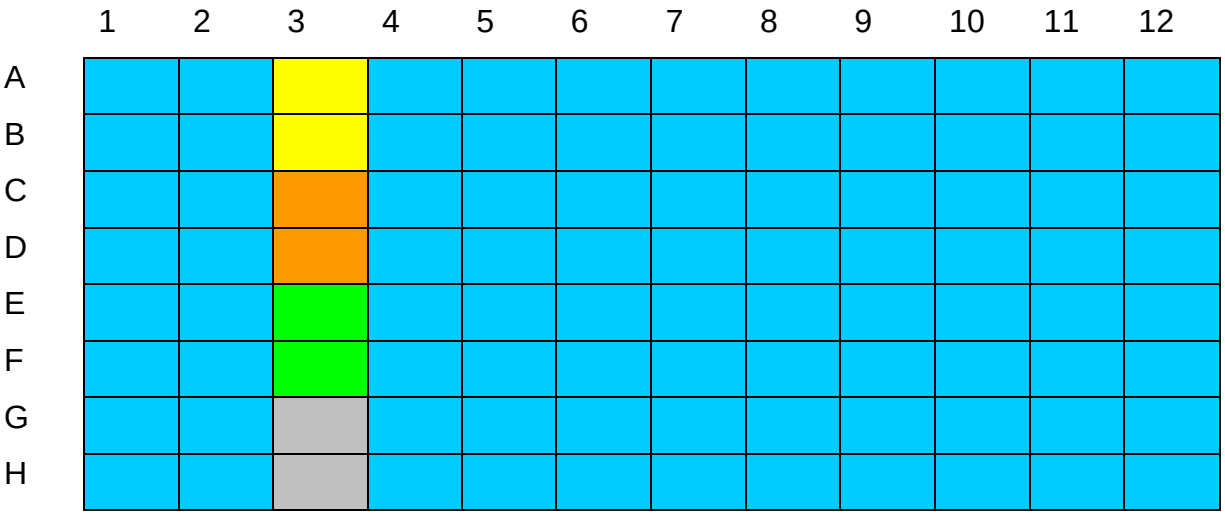

Figure 14: Schematic view of a 96-well deep well plate. transformant, host strain *Δdas1das2* + BDH host strain CBS 7435 + BDH; corresponding wildtype CBS 7435, sterile control.

4.3 Results and discussion

4.3.1*P. pastoris* CBS 7435 MUT over-expression strains

Herein the host strain CBS 7435, which already harbors one copy of the BDH gene, was used as platform for the over-expression of the MUT genes, and for comparison reasons used as control strain in every DWP.

All overxpression strains generated during this study were cultivated, MeOH induced and harvested after 106 hours as described in 3.8.8 and screened for enhanced NADH generation activity.

AOX1 over-expression

Activity screening was done according to method described in chapter 3.9

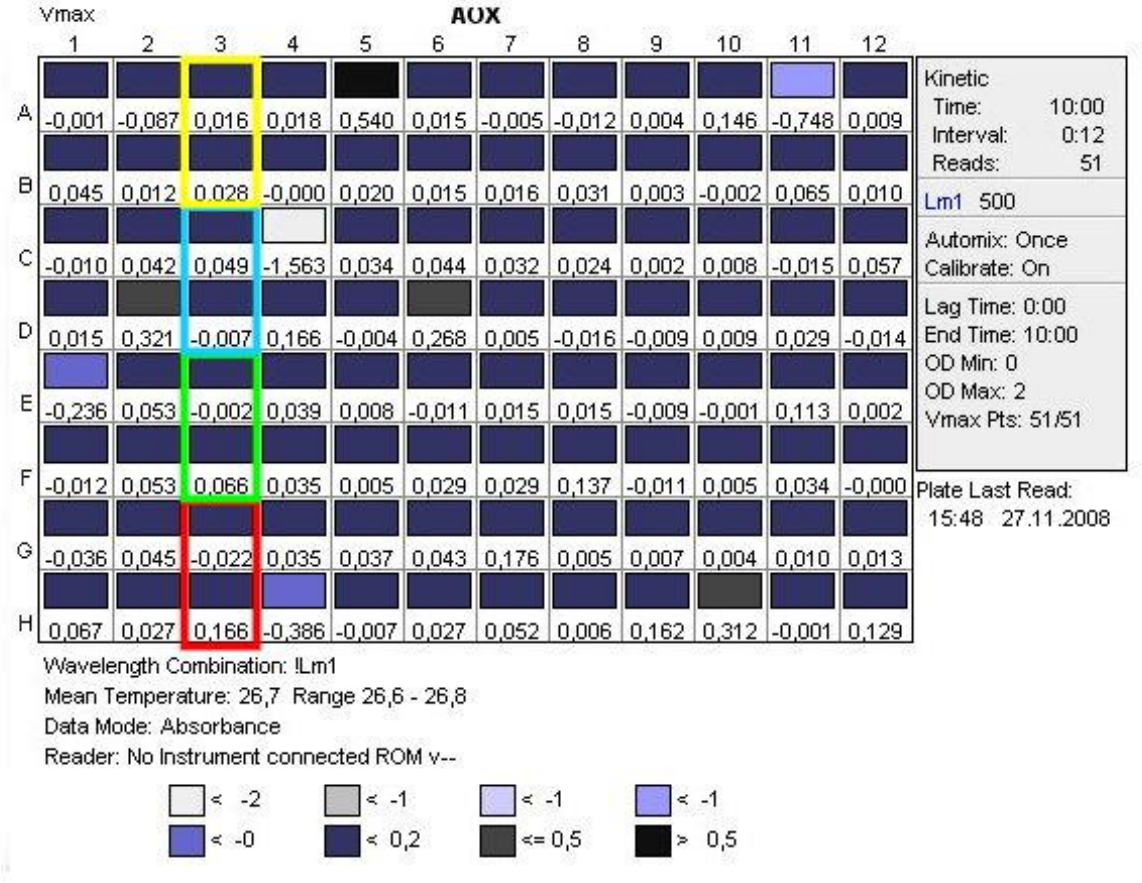

Figure 15: Results of AOX1 assay. Screenshot from SoftMax Pro 4.8. *P. pastoris Δdas1das2* + BDH, *P. pastoris* CBS 7435 + BDH, *P. pastoris* CBS 7435, sterile control.

All results of the activity assay using the cell lysate are in the same range as the sterile control. Hence, cultivation, harvest and analysis were repeated, unfortunately with the same results. No significant Aox1 activity was measurable.

FLD over-expression

Due to a lower rate of transformants, only 50 instead of 88 colonies were picked, cultivated and prepared for measurement.

The analysis of the photometric raw data was done via MS-Excel and is shown in Figure 16.

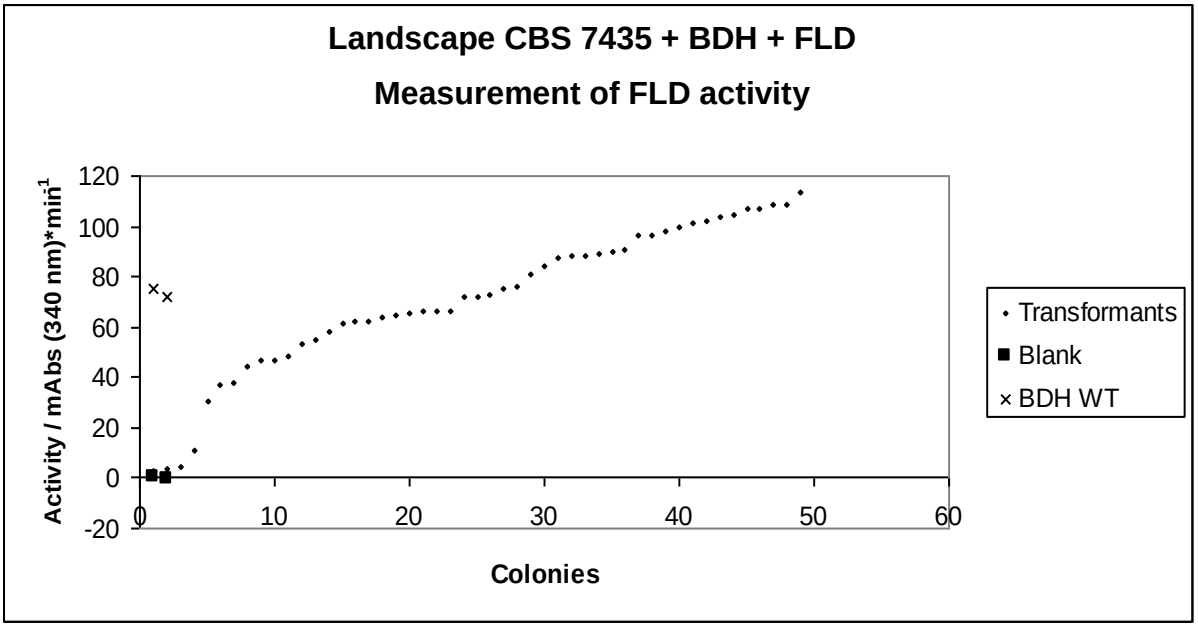

Figure 16: Landscape of *P. pastoris* CBS 7435 transformants with over-expressed BDH and FLD. Square dots mark the sterile controls of the cultivations. The x-shaped dots mark the FLD activities of the host strain *P. pastoris* CBS 7435 + BDH.

According to the results, about 50% of all analyzed transformants showed a higher performance compared to the host strain.

Four transformants with the highest relative activity were chosen for a re-screen under the same cultivation and analysis conditions.

FDH over-expression

As also mentioned for the FLD co-expression, a lower rate of transformants was observed after the FDH co-transfromation, consequently only 39 instead of 88 colonies were available for measurement.

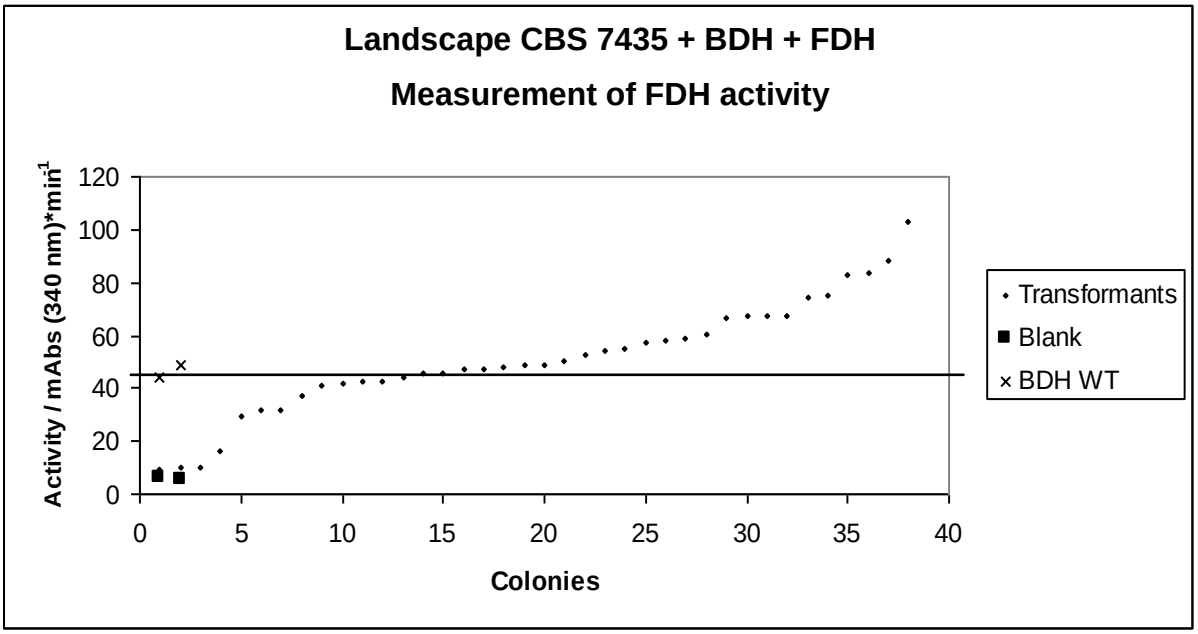

Figure 17: Landscape of *P. pastoris* CBS 7435 transformants with over-expressed BDH and FDH. Square dots mark the sterile controls of the cultivations. The x-shaped dots mark the FDH activities of the host strain *P. pastoris* CBS 7435 + BDH

Despite a low transformation rate, many transformants had a better BDH performance than the control strain. Again, the top four transformants were chosen for re-screen.

Over-expression of FDH + FLD

The cell crude extract of the transformants with the FLD and FDH co-expression was used for both activity assays.

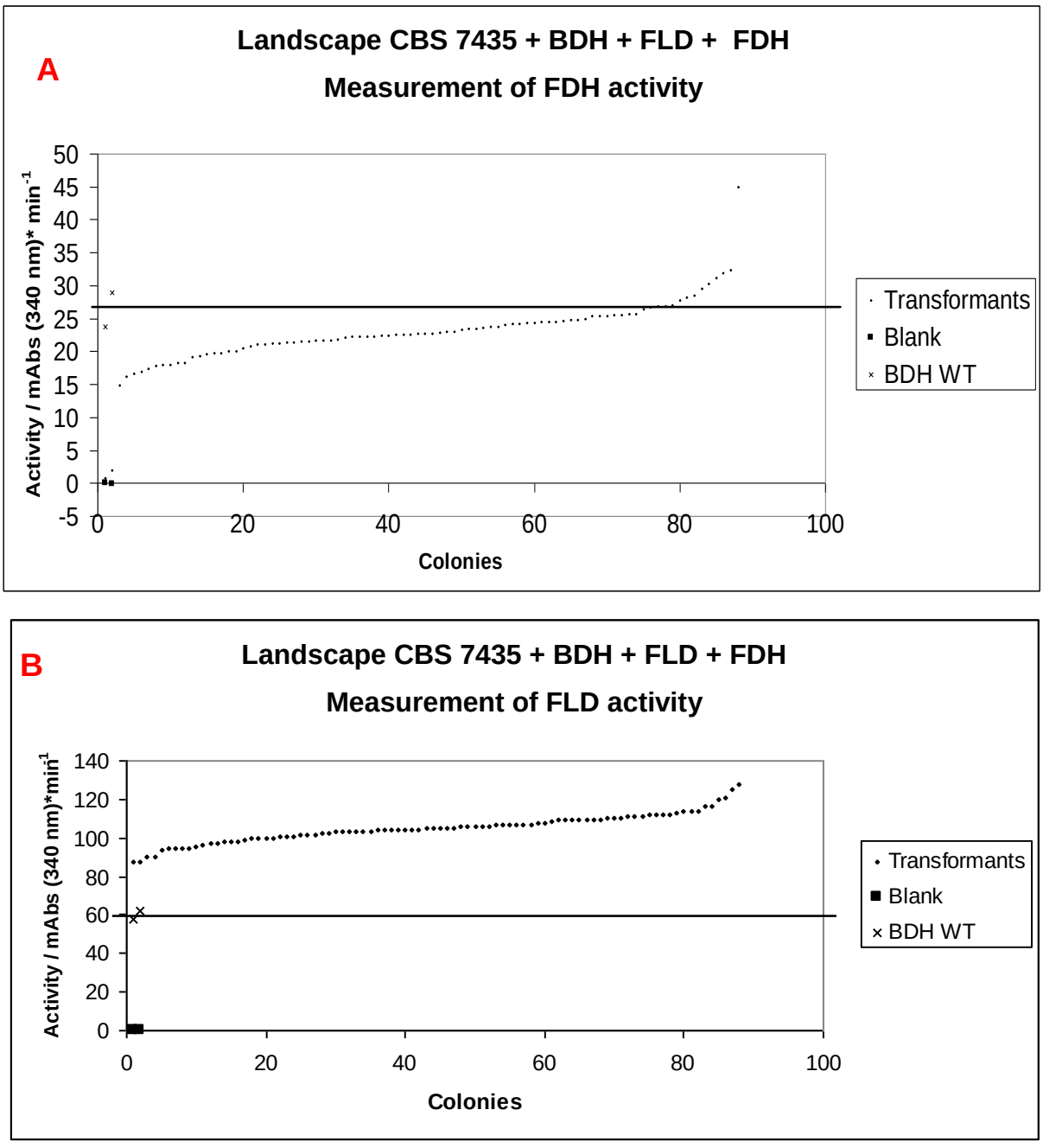

Figure 18: Landscape of *P. pastoris* CBS 7435 transformants with over-expressed BDH, FLD and FDH. Square dots mark the sterile controls of the cultivations. The x-shaped dots mark the correspondent activities of the host strain *P. pastoris* CBS 7435 + BDH and are extended through the black line. **A:** Measurement of FDH activity. **B:** Measurement of FLD activity

While all of the transformants showed a significant higher activity with the *FLD* activity assay, the results for *FDH* activity range mostly about the same value or even lower than the host strain. The top four transformants of each measurement were again chosen for a re-screen under the same conditions.

Re-screen results

The results of the re-screen confirmed the enhanced FLD and FDH activites in most of the chosen stains (see Table 17). Some strains however, couldn't reproduce the results of the first screening. The strain with the highest relative activity (FLD 1) compared to the host strain was selected for further studies on this topic.
In the case of the over-expression of *FLD*+*FDH*, the strain with the best combination of *FLD* and *FDH* activity was chosen. Also the reduced FDH activity of these strains was reproduced.

Table 17: Re-screen results of *P. pastoris* CBS 7435 strains.

Name of transformant	FLD re-screen activities	FDH re-screen activities
Host strain CBS 7435 + BDH	100 ± 11%	100 ± 12%
FLD 1	197 ± 9%	-
FLD 2	159 ± 11%	-
FLD 3	181 ± 10%	-
FLD 4	174 ± 6%	-
FDH 1	-	216 ± 10%
FDH 2	-	88 ± 27%
FDH 3	-	73 ± 5%
FDH 4	-	197 ± 20%
FLD+FDH 1	196 ± 7%	113 ± 2%
FLD+FDH 2	176 ± 4%	73 ± 17%
FLD+FDH 3	128 ± 54%	90 ± 5%
FLD+FDH 4	168 ± 6%	95 ± 9%

4.3.2 *P. pastoris Δdas1das2* MUT over-expression strains

Over-expression of AOX1

Due to previously described *AOX1* over-expression results in the *P. pastoris* CBS 7435 strain, no *AOX1* related experiments were planned for the *Δdas1das2* strain. (see 4.3.3)

Over-expression of FLD

The majority of the screened transformants showed higher FLD activity than the control strain CBS 7435 + BDH as could be detected with the FLD activity assay. (See Figure 19)

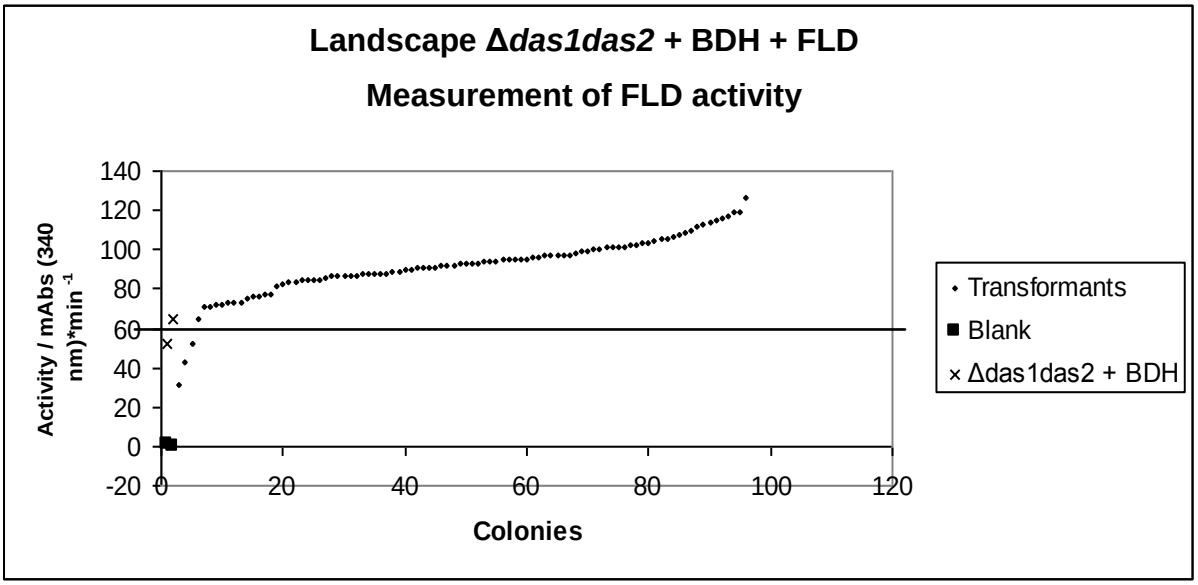

Figure 19: Landscape of *P. pastoris Δdas1das2* transformants with over-expressed BDH and FLD. Grown Square dots mark the sterile controls of the cultivations. The x-shaped dots mark the FLD activities of the host strain *P. pastoris Δdas1das2* + BDH.

Apparently, and as expected the co-expression of the FLD gene in the das1 das2 double knockout strain has a bigger impact on the MeOH dissimilation pathway than in the *P. pastoris* CBD 7435 strain. In order to confirm these preliminary results, four transformants displaying the highest performances were chosen for a re-screen.

Over-expression of FDH

The over-expression of the FDH gene in the das1 das2 double knock out strain resulted in a higher NADH generation performance compared to the starting strain, which only contains the endogenous FDH gene. And is in line with the observations done for the FLD over-expression strains (See Figure 20)

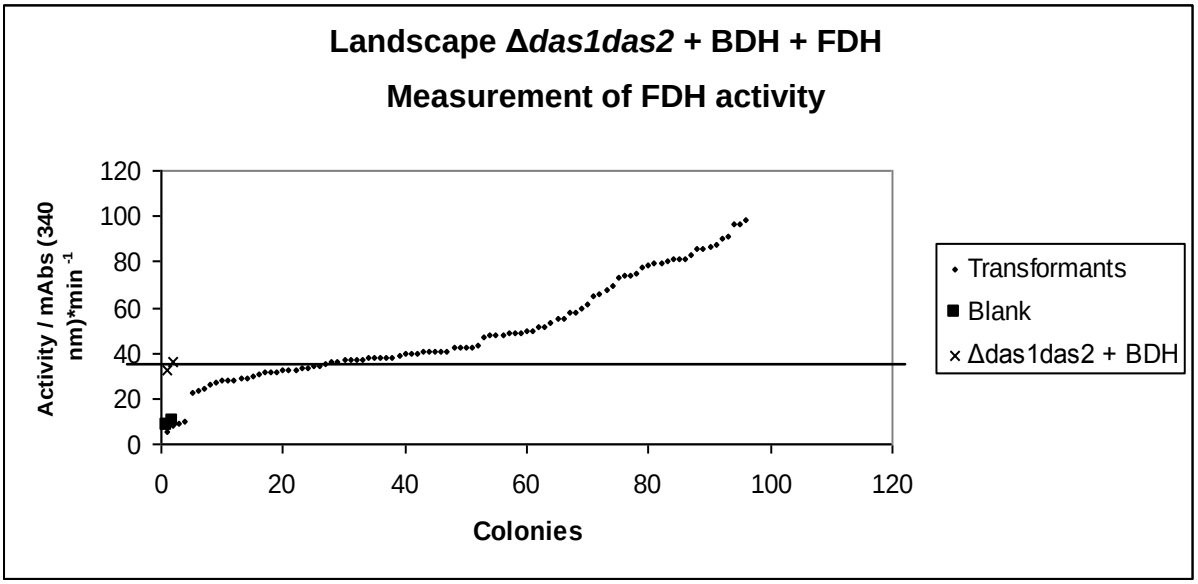

Figure 20: Landscape of *P. pastoris Δdas1das2* transformants with over-expressed BDH and FDH. Square dots mark the sterile controls of the cultivations. The x-shaped dots mark the FDH activities of the host strain *P. pastoris Δdas1das2* + BDH and are extended through the black line.

Also here the activity landscape shows that the over-expression of this MUT-gene enhances the co-factor regeneration in a more obvious manner than in the wild type strain. The top four transformants were chosen for a re-screen.

Over-expression of FLD + FDH

The promising results obtained by the co-expression of FDH and FLD demanded the simultaneous co-expression of both enzymes. Herein, the resulting transformants were subjected to both, FDH and FLD assay in order to elucidate the effect of each enzyme in terms of co-factor regeneration.

The assay results depicted in an activity landscape (Figure 21) displayed a high FLD performance of these strains. Interestingly, a rather low NADH generation performance was detected with the FDH assay, which suggests that this enzyme

might be a bottleneck during the MeOH dissimilation pathway in the engineered strains. For confirmation of the previous results four transformants displaying the highest FLD and FDH activity were chosen for a re-screen.

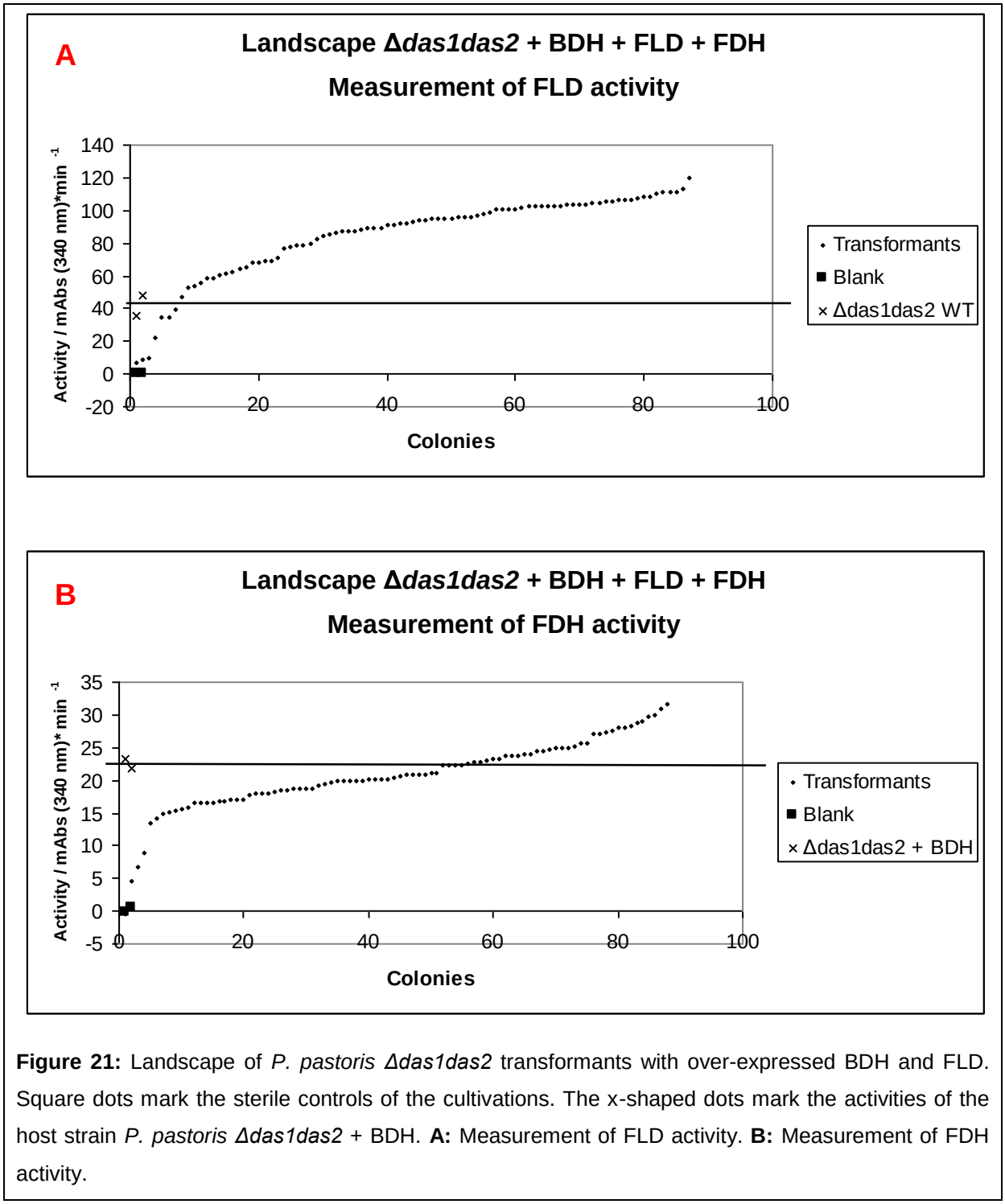

Figure 21: Landscape of *P. pastoris Δdas1das2* transformants with over-expressed BDH and FLD. Square dots mark the sterile controls of the cultivations. The x-shaped dots mark the activities of the host strain *P. pastoris Δdas1das2* + BDH. **A:** Measurement of FLD activity. **B:** Measurement of FDH activity.

Re-screen results

The majority of the re-screened strains confirmed the enhanced NADH generation rate compared to the host strain. (See Table 18)

Table 18: Re-screen results of *P. pastoris Δdas1das2* strains.

Name of transformant	FLD re-screen activities	FDH re-screen activities
Host strain CBS 7435 *Δdas1das2* + BDH	100 ± 6%	100 ± 7%
FLD 1	161 ± 11%	-
FLD 2	146 ± 6%	-
FLD 3	142 ± 4%	-
FLD 4	142 ± 5%	-
FDH 1	-	380 ± 3%
FDH 2	-	129 ± 16%
FDH 3	-	333 ± 8%
FDH 4	-	343 ± 10%
FLD+FDH 1	296 ± 14%	122 ± 15%
FLD+FDH 2	212 ± 12%	103 ± 15%
FLD+FDH 3	268 ± 6%	89 ± 13%
FLD+FDH 4	282 ± 17%	115 ± 7%

In case of the over-expressed FLD+FDH strains, the one with the best combination of FLD and FDH activity was chosen and handed over to Kirsten Schroer for further work on this topic.

4.3.3Final discussion

AOX1 screening

The *AOX1* over-expression strains showed no detectable *AOX1* activity in the DWP-scale. All measured strains displayed values in the same range as the sterile control, which might suggest errors in the activity SOP. On the other hand, studies on shake flask cultivations performed by Kirsten Schroer showed *AOX1* activity using the same protocol, and therefore validates the application of this assay for this purposes.

At the same time it underlines that the cultivation procedure, which is the main difference between both experiments might have a dramatic impact on the outcome of the assay.

The *AOX1* assay is an enzyme coupled assay that relies on the generation of H_2O_2, which reacts with horse radish peroxidase. If this by-product reacts with other enzymes like e.g. catalase present in high amounts in the crude extract of *P. pastoris*, then no oxidase activity would be detectable. The fact, that the assay only delivered positive values with shake flasks cultivated samples and not with DWP cultivated samples suggests that in small scale cultivations there might be a higher catalase expression, maybe due to the O_2 influence.

This explanation is supported by the lack of *AOX1* activity in the *P. pastoris* wild type strain cultivated in DWP, which generally is known to be a good *AOX1* producer. Therefore, and due to the reports [27] describing *AOX1* as a major participant of the MUT pathway in *P. pastoris* we assume that this enzyme is present in large quantities in the peroxisome, and the focus of this study will be posed on the other enzymes of the MUT pathway.

P. pastoris CBS 7435 as host strain

The *FDH* and *FLD* activity screenings showed promising results and are supported by the re-screens of the strains with the overall best performance. The activity landscapes obtained showed typical characteristics with a variety of strains beneath or around the activity level of the host strain and some transformants with a significant higher NADH generation rate.

Probably the most interesting results were obtained with the co-expression of *FLD* and *FDH*. When measuring the NADH generation rate via the *FLD* activity assay, every transformant showed significant higher results compared to the host strain, while on the other hand just average results in terms of the FDH activity assay.

The surprisingly high results of *FLD* screening could quite easily be explained by the fact, that the photometric measurement of NADH generation at 340 nm and the usage of the crude cell extract, the results included not only the enhancement of an

over-expressed *FLD*, but also the enhancements of the over-expressed FDH as well. The generated formate is immediately converted by *FDH* and therefore the *FLD* activity assay showed the sum of both reactions.

However, this hypothesis does not explain the average results of the FDH screening, in which all of the transformants perform in the same range as the host strain although FDH should be overexpressed. In the case of a successful co-expression of both enzymes, the landscape of the single over-expression of *FDH* was reproducible. The lack of this typical characteristic suggests a problem of over-expression itself, maybe due to the design of the expression cassette. The integration of the linearized cassette in the *P.* pastoris genome should occur at the *AOX1* locus. In the present case, the co-expression cassette had two *AOX1 prom* sequences shortly after another. It could be possible, that the one promoting the *FLD* expression had been preferred.

A summary of the results is shown in the following Table 19:

Table 19: Summary of best strains after re-screen.

Name of strain	FLD activity	FDH activity
P. pastoris CBS 7435 + BDH	100 ± 11%	100 ± 12%
WT BDH FLD	197 ± 9%	-
WT BDH FDH	-	216 ± 10%
WT BDH FLD+FDH	196 ± 7%	113 ± 2%

P. pastoris Δdas1das2 as host strain

Similar to the results discussed before, the *P. pastoris Δdas1das2* transformants showed the same significant activity enhancements as the strains with *P. pastoris* CBS 7435 as a host strain.
Table 20 shows a summary of these results.

Table 20: Summary of best strains after re-screen.

Name of strain	FLD activity	FDH activity
P. pastoris Δdas1das2 + BDH	100 ± 6%	100 ± 7%
d12 BDH FLD	161 ± 11%	-
d12 BDH FDH	-	380 ± 3%
d12 BDH FLD+FDH	296 ± 14%	122 ± 15%

Comparison CBS 7435 ↔ *Δdas1das2*

A direct comparison of both starting strains in terms of NADH generation employing the MUT enzymes FLD and FDH, respectively as well as the co-expression of both, the engineered *Δdas1das2* strains showed significant higher activities.

Apart from the higher activities, there are no other differences between the transformants of both host strains in terms of growth rate, cell lysis or other cell characteristics. .

Future perspectives

In this diploma thesis, the sequences of *P. pastoris* endogenous FLD and FDH were used, although previous work on this topic showed, that recombinant enzymes from different origins, such as *Saccharomyces cerevisiae, Paracoccus sp.* or *E. coli* delivered higher specific activities. [48, 51-53] Consequently, further studies and enhancements on the NADH regeneration system could be still focused on the optimization of the MUT pathway responsible enzymes.

Besides using codon optimized sequences of *P. pastoris* MUT genes, directed evolution in order to engineer mutants with enhanced performances and/or more desired characteristics, like e.g. a higher thermostability, higher resistances to acidic/alkaline environments, or a higher long-term stability. More detailed research on this topic can also provide starting points for a (semi-) rational design.

Further studies could also be related to find more worthwhile and suitable biotransformations in terms of industrial applications employing other oxidoreductases, which could handle more complex substrates or conversions. The second topic of this diploma thesis, concerning the work done on xylose reductase, shows such a possible application.

5 Xylose reductase strains

5.1 Strategy description

The studies on butanediol dehydrogenase showed not only promising results in terms of enhanced cofactor regeneration, but also the limitations of this employed oxidoreductase in terms of only accepting NADH as a cofactor.

Since one of the topics of this diploma thesis concentrates on the enhancement of biotransformations of NADPH dependent oxidoreductases, and BDH is strictly NADH-dependent, a different enzyme was chosen for further studies on this topic.

Candida tenuis xylose reductase (*Ct*XR) as well as an engineered strain of the same enzyme with enhanced acceptance of NADH as a cofactor (XR-M) were used in this context. Both enzymes were characterized and described before [42-44] and catalyze the reaction shown in Figure 22.

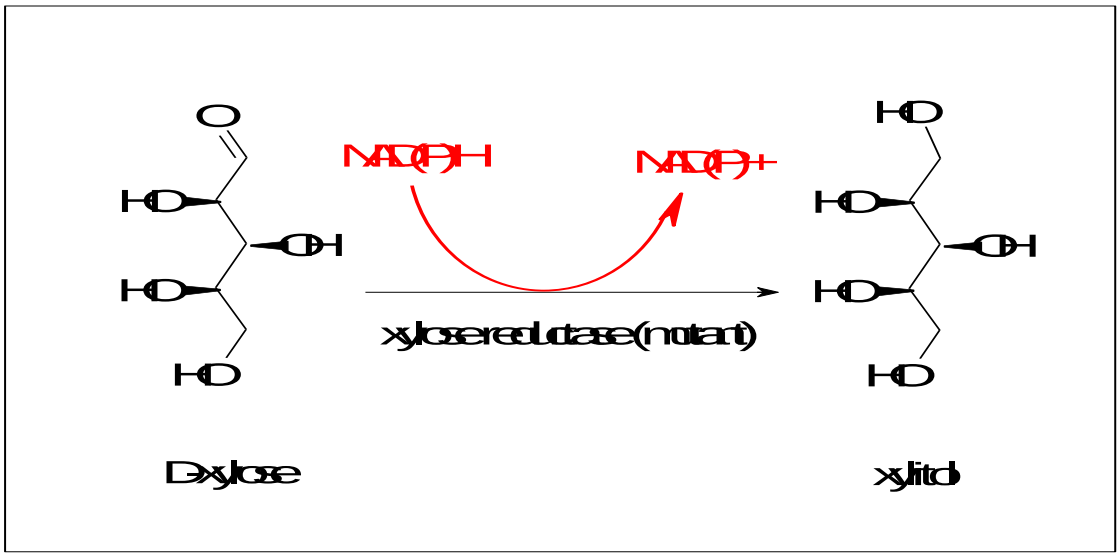

Figure 22: Catalyzed reaction of xylose reductase

The genes of interest were designed and amplified from plasmid DNA kindly provided by Prof. Nidetzky (*E. coli* plasmid *Ct*XRwt for XR and CtXR-K274R-N276D for XR-M) and cloned into an in house available *E. coli* / *P. pastoris* shuttle vector T2 under the control of the *P. pastoris* endogenous *AOX1* promoter and can be selected using Zeocin™. After *P. pastoris* transformation, cultivation in DWP and analysis of xylose

reductase activity, the enzymes of the MUT pathway were integrated into the chosen XR expressing strain using the already described pKan 3,2-8 *E. Coli* / *P. pastoris* shuttle vector. Similar to the procedure already established in the studies of BDH strains, the *P. pastoris* wildtype CBS 7435, as well as the previously described *Δdas1das2* knockout strain was used as starting strains for this metabolic engineering approach. Enhanced strains were again given to Kirsten Schroer for further studies on the effects of the over-expression to the overall biotransformation rate of XR and XR-M.

5.2 Experimental

5.2.1 Identification of genes of interest

The DNA sequence of *Ct*XR is online available in the NCBI GeneBank. (Acc. Nr.: AF074484). Furthermore the DNA sequence of the engineered strain CtXR-K274R-N276D was published and described by Petschacher and Nidetzky *et al* [42-44].
The DNA sequences of the MUT pathway enzymes are the same as described in the previous chapter.

5.2.2 Construction of *Pichia pastoris* strains for enhanced cofactor recycling

To study the various effects of over-expression of different genes from the MUT pathway in terms of cofactor regeneration combined with the over-expression of the oxidoreductase XR or XR-M, in total X *P. pastoris* strains were targeted.
Following Table 21 and Table 22 show a detailed overview of the targeted strains.

Table 21: Construction of *P. pastoris* strains for further co-expression

P. pastoris strain	Over-expression of
CBS 7435	FLD
	FDH
	FLD + FDH
Δdas1das2 (D12-B1H)	XR
	XR-M

Table 22: Construction of *P. pastoris* co-expression strains for enhanced NAD(P)H regeneration

P. pastoris strain	Employing oxidoreductase	Co-expression of
CBS 7435	XR	FLD
		FDH
		FLD + FDH
	XR-M	FLD
		FDH
		FLD + FDH
Δdas1das2 (D12-B1H)	XR	FLD
		FDH
		FLD + FDH
	XR-M	FLD
		FDH
		FLD + FDH

As already described in 4.3.3 no further studies on AOX1 were targeted. .

5.2.3Amplification of expression cassettes

The amplification of the single enzymes of the MUT pathway, as well as the combined FLD + FDH expression cassette, was done under the same conditions and the same protocols as mentioned in the previous chapter 4.2.3.

PCR

For the over-expression of XR, the coding gene was amplified via PCR. Template of the PCR was the plasmid DNA of native *Ct*XRwt which was subcloned by the GenScript into the pUC57-plasimd. Details about the PCR can be seen in Table 11 and 4.

Table 23: Standard composition of PCR of XR

	Name	Concentration	Volume
Template	*Ct*XRwt	10 ng/µL	3 µL
Primer (fw and rv)	XR-Eco_f	10 pmol/µL	2 µL
	XR-Not-r	10 pmol/µL	2 µL
Buffer	HF-Buffer 5x	1x	10 µL
dNTPs	dNTP Mix	10 mM	1 µL
Polymerase	Phusion™	2 U/µL	0,3 µL
ddH_2O			31,7 µL
Σ			50 µL

Table 24: Standard PCR program used in thermocyclers

Temperature	Time	
98°C	30 sec	
98°C	10 sec	30 cycles
60°C	20 sec	
72°C	1 min 20 sec	
72°C	7 min	
4°C	∞	

The PCR product was purified with QIAquick Kit, and diluted with 30 µL of ddH_2O. Purified DNA was further digested with *Eco*RI / *Not*I for later ligation in an equally digested T2 *E. coli* / *P. pastoris* shuttle vector with Zeocin™ as a selection marker.

Overlap Extension PCR (OE-PCR)

For over-expression of XR-M, an internal *Bgl*II restriction site had to be removed. This was done during the assembly of the expression cassette via OE-PCR by introducing a silent mutation at the restriction site.

The OE-PCR was performed as described before (see 4.2.3) using primers listed in Table 4.

Table 25: Used templates and primers in OE-PCR

Fragment name	Template	Primer
XR-M 1/2	CtXR-K274R-N276D	XR-Eco_f Bgl_remo_r
XR-M 2/2		Bgl_remo_f XR-Not-r

Briefly, the single components were amplified by standard PCR (see Table 25), purified and their concentrations were determined by gel electrophoresis. Afterwards, approximately 5 ng of each fragment was used as template for OE-PCR.

A more detailed composition of the OE-PCR can be seen in Table 26.

Table 26: Standard composition of OE-PCR (1st step)

	Name	Concentration	Volume
Template	XR-M 1/2	5 ng/µL	1 µL
	XR-M 2/2	5 ng/µL	1 µL
Buffer	HF-Buffer 5x	1x	10 µL
dNTPs	dNTP Mix	10 mM	1 µL
Polymerase	Phusion	2 U/µL	0,3 µL
ddH_2O			36,7 µL
Σ			50 µL

Thereafter followed a shortened PCR program:

Table 27: Standard program used for OE-PCR in thermocyclers

Temperature	Time	
98°C	30 sec	
98°C	10 sec	15 cycles
60°C	20 sec	
72°C	1 min 20 sec	
72°C	7 min	
4°C	∞	

After cooling down of samples, a 50 µL mixture of ddH_2O, buffer, primers and polymerase to an end volume of 100 µL were added and the same, shortened PCR program with 15 cycles was used again.

Table 28: Standard composition of OE-PCR (2^{nd} step)

	Name	Concentration	Volume
Primer (fw and rv)	XR-Eco_f	10 pmol/µL	2 µL
	XR-Not-r	10 pmol/µL	2 µL
Buffer	HF-Buffer 5x	1x	10 µL
dNTPs	dNTP Mix	10 mM	1 µL
Polymerase	Phusion	2 U/µL	0,3 µL
ddH_2O			34,7 µL
Σ			50 µL

All DNA purification steps were done via QIAquik Kits according to the standard protocol an eluted in 30 µL ddH_2O.
Purified DNA was further digested with *Eco*RI / *Not*I for later ligation in an equally digested T2 *E. coli / P. pastoris* shuttle vector with Zeocin™ as a selection marker.

Ligation into shuttle vector

After purification and determination of the product via gel electrophoresis, the PCR products were digested with *Eco*RI and *Not*I according to the producer's manual. The ligation into the *E. coli / P. pastoris* shuttle vector was performed as previously described in 4.2.4.

5.2.4*P. pastoris* transformation

The vectors for *XR*, and *XR-M* as well as the vectors for enhanced cofactor recycling were linearised with *Bgl*II and used for *P. pastoris* transformation according to Lin-Cereghino *et al* [45]. In each transformation, about 1 µg of linearized vector DNA was used, which resulted in an average number of about 300 transformants.

The transformants were selected on YPD/Zeocin™ (50 µg/mL) in case of the XR and XR-M strains and YPD/Zeocin™/Geneticin (50/300 µg/mL)-agar plates in case of the strains with additional over-expressed enzymes of the MUT pathway.

After successful over-expression of the *XR* and *XR-M* genes in *P. pastoris*, the cofactor recycling enzymes of the MUT pathway were co-expressed in an additional step. Linearized vector DNA was available from the previous experiments on BDH. The transformation was done according to the already established protocol of Lin-Cereghino *et al*. The transformants were selected on YPD/Zeocin™/Geneticin (50/300 µg/mL)-agar plates.

Resulting transformants were cultivated in 96-well deep well plates as described earlier in chapter 4.2.5 and assayed for increased FDH and FLD activity as well as *XR* activity.

5.2.5Cultivation and induced protein expression

The cultivation of *P. pastoris* transformants in 96-well deep well plates and the subsequent cell lysis with Y-PER® were performed as described in 4.2.5

For each construct, 88 transformants were cultivated, along with the wildtype and host strains as depicted in Figure 14.

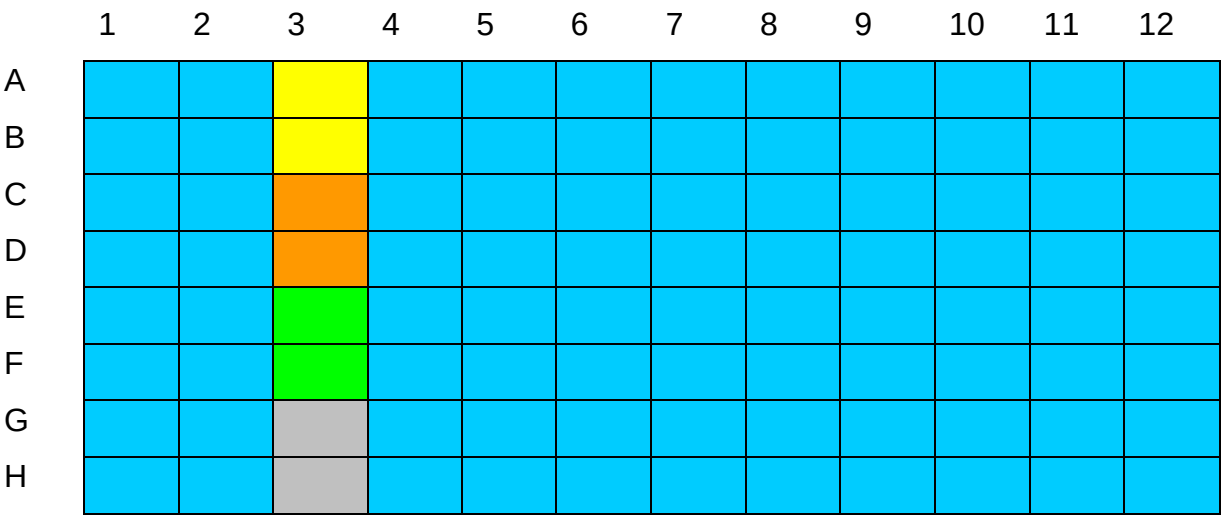

Figure 23: Schematic view of a 96-well deep well plate. transformant, host strain *Δdas1das2* + XR(-M) host strain CBS 7435 + XR(-M); correspondent wildtype, sterile control.

5.3 Results and discussion

All screening experiments were done under the same conditions in terms of cell lysis and reprocessing, microtiter plates, room temperature (23°C) and photometer.
The results of the photometric raw data were analyzed via MS-Excel™ and were graphically presented in form of landscapes with the activities in ascending (in case of all the MUT enzymes) or decreasing (in case of the XR and XR-M measurements) order.

In all experiments, the top 4 performing strains were targeted for re-screen.

5.3.1 *P. pastoris* CBS 7435 MUT + XR over-expression strains

Herein, the host strain *P. pastoris* CBS 7435, which already harbors the over-expressed XR, was used as a platform for the over-expression of the enzymes of the MUT pathway, and for comparison reasons, was used as a control strain in every DWP.

Over-expression of MUT

To achieve the flexible Pichia platform, as mentioned before in chapter 2, strains with enhanced cofactor recycling but without an oxidoreductase employed for the main biotransformation were produced.

These strains were designed for easy accessibility of new oxidoreductases.

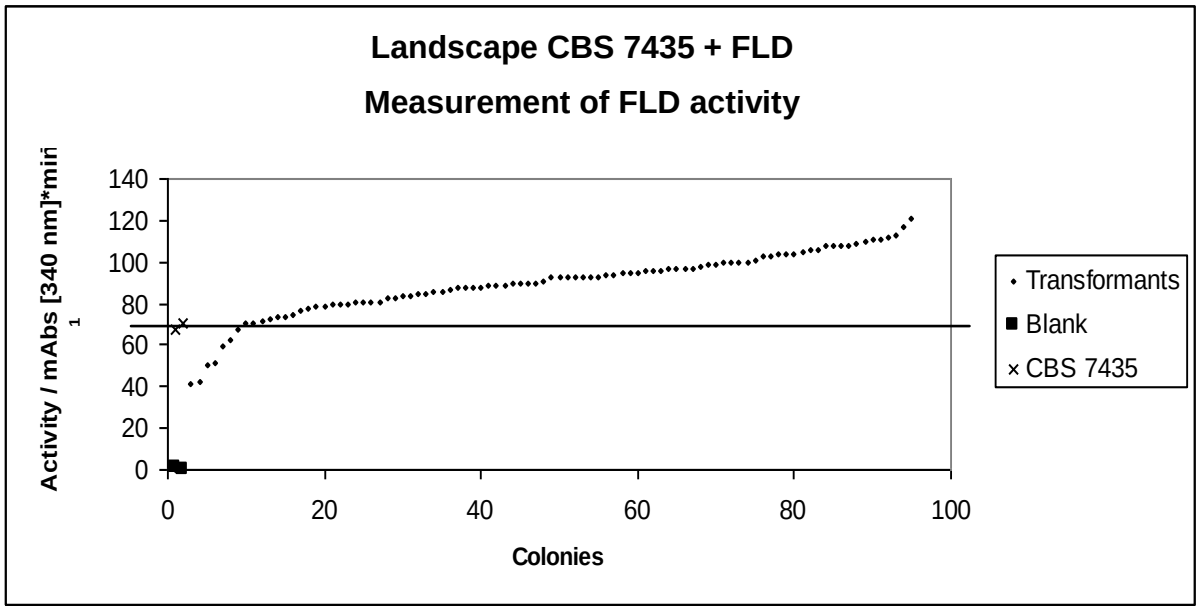

Figure 24: Landscape of *P. pastoris* CBS 7435 transformants with over-expressed FLD. Square dots mark the sterile control of the cultivation. The x-shaped dots mark the FLD activity of the wild type strain *P. pastoris* CBS 7435 and are visualized through the extended black line.

The top 4 strains with the highest activity were chosen for re-screen.

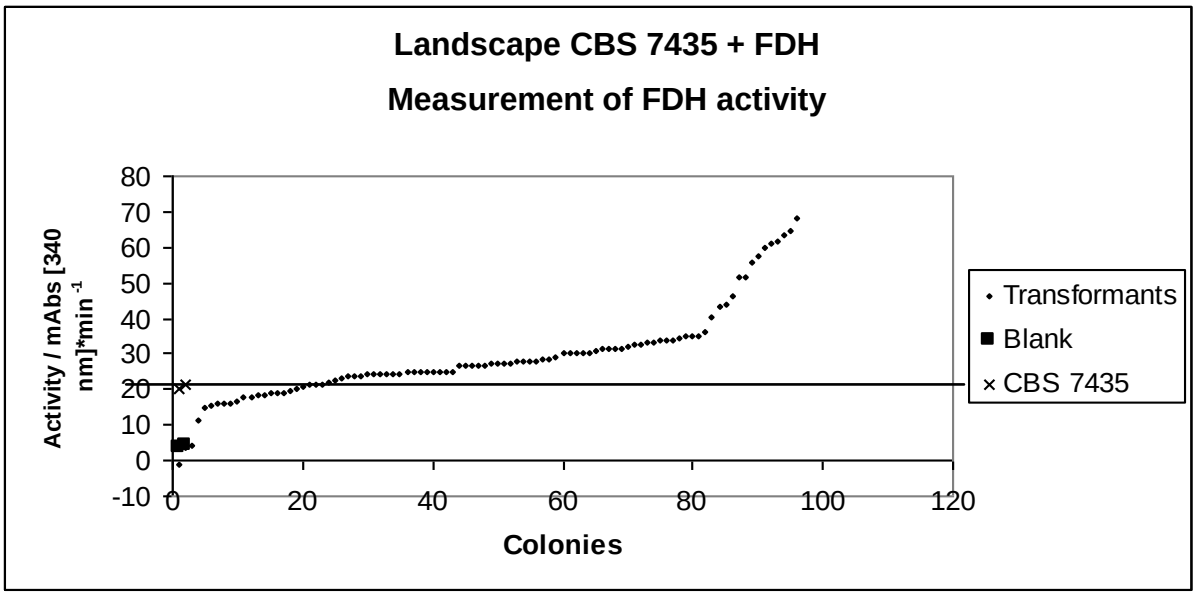

Figure 25: Landscape of *P. pastoris* CBS 7435 transformants with over-expressed FDH. Square dots mark the sterile control of the cultivation. The x-shaped dots mark the FDH activity of the wild type strain *P. pastoris* CBS 7435 and are visualized through the extended black line.

Again, the 4 best performing strains were chosen for re-screen.

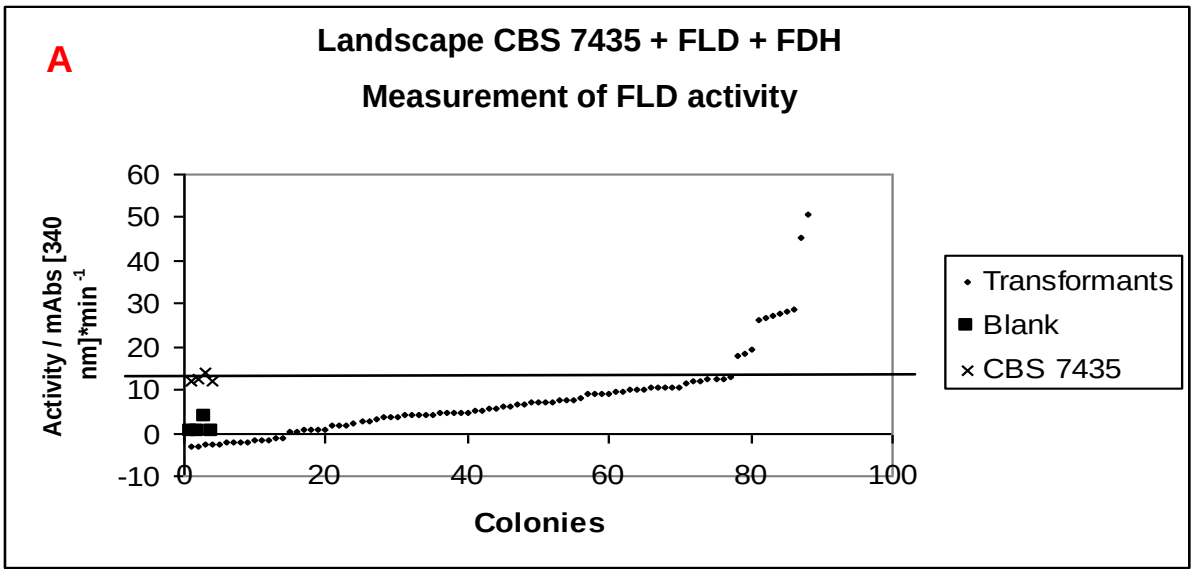

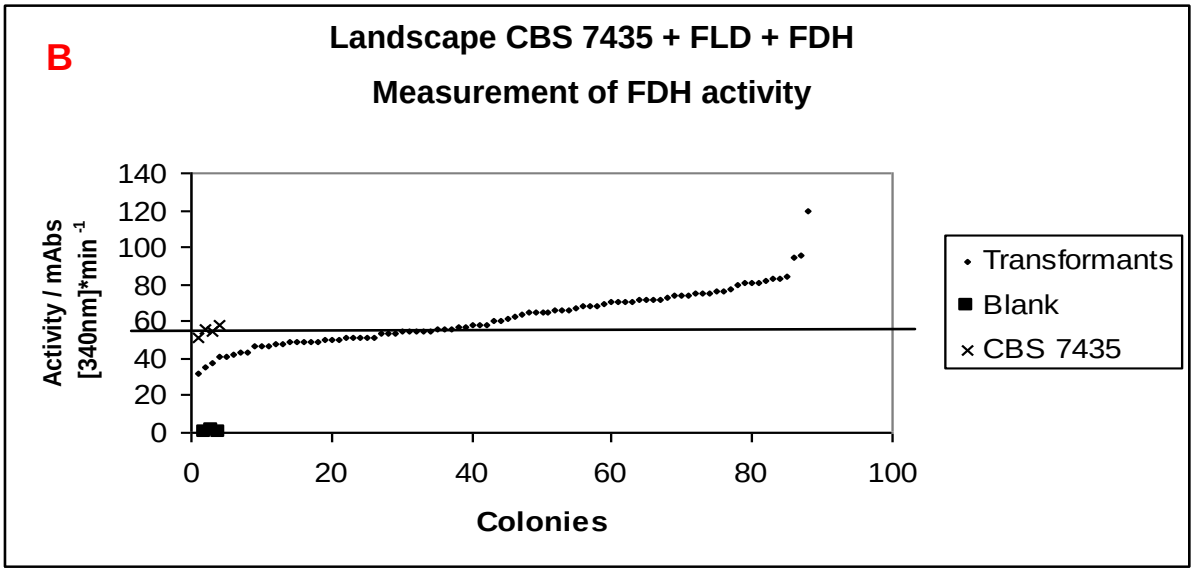

Figure 26: Landscapes of *P. pastoris* CBS 7435 transformants with over-expressed FLD and FDH. Square dots mark the sterile controls of the cultivations. The x-shaped dots mark the activities of the wild type strain *P. pastoris* CBS 7435 and are visualized through the extended black lines. **A:** Measurement of FLD activity. **B:** Measurement of FDH activity.

According to the previous established screening method on the BDH strains, the transformants for re-screen were chosen out of the highest combinations of *FLD/FDH* activity.

Co-expression of *XR* and *FLD*

All measurements of the *XR* activity assay result in a negative valued Landscape, due to the designed fact that NADPH is depleted during the measurement.

For all landscapes of the MUT enzymes, the same methods and procedures came into play as in the previous chapter. Therefore, the landscapes have positive values compared to the wildtype CBS 7435.

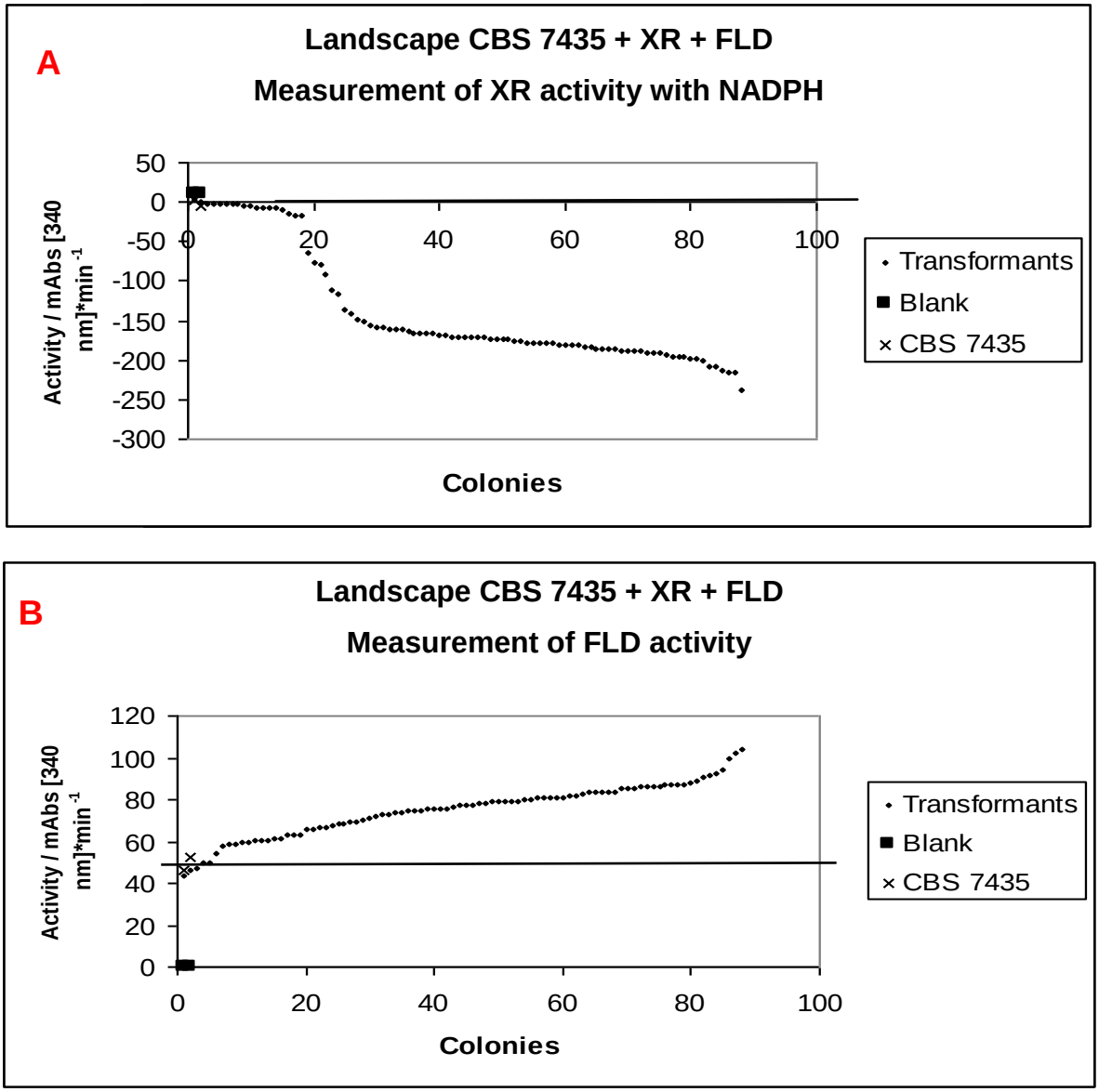

Figure 27: Landscapes of *P. pastoris* CBS 7435 transformants with over-expressed XR and FLD. Square dots mark the sterile controls of the cultivations. The x-shaped dots mark the activities of the wild type strain *P. pastoris* CBS 7435 and are visualized through the extended black lines. **A:** Measurement of XR activity with NADPH. **B:** Measurement of FLD activity.

The four strains with the highest combination of XR/FLD activity were chosen for re-screen.

Co-expression of XR and FDH

The over-expression of XR in the already existing CBS 7435 + FDH strains resulted in a high number of transformants with significant activities in xylose degradation. (see Figure 28)

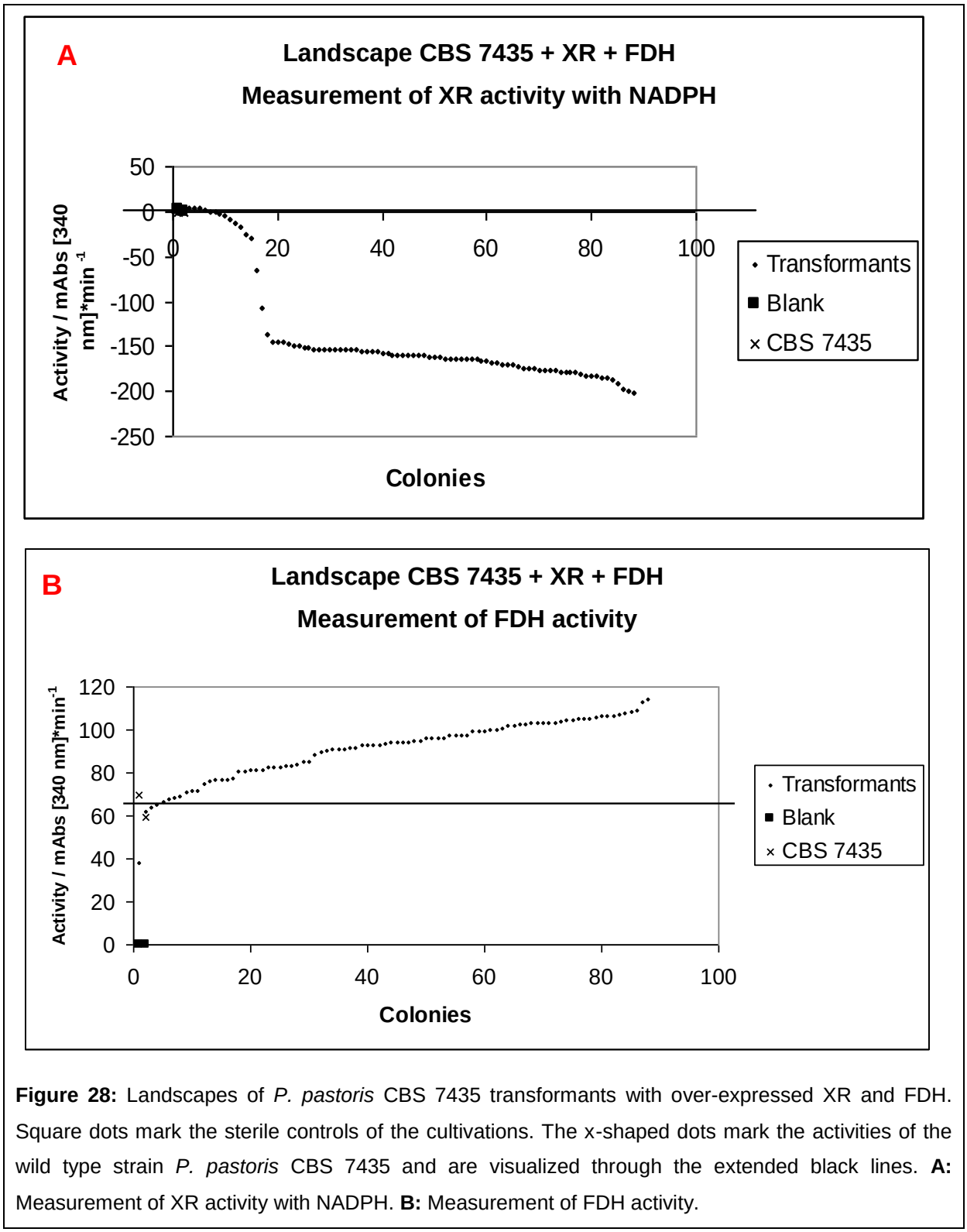

Figure 28: Landscapes of *P. pastoris* CBS 7435 transformants with over-expressed XR and FDH. Square dots mark the sterile controls of the cultivations. The x-shaped dots mark the activities of the wild type strain *P. pastoris* CBS 7435 and are visualized through the extended black lines. **A:** Measurement of XR activity with NADPH. **B:** Measurement of FDH activity.

The results of the FDH activity are as expected. Because the best CBS 7435 + FDH strain was used as host, all of the produced transformants have a higher FDH activity compared to the wildtype, even if there is a quite large normal derivation between the transformants.

Co-expression of *XR, FLD* and *FDH*

The co-expression of three enzymes.

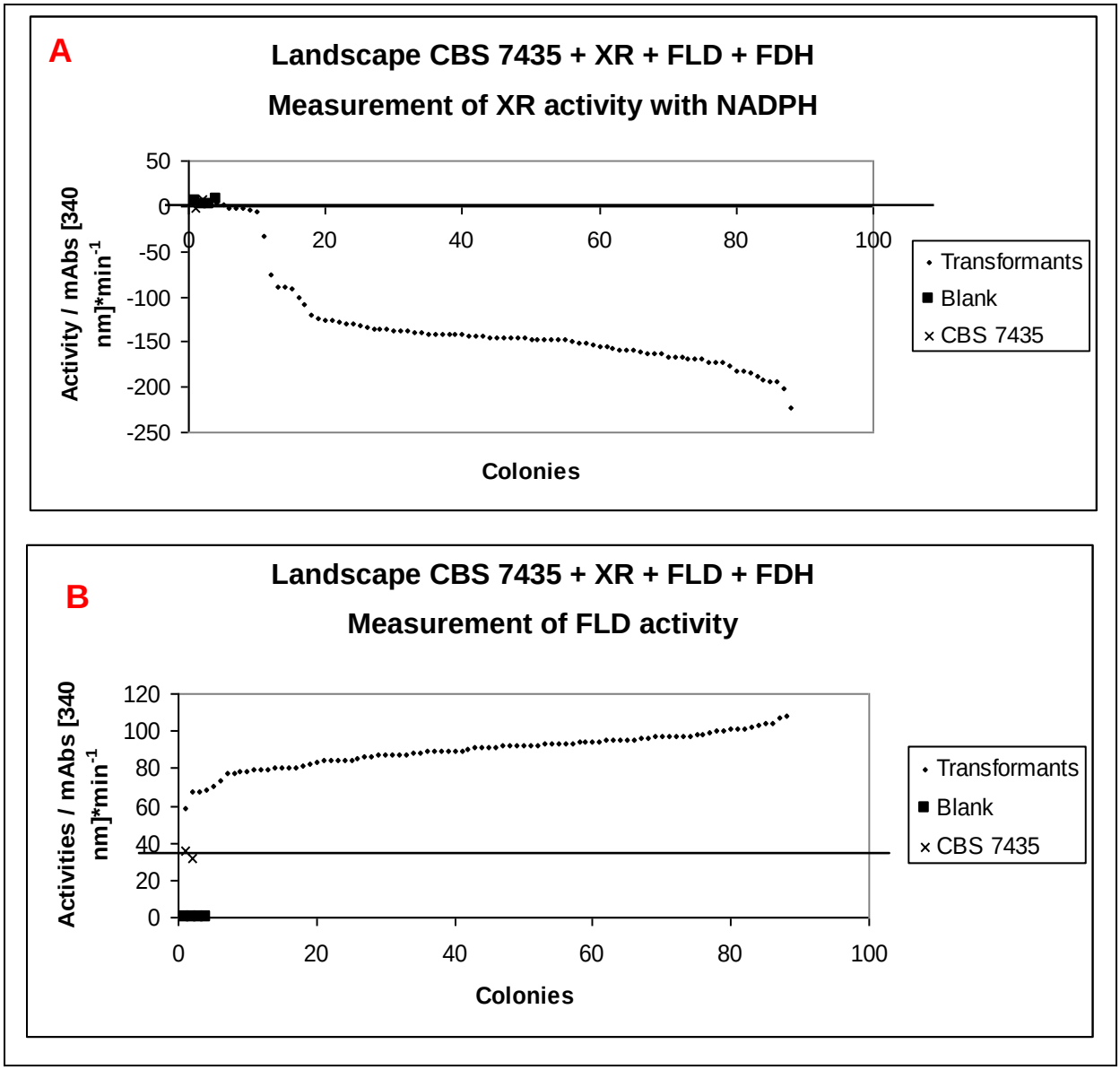

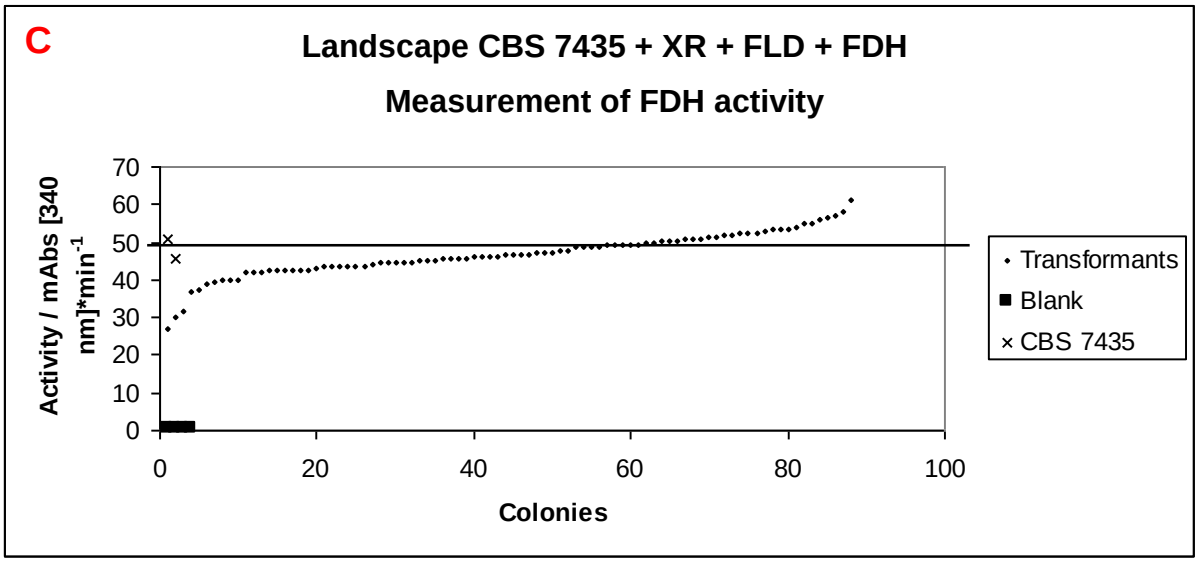

Figure 29: Landscapes of *P. pastoris* CBS 7435 transformants with over-expressed XR, FLD and FDH. Square dots mark the sterile controls of the cultivations. The x-shaped dots mark the activities of the wild type strain *P. pastoris* CBS 7435 and are visualized through the extended black lines. **A:** Measurement of XR activity with NADPH. **B:** Measurement of FLD activity. **C:** Measurement of FDH activity.

The results are very similar to the results of the BDH strains. Again, the measurement of FLD showed high activities throughout all transformants, while the activities of FDH are in range of the wild type CBS 7435.

According to the already established procedure, the strains with the highest combined activities of all three screenings were chosen for a re-screen. The priority of this breakdown was on the enhanced MUT activities.

5.3.2 *P. pastoris* CBS 7435 MUT + XR-M over-expression strains

The host strain *P. pastoris* CBS 7435 is over-expressed with the mutant of xylose reductase, which has a high acceptance for NADH as a cofactor for biotransformation. Therefore, all activity screenings were done with NADH.

In case of the co-expression of XR-M, FLD and FDH, the strain was also measured with NADPH as a cofactor to obtain a direct comparison between both activity screens.

Co-expression of XR-M and FLD

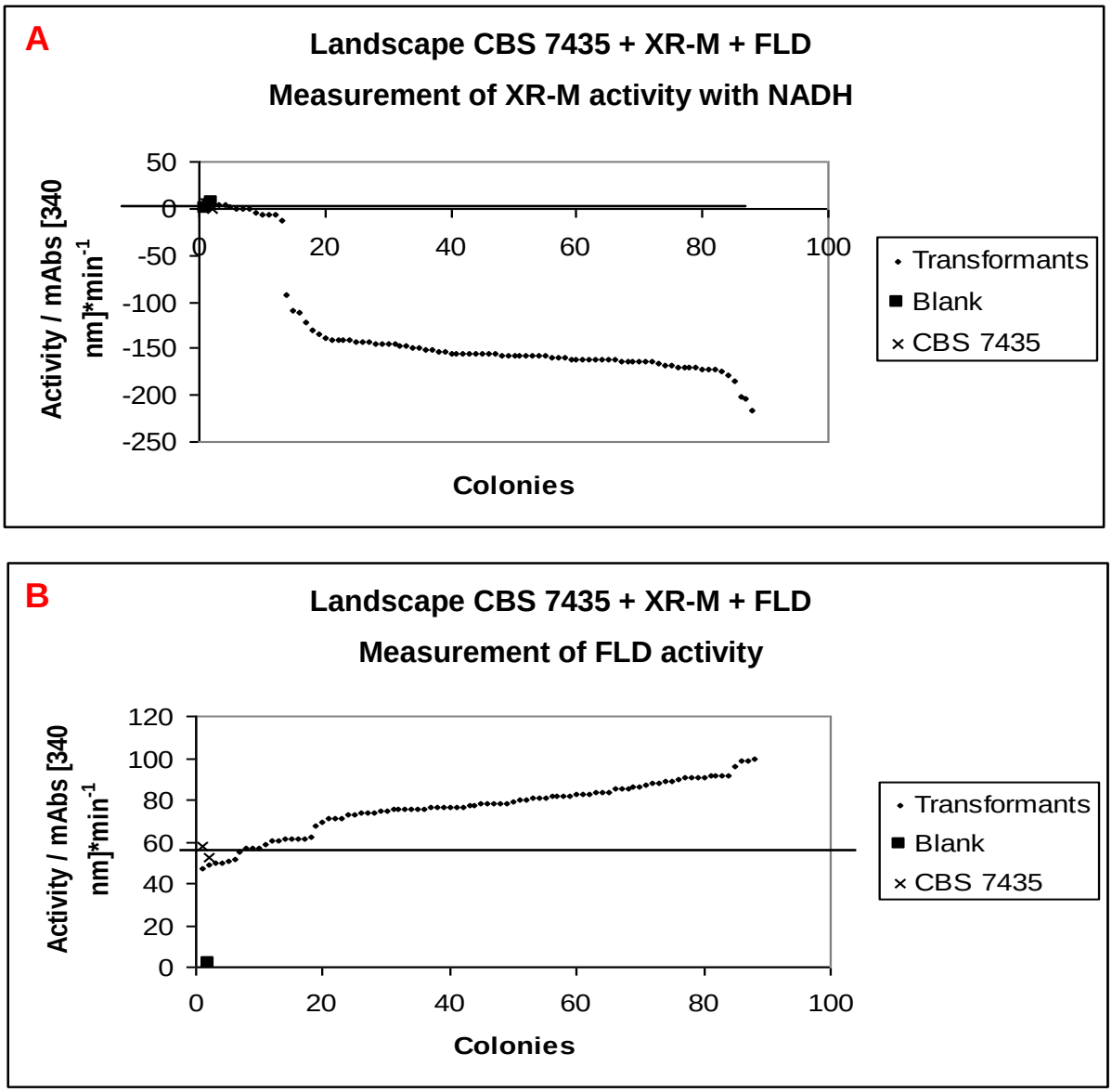

Figure 30: Landscapes of *P. pastoris* CBS 7435 transformants with over-expressed XR-M and FLD. Square dots mark the sterile controls of the cultivations. The x-shaped dots mark the activities of the wild type strain *P. pastoris* CBS 7435 and are visualized through the extended black lines. **A:** Measurement of XR-M activity with NADH. **B:** Measurement of FLD activity.

Co-expression of *XR-M* and *FDH*

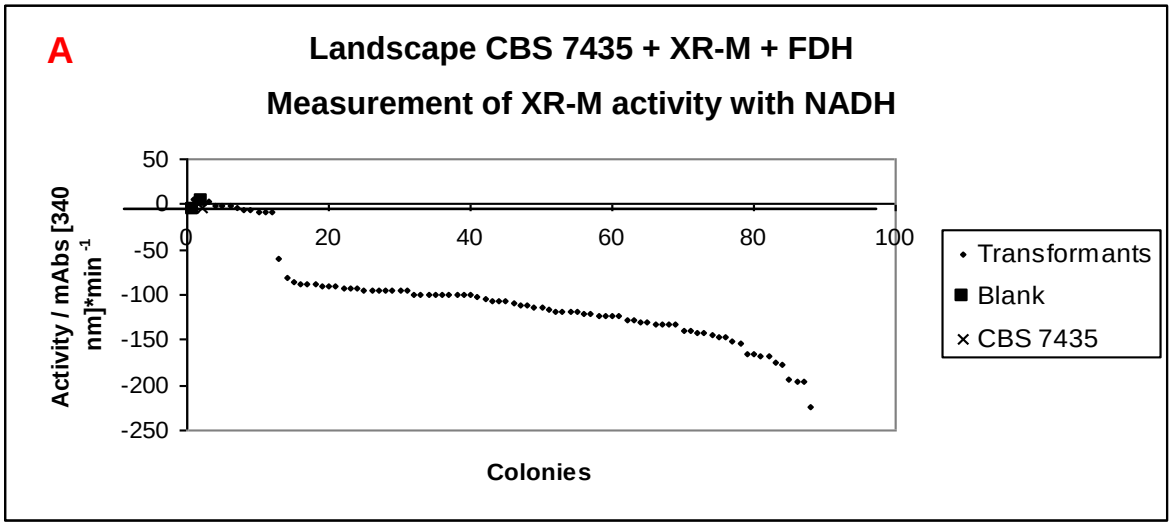

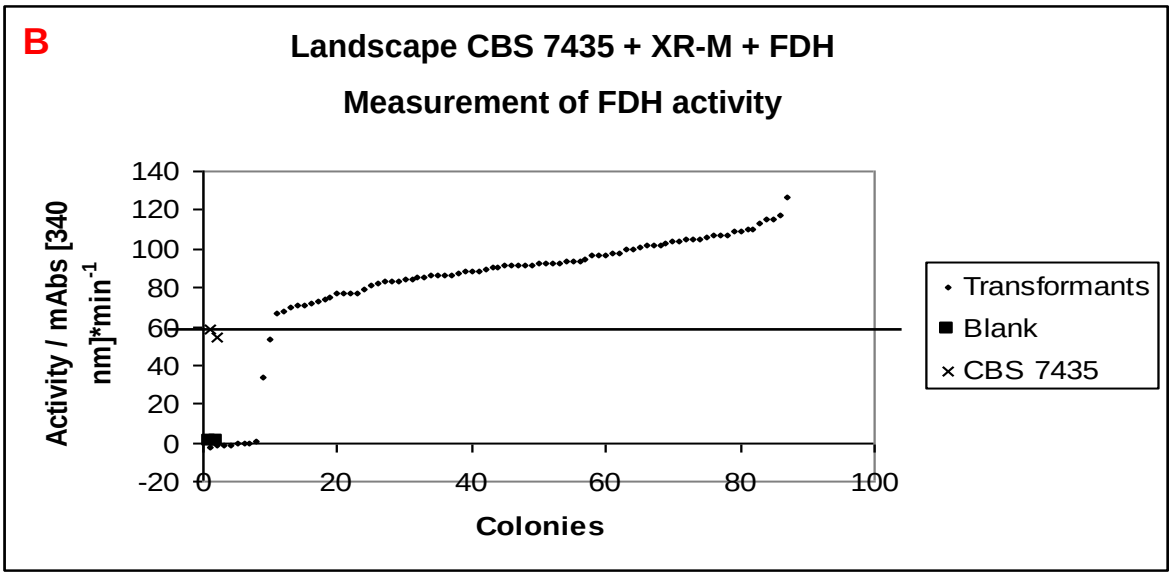

Figure 31: Landscapes of *P. pastoris* CBS 7435 transformants with over-expressed XR-M and FDH. Square dots mark the sterile controls of the cultivations. The x-shaped dots mark the activities of the wild type strain *P. pastoris* CBS 7435 and are visualized through the extended black lines. **A:** Measurement of XR-M activity with NADH. **B:** Measurement of FDH activity.

Co-expression of XR-M, FLD + FDH

The produced strain was measured for XR activity once using NADPH as the cofactor for the reaction and once using NADH. A direct comparison of both strains showed very similar results.

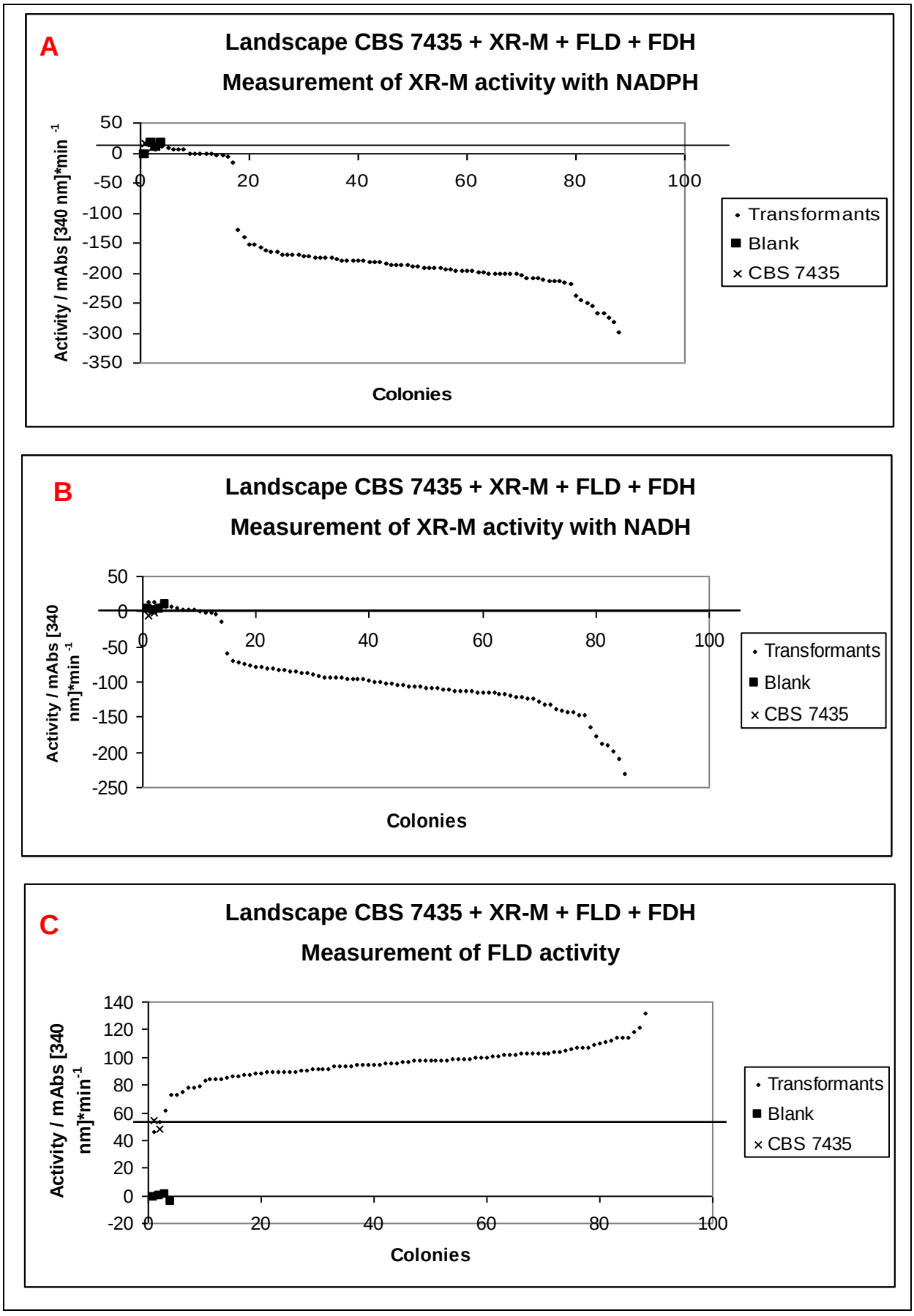
A
Landscape CBS 7435 + XR-M + FLD + FDH
Measurement of XR-M activity with NADPH
Activity / mAbs [340 nm]*min -1
50
0
-50
-100
-150
-200
-250
-300
-350
0
20
40
60
80
100
Colonies
Transformants
Blank
CBS 7435
B
Landscape CBS 7435 + XR-M + FLD + FDH
Measurement of XR-M activity with NADH
Activity / mAbs [340 nm]*min -1
50
0
-50
-100
-150
-200
-250
0
20
40
60
80
100
Colonies
Transformants
Blank
CBS 7435
C
Landscape CBS 7435 + XR-M + FLD + FDH
Measurement of FLD activity
Activity / mAbs [340 nm]*min -1
140
120
100
80
60
40
20
0
-20
0
20
40
60
80
100
Colonies
Transformants
Blank
CBS 7435

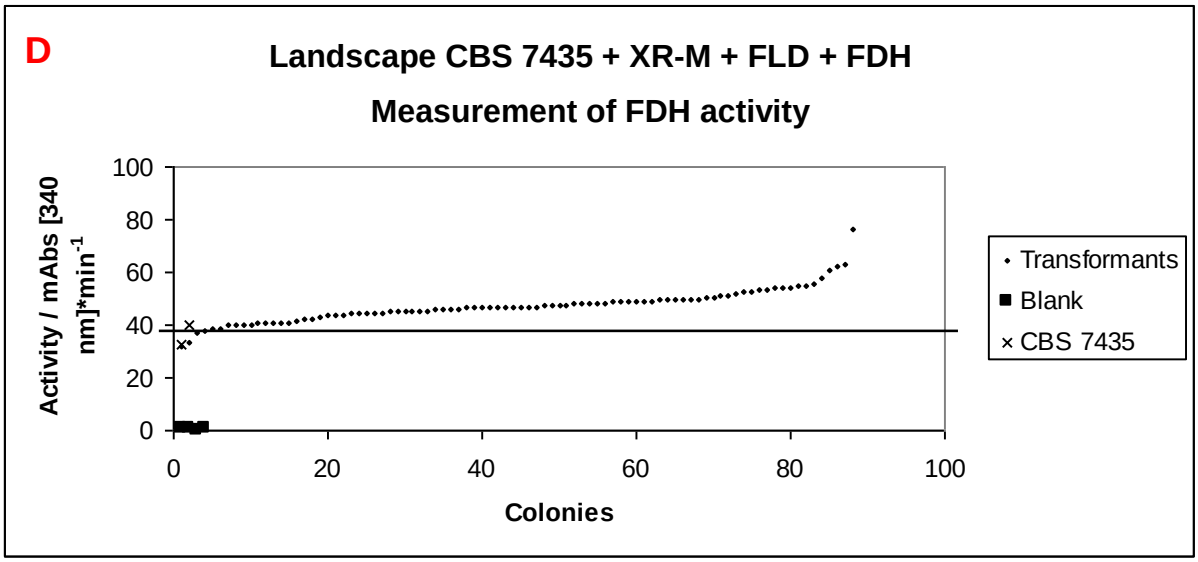

Figure 32: Landscapes of *P. pastoris* CBS 7435 transformants with over-expressed XR-M, FLD and FDH. Square dots mark the sterile controls of the cultivations. The x-shaped dots mark the activities of the wild type strain *P. pastoris* CBS 7435 and are visualized through the extended black lines. **A:** Measurement of XR-M activity with NADPH as cofactor. **B:** Measurement of XR-M activity with NADH as cofactor. **C:** Measurement of FLD activity. **D:** Measurement of FDH activity.

Comparing the measurements for XR-M activity with cofactor NADH and NADPH, both Landscapes are very similar to each another. The activities are all in the same range and the curves look alike.

For FDH activities, the results showed a steady enhancement compared to the wildtype.

5.3.3 *P. pastoris Δdas1das2* MUT + XR over-expression strains

According to the previous work on BDH, the implementation of the MUT enzymes into the *das1 das2* knock-out strain should result into an even more efficient platform strain. For a direct comparison a control strain of the Δ*das1das2* was picked in every DWP.

Over-expression of XR

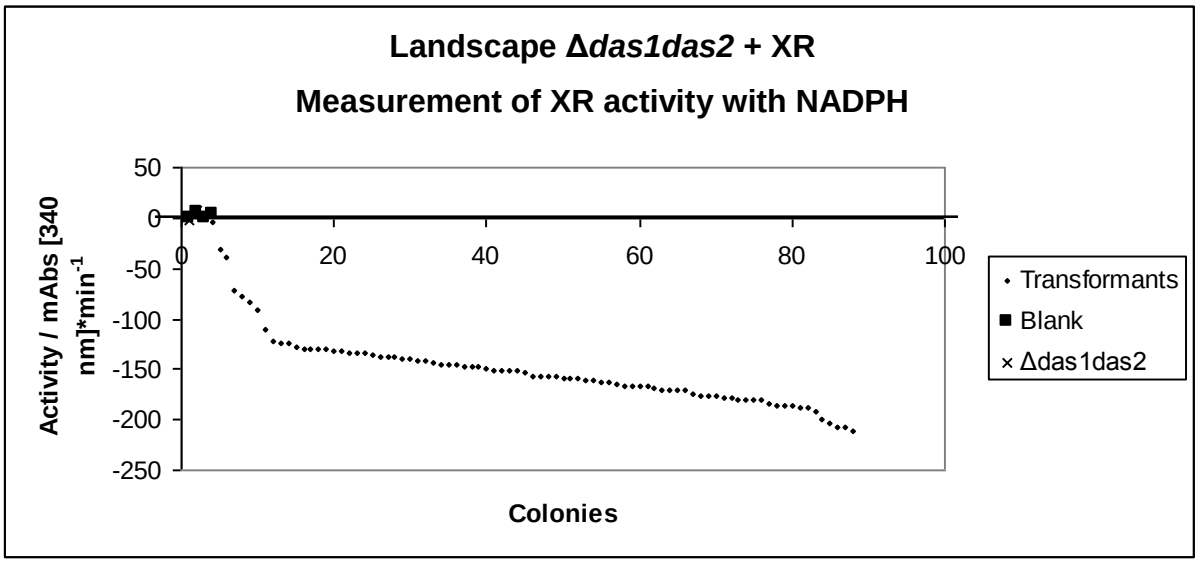

Figure 33: Landscape of *P. pastoris Δdas1das2* transformants with over-expressed XR. Square dots mark the sterile control of the cultivation. The x-shaped dots mark the activity of the host strain *P. pastoris Δdas1das2* and are visualized through the extended black line.

The results showed a very similar landscape to the results of the CBS 7435 wildtype strains. The *XR* activities of most transformants are in a narrow range with just a few outliners towards significant higher or lower activity.

Co-expression of FLD

Due to a lower rate of transformation, only 48 colonies instead of 88 were picked, cultivated and prepared for measurement.

After analysis, the results were ordered and depicted in following Figure 34:

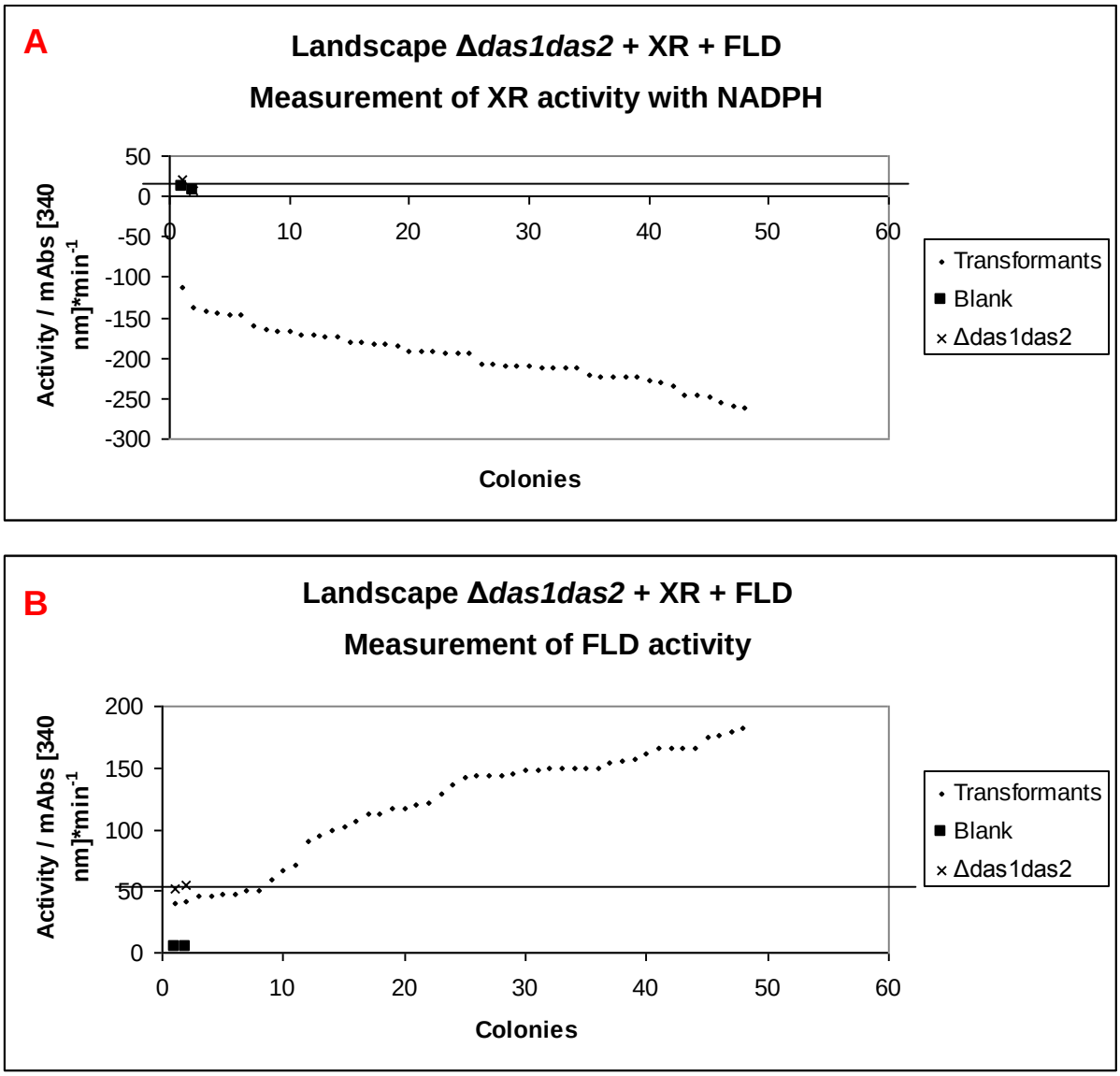

Figure 34: Landscapes of *P. pastoris Δdas1das2* transformants with over-expressed XR and FLD. Square dots mark the sterile controls of the cultivation. The x-shaped dots mark the activities of the host strain *P. pastoris Δdas1das2* and are visualized through the extended black lines. **A:** Measurement of XR activity. **B:** Measurement of FLD activity.

Screens of FLD + XR activity show suspected, yet interesting results. The XR activities range around the normal deviation of the host strain, whereas the FLD screen showed a known shape of the landscape with significant enhancements on most transformants.

Co-expression of FDH

Transformation rates of FDH + XR co-expression showed again normal quantities.

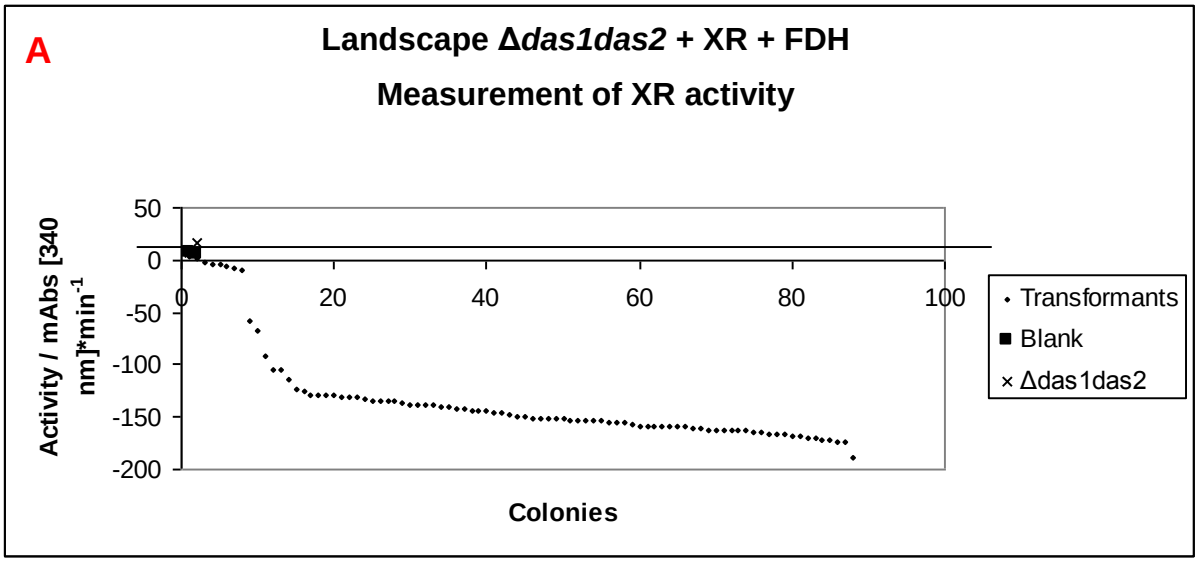

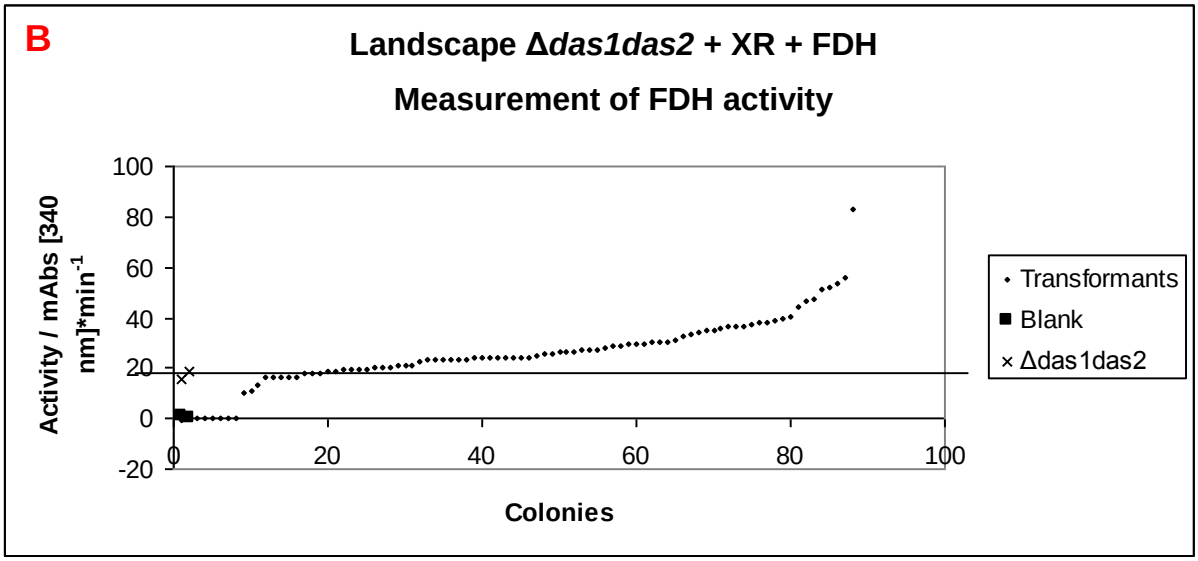

Figure 35: Landscapes of *P. pastoris Δdas1das2* transformants with over-expressed XR and FDH. Square dots mark the sterile controls of the cultivation. The x-shaped dots mark the activities of the host strain *P. pastoris Δdas1das2* and are visualized through the extended black lines. **A:** Measurement of XR activity. **B:** Measurement of FDH activity.

The activity screening of XR resulted in a more distinctive shape. The transformants are in a much narrower spectrum around the host strain.

Screening of FDH activity resulted in about the same landscape as the previous strain.

Co-expression of XR, FLD and FDH

The co-expression of both MUT enzymes and XR

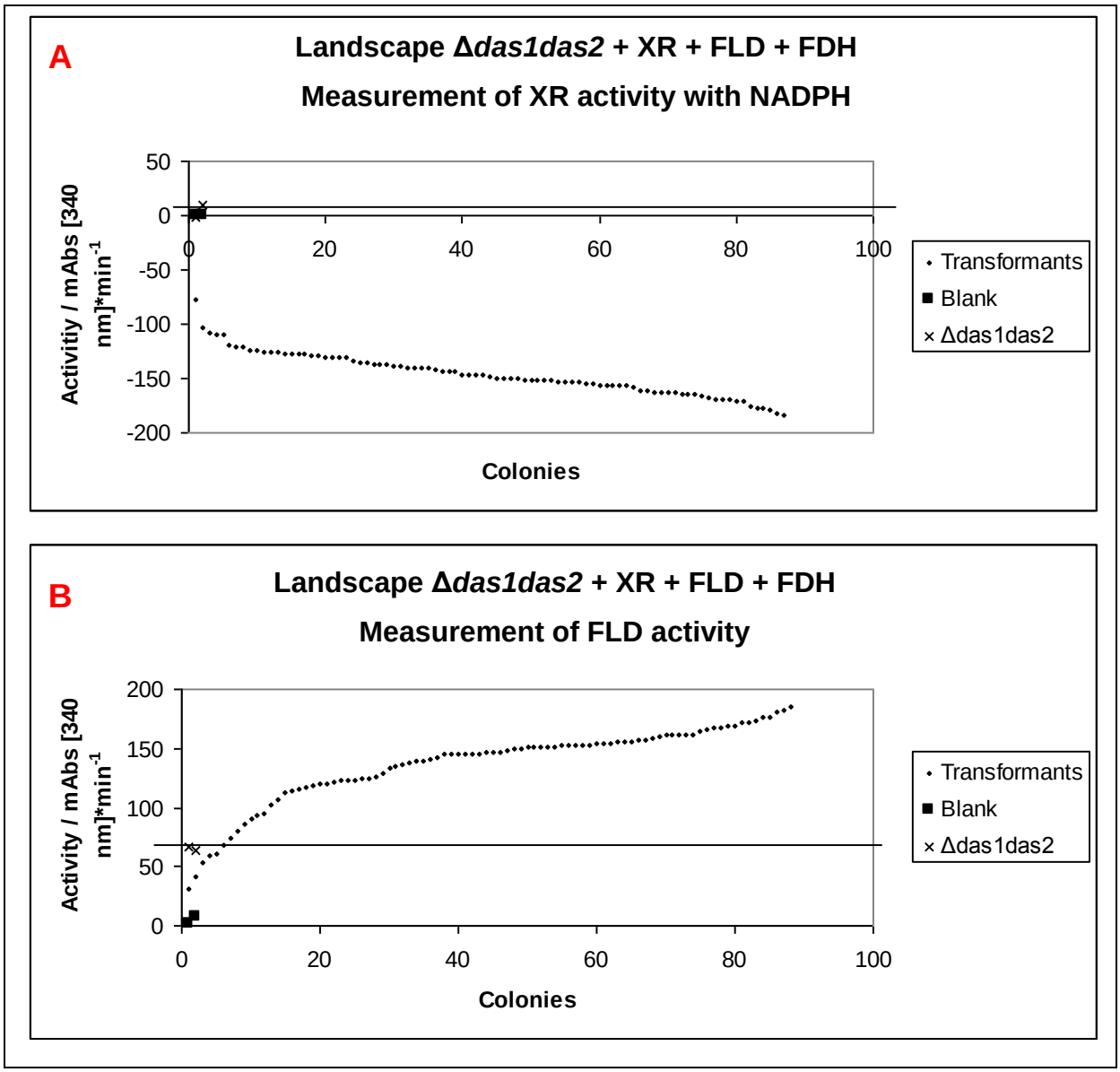

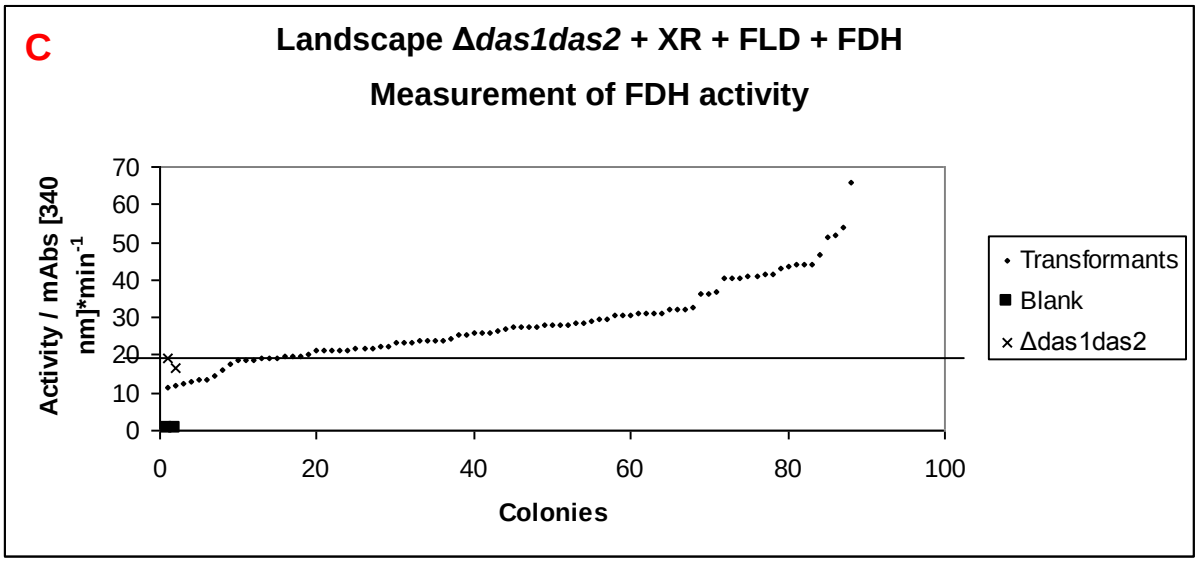

Figure 36: Landscapes of *P. pastoris Δdas1das2* transformants with over-expressed XR, FLD and FDH. Square dots mark the sterile controls of the cultivation. The x-shaped dots mark the activities of the host strain *P. pastoris Δdas1das2* and are visualized through the extended black lines. **A:** Measurement of XR activity with NADPH. **B:** Measurement of FLD activity. **C:** Measurement of FDH activity.

Activity measurements of all three enzymes showed transformants with enhanced activities of all three respective enzymes.

5.3.4 *P. pastoris Δdas1das2* MUT + XR-M over-expression strains

Combination of *Δdas1das2* strains with the XR mutant strains.

Over-expression of XR-M

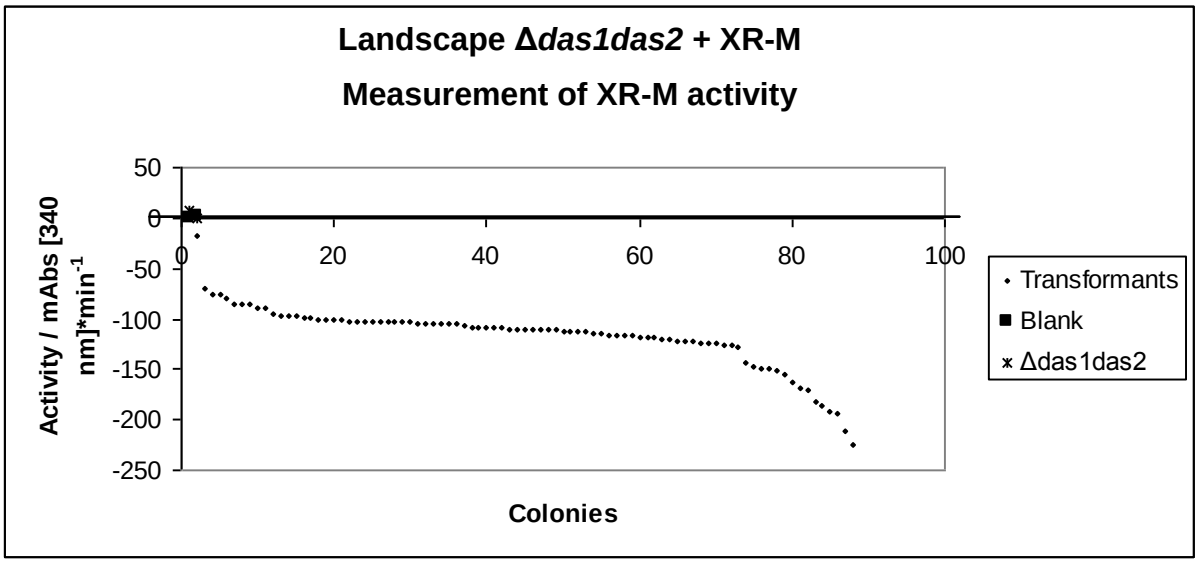

Figure 37: Landscape of *P. pastoris Δdas1das2* transformants with over-expressed XR-M. Square dots mark the sterile control of the cultivation. The x-shaped dots mark the XR-M activity of the host strain *P. pastoris Δdas1das2* and are visualized through the extended black line.

Co-expression of FLD

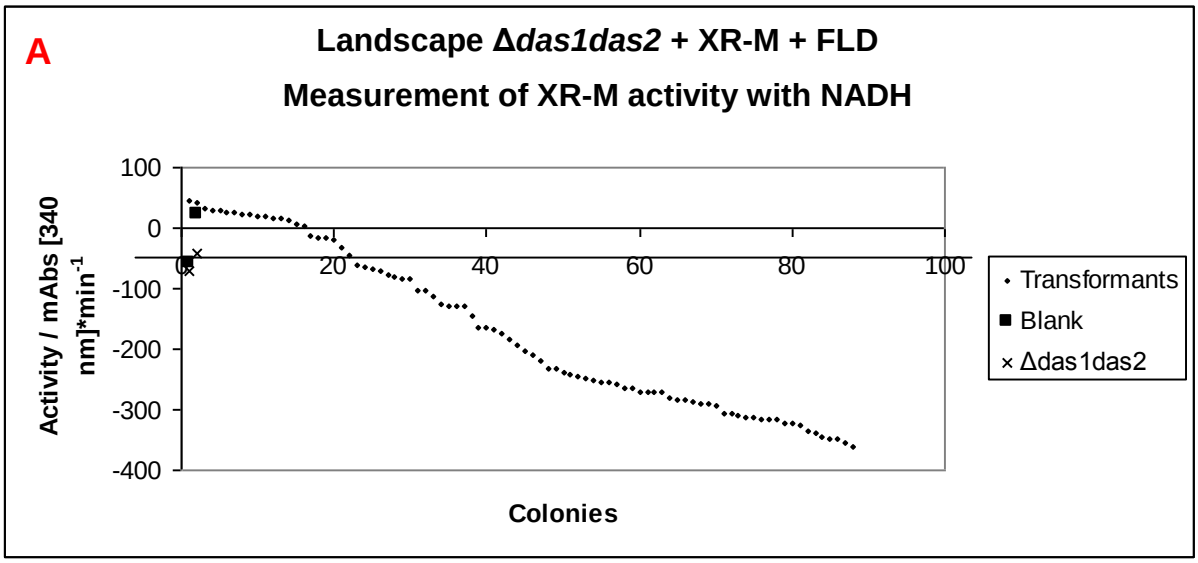

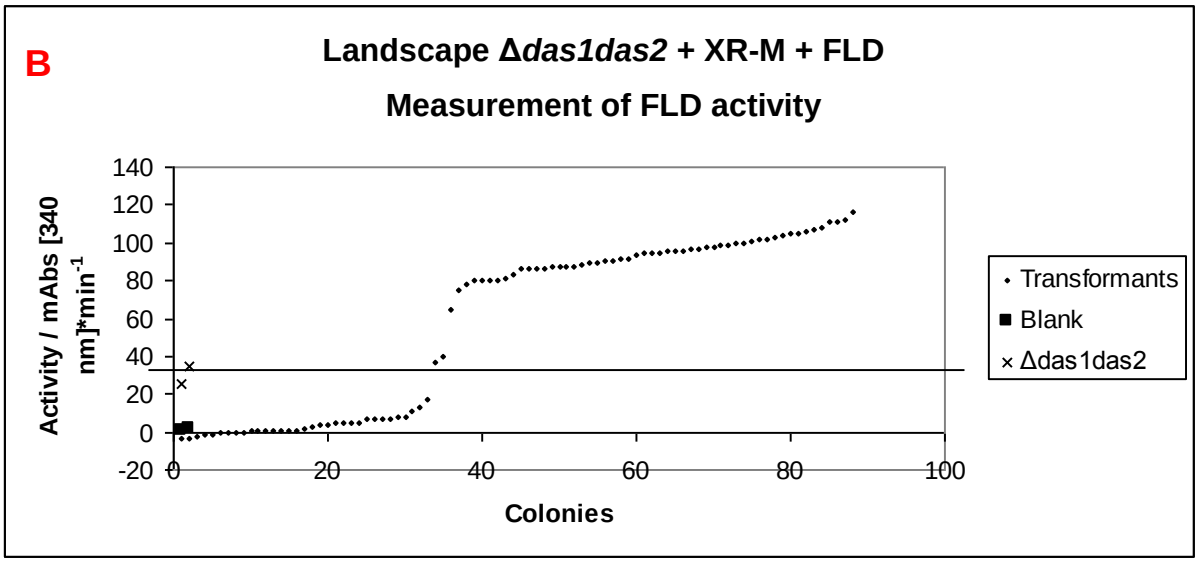

Figure 38: Landscapes of *P. pastoris Δdas1das2* transformants with over-expressed XR-M and FLD. Square dots mark the sterile controls of the cultivation. The x-shaped dots mark the activities of the host strain *P. pastoris Δdas1das2* and are visualized through the extended black lines. **A:** Measurement of XR-M activity with NADH. **B:** Measurement of FLD activity.

Interesting in these landscapes are the transformants showing a lower acivity than the regular Δ*das1das2* strains. Due to the possible presence of MeOH, these transformants maybe already compensate the NADH consumption of the system.

Co-expression of FDH

Same results as discussed before.

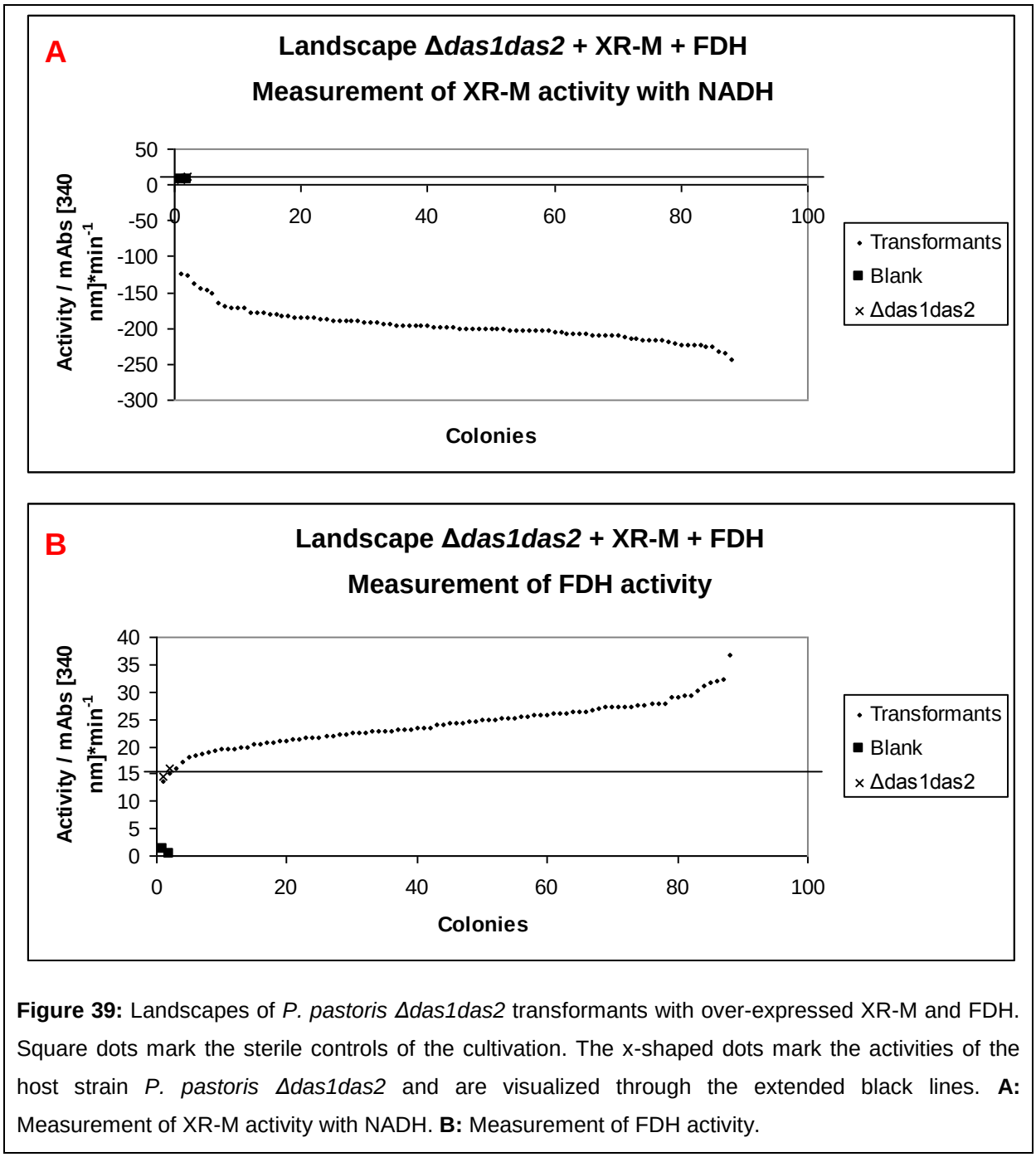

Figure 39: Landscapes of *P. pastoris Δdas1das2* transformants with over-expressed XR-M and FDH. Square dots mark the sterile controls of the cultivation. The x-shaped dots mark the activities of the host strain *P. pastoris Δdas1das2* and are visualized through the extended black lines. **A:** Measurement of XR-M activity with NADH. **B:** Measurement of FDH activity.

Co-expression of FLD and FDH

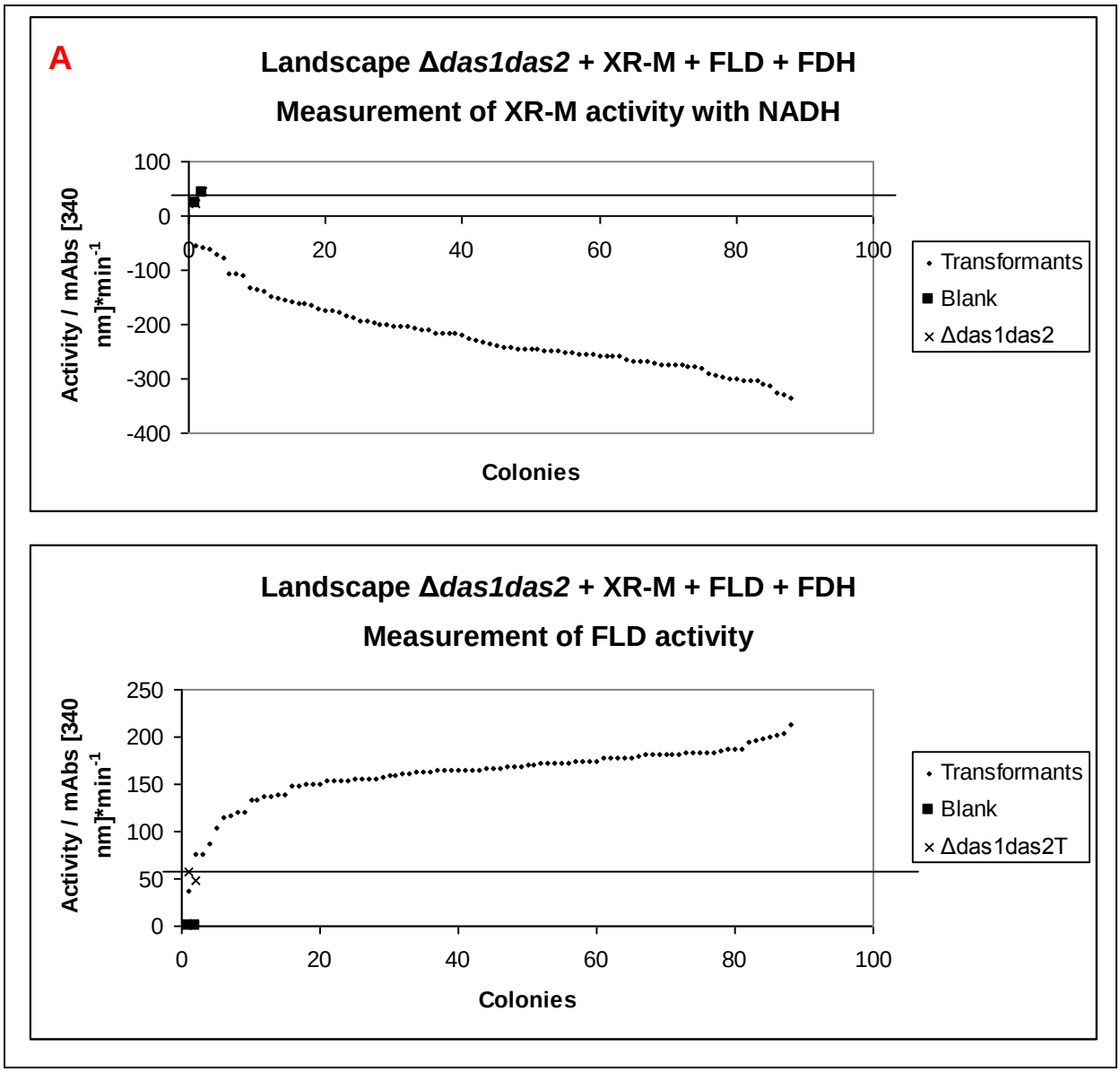

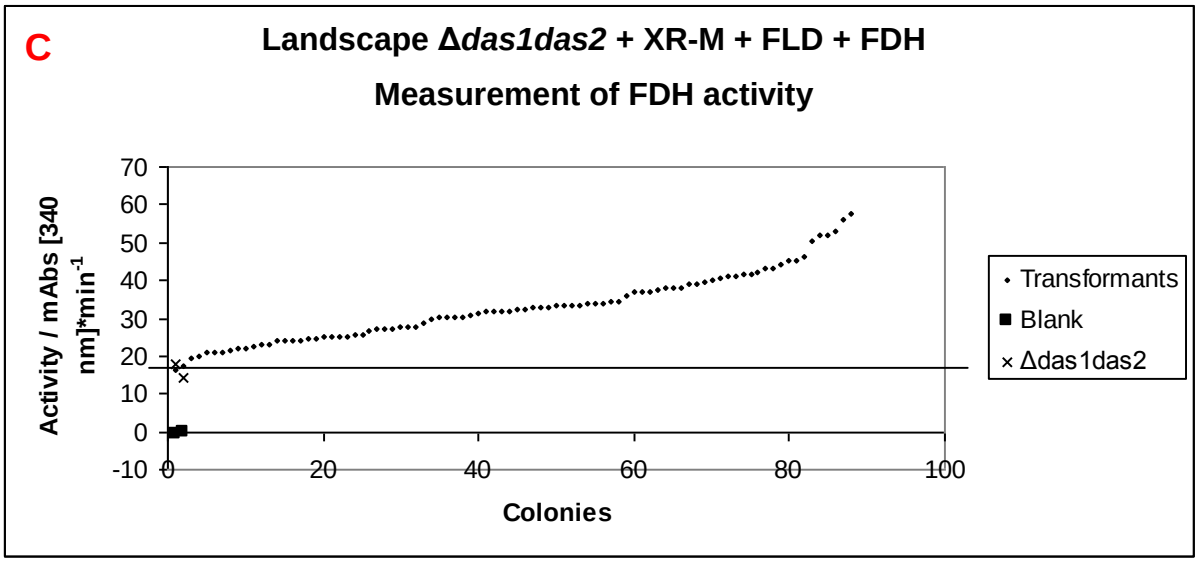

Figure 40: Landscapes of *P. pastoris Δdas1das2* transformants with over-expressed XR-M, FLD and FDH. Square dots mark the sterile controls of the cultivation. The x-shaped dots mark the activities of the host strain *P. pastoris Δdas1das2* and are visualized through the extended black lines. **A:** Measurement of XR-M activity with NADH. **B:** Measurement of FDH activity. **C:** Measurement of FLD activity.

5.3.5Final discussion

P. pastoris CBS 7435 as a host

The FLD and FDH activity screenings showed the expected results with significant enhancements in both cases. The re-screens of the overall best performing strains supported and confirmed the screening results and led to the conclusion, that the over-expression of the targeted strains was successful.

The obtained activity landscapes showed typical characteristics with the majority of the transformants in about the range of the host strain, as well as some with significant higher or lower activities. In case of the XR and XR-M strains, their significant enhanced ability reduce xylose ranged in a quite tight spectrum with just a few outlier showing significant differences in activity.

Activity screenings and re-screenings of XR and XR-M showed a highly active and efficient reduction of the substrate. Compared to the wyldtype host strain, which

provides xylose degradation only via the endogenous aldose reductase of *P. pastoris*, the engineered strains enhance the reduction of xylose with factor 200-300. Hence, the conversion of high amounts of substrate was easily achieved by the generated strains.

Re-screen proved the XR/-M activity in all of the chosen strains. The strain with the best combination of enhanced MUT activity and XR/-M activity was picked for further studies on behalf of whole-cell biotransformation done by Beate Pscheidt and Kirsten Schroer in bigger scale on 1,5 L bioreactors.

P. pastoris Δdas1das2 as a host

According to the previously discussed results of the CBS 7435 strains, the *Δdas1das2* transformants showed the same enhanced activities and likewise the same screening landscapes.

Comparison CBS 7435 ↔ *Δdas1das2*

Acording to the results with the BDH strains, a similar performance in terms of activity was expected. Due to the lack of the *DAS1* and *DAS2* the MUT pathway had to lead towards the dissimilation of MeOH resulting in CO_2.

Surprisingly, the results did not show any significant differences between both host strains in terms of relative activity. Based on the studies of this thesis it remains to be clarified if this effect is due to different expression levels of the reductase or if the different strain background indeed does not provide any advantages for the bioconversion since the availability of NADH is not the limiting factor.

Comparison XR ↔ XR-M

In terms of cell growth, lysis, preparation or overall handling, there are no differences between the strains with over-expressed XR and the ones with over-expressed XR-M.

In terms of cofactor dependency, the published results were confirmed.

Whole-cell biotransformations

Even though all the screening work was done with the crude cell extract due to reasons of time management, the focus of these experiments lied in the adaptation as a platform for whole-cell biotransformations.
Sadly, the first experiments concerning the conversion rate of the whole-cell system showed an unidentified problem. Not any of the produced strains was capable of reproducing the conversion rates confirmed in-vitro.

Future perspectives

The screening results in this diploma thesis showed the successful over-expression of C. tenuis XR within the genome of *P. pastoris*. Sadly, the results of the first whole cell biotransformations were not nearly as promising.

Further studies on this topic may concern the occurring problem in detail. It is yet not clear, why exactly the biotransformations result in such low conversion rates or non at all. Segregation of the enzyme, as well as the transport mechanisms of the substrate xylose are unresolved issues.

The studies on the XR as well as the mutant of same enzyme showed the advantages, but also the limitations of this platform. Although the screening proved efficient XR activities on both cofactors in the mutant strains, all strains had their limitations depending the whole cell biocatalysis.

Interestingly, *P. pastoris* has an endogenous aldose reductase, theoretically capable of converting xylose [10]. Therefore, another study of interest could be the over-expression and further analysis of this enzyme and the comparison to the already established XR.

Still, many interesting redox biocatalysts deed NADPH and therefore a platform for the regeneration of both nicotine cofactors would be a desirable improvement to the platform. Hence, the further work in this thesis deals with the engineering of *P. pastoris* FDH for enhanced regeneration of NADPH.

6 Cofactor dependency of FDH

6.1 Strategy description

The *P. pastoris* endogenous cofactor regeneration employing the methanol utilization pathway is expected to be strictly NAD+ dependent. Many oxidoreductases, however, are solely NADPH dependent. Consequently, another main topic of this diploma thesis focuses on two different engineering approaches to establish an efficient NADPH recycling in *P. pastoris*. Therefore*, P. pastoris* (*FDH*) was chosen as a model enzyme to engineer for enhanced cofactor acceptance of NADP*.

As mentioned before in chapter 1.3.2, Former studies showed the superiority of FDH as a NAD+ dependent cofactor regeneration system due to different reasons such as the wide pH-optimum of catalysis, the low cost of regeneration enzyme as well as substrate, and the high processing stability combined with the maximum yield of target product.

Previous published work on this topic [20, 21] showed a successful adaptation by site directed mutagenesis of one or two specific amino acids within the Rossman fold of the *S. cerevisiae* FDH. The exchange of specific amino acids in this area leads to a different acceptance of NADH, or NADPH respectively, due to steric effects at the cofactor binding site. Through a high FDH sequence similarity (77% aa) between both yeast, namely *S. cerevisiae* and *P. pastoris*, a similar approach seems promising.

The Rossman fold structural motif consisting of three or more parallel β-strands and linked together by two α-helices is the binding site for the two nicotine cofactors on the surface of the FDH enzyme. (See Figure 41 A - C)

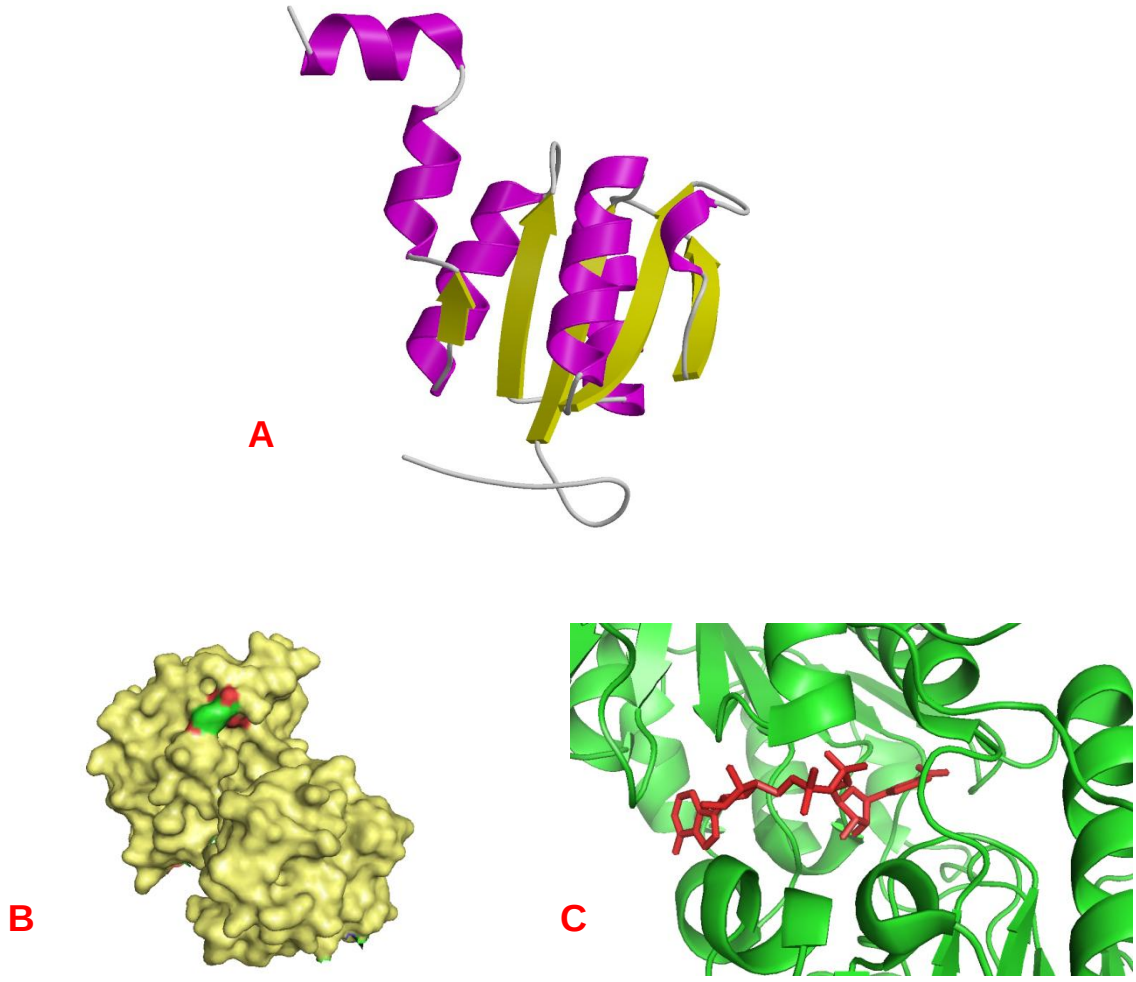

Figure 41 A: Schematic view of a typical Rossman fold **B:** Surface of *P.pastoris* FDH. Marked in green (C-atoms) and red (O-Atoms) are the sidechaines of residue D195 and Y196. **C:** Magnification of NAD^+ (marked in red) binding site in *P. pastoris* FDH

Structural analysis of *Pp*FDH was done by modeling of the crystal structure with the online available software pHyre (See chapter 3.4)

Using the FDH structure model as a starting point and comparing it with the analyzed structures to the available data, two hotspots, namely D195 and Y196 would have a dramatic effect in terms of size and shape of the cofactor binding pocket of the enzyme. Since, an amino acid substitution towards smaller residues at these positions could greatly improve the acceptance of NADP+ compared to the wildtype enzyme.

Therefore, a set of strains harboring different mutations, which are listed on Table 29 were constructed. Furthermore, a screening employing site saturation mutagenesis

of the hotspots should provide additional insight of the binding area and clones with higher acceptances.

6.2 Experimental

6.2.1 Identification of genes of interest

The DNA sequence of *P. pastoris* FDH was the same as in previous chapter 4.2.1.

6.2.2 Construction of *P. pastoris* strains with enhanced NADPH acceptance

Table 29 shows in detail the *P. pastoris* strains produced in the course of these studies.

Table 29: Constructed *P. pastoris* strains

Host strain	FDH mutations	Method
P. pastoris CBS 7435	Random mutation at position 195 and 196	Site-saturated mutagenesis
	D195A, Y196R	Two-step PCR (QuikChange™)
Δdas1das2 (D12-B1H)	D195A, Y196R	Two-step PCR (QuikChange™)

The experiment on the (semi-)rational design of D195Y-Y196R-FDH was conducted to target, cultivate and analyze 88 transformants on a DWP. Site-saturated mutagenesis on positions 195 and 196 was designed for a statistically firmness of over 95% and therefore targeted 3608 transformants on 41 DWPs.

6.2.3 Generation of expression cassettes

Two-step PCR

For generation of the FDH double mutant (FDHdMut), a two-step PCR was performed according to in house SOP AA.04. (Stratagene *QuikChange*™)

Table 30: Standard composition of two-step PCR

	Name	Concentration	Volume
Template	3,2-8 Kan FDH	5 ng/µL	1 µL
Buffer	Pfu Reaction Buffer 10x	1x	5 µL
Primer	P08-801 or P08-802	10 pmol/µL	1,5 µL
dNTPs	dNTP Mix	10 mM	1 µL
Polymerase	*PfuTurbo*®	2,5 U/µL	1 µL
ddH_2O			40,5 µL
Σ			50 µL

Thereafter followed the first PCR cycle as described in following Table 31

Table 31: Program used in the 1st step of two-step PCR

Temperature	Time	
95°C	60 sec	
95°C	50 sec	repeat for 4 cycles
60°C	50 sec	
72°C	5 min	
72°C	7 min	
4°C	∞	

After cooling down of the product, the 2nd step was initiated by mixing of 25 µL of the product amplified with the forward primer and 25 µL of the product with the reverse primer. This mixture was again put into the thermocycler with a prolonged program.

Table 32: Program used in the 2nd step of two-step PCR

Temperature	Time	
95°C	60 sec	
95°C	50 sec	repeat for 18 cycles
60°C	50 sec	
72°C	5 min	
72°C	7 min	
4°C	∞	

2 µL of *Dpn*I restriction enzyme was added and the PCR product was digested for two hours. Afterwards, the DNA purification was done via QIAquik Kits according to the standard protocol and the DNA was eluted in 30 µL ddH_2O.

Ligation into shuttle vector

After purification and determination of the product via gel electrophoresis, the PCR products of the single and double mutated variants were digested with *Eco*RI and *Not*I according to the producer´s manual. The following ligation step into the *E. coli / P. pastoris* shuttle vector was performed according to previously described method. (See chapter 3.8.3)

Site-saturated mutagenesis

A non rational approach was followed by SSM. The obtained expression cassette was obtained via OE-PCR and directly used for *P. pastoris* transformation, in order to avoid a loss of diversity during DNA amplification in *E. coli* prior to transformation into *P. pastoris.*

Two Primers regarding the expression cassette were kindly provided by Alexander Gutmann, [25] the template was the already existing 3,2-8 Kan vector with the FDH insert previously described in chapter 4.2.3. OE-Primers were designed for random

mutagenesis on positions 195 and 196 of enzyme changing the codons to random combination NNK. (see Figure 42)

OE-PCR was done after standard protocol.

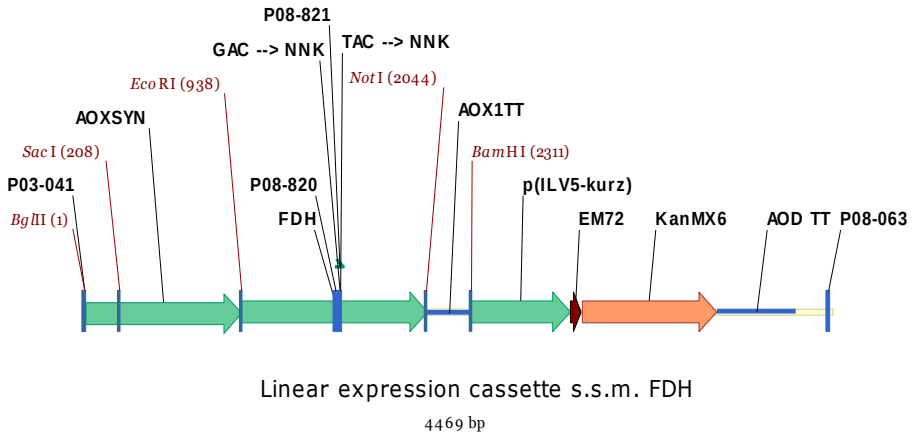

Figure 42: Schematic view of the linear expression cassette of FDH

After linearizion of the template plasmid and amplification of the two fragments, the linear cassette, including promoter region and Geneticin resistance information for usage as selection marker as well as the terminator region was amplified via OE-PCR. (see Figure 42 and Figure 43)

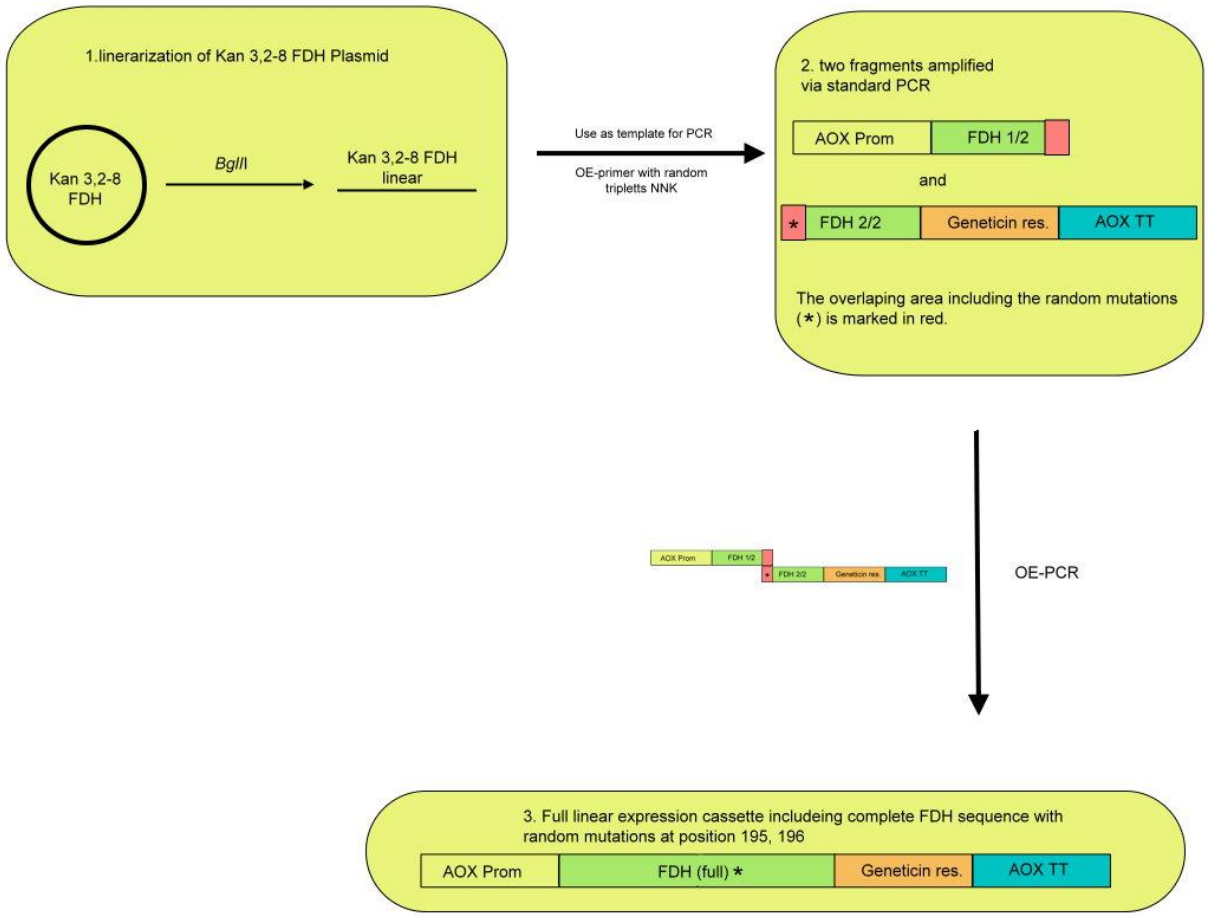

Figure 43: Simplified construction scheme of the linear FDH expression cassette

DNA purification was done via QIAquik Kits according to the standard protocol and the DNA was eluted in 30 µL ddH_2O.

*6.2.4*Transformation into *P. pastoris*

For site-saturated mutagenesis, about 1 µg of the purified PCR product was directly used in *P. pastoris* transformation.

In case of the double mutant, the vectors were linearized with *Bgl*II and used for *P. pastoris* transformations according to Lin-Cereghino *et al*. [45] In each transformation, about 1 µg of linearized vector DNA was used, which resulted in an average number of about 800 transformants per approach.

The transformants were selected on YPD/Geneticin (300 µg/mL)-agar plates and then cultivated in 96-well deep well plates as described earlier in 5.2.5 and assayed for increased NADP+ acceptance of *P. pastoris* FDH.

6.2.5Cultivation and induced protein expression

The cultivation of *P. pastoris* transformants in 96-well deep well plates following the standard protocol. For activity determination, the cells were disrupted with Y-Per® as described in 3.8.9.

For the FDHdMut variants, 88 transformants were cultivated, along with the wild type and host strains as depicted in Figure 14.

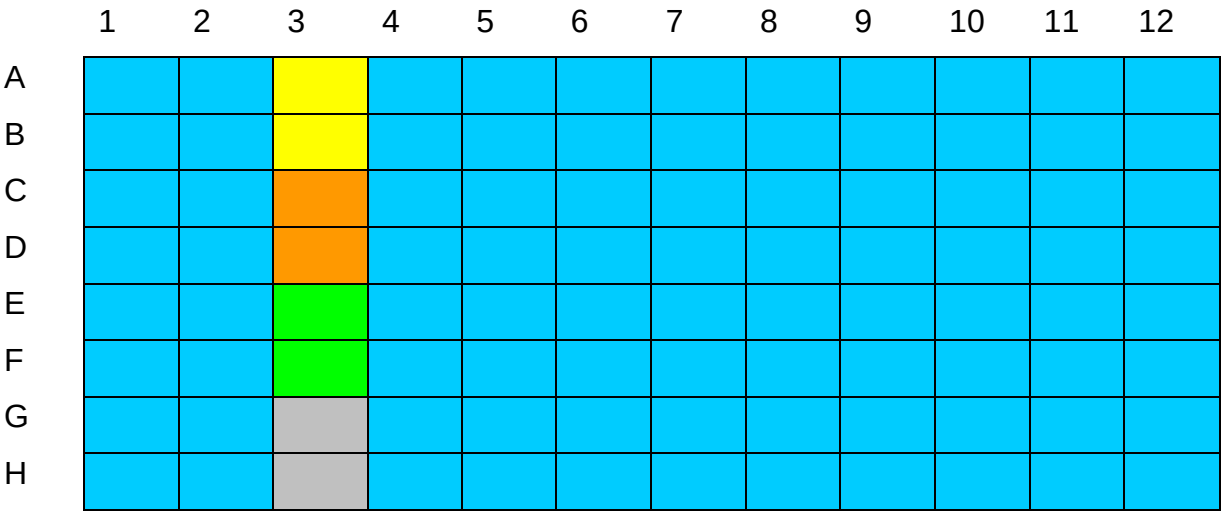

Figure 44: Schematic view of a 96-well deep well plate. Blue fields indicate a transformant, yellow and orange fields indicate one or two host strains. In the green fields, the correspondent wildtype was cultivated, while the grey fields were sterility control wells only filled with medium.

For the site-saturated mutagenesis, a larger number of about 3600+ transformants were targeted, but only 352 transformants could be analyzed due to a poor yield in transformation.

6.3 Results and discussion

6.3.1FDH double mutant

Over-expressed FDHdMut transformants were measured twice with NAD+ and NADP+ as cofactor. A previously produced strain of *Δdas1das2* + FDH was cultivated on the DWP for later comparison with mutated strains.

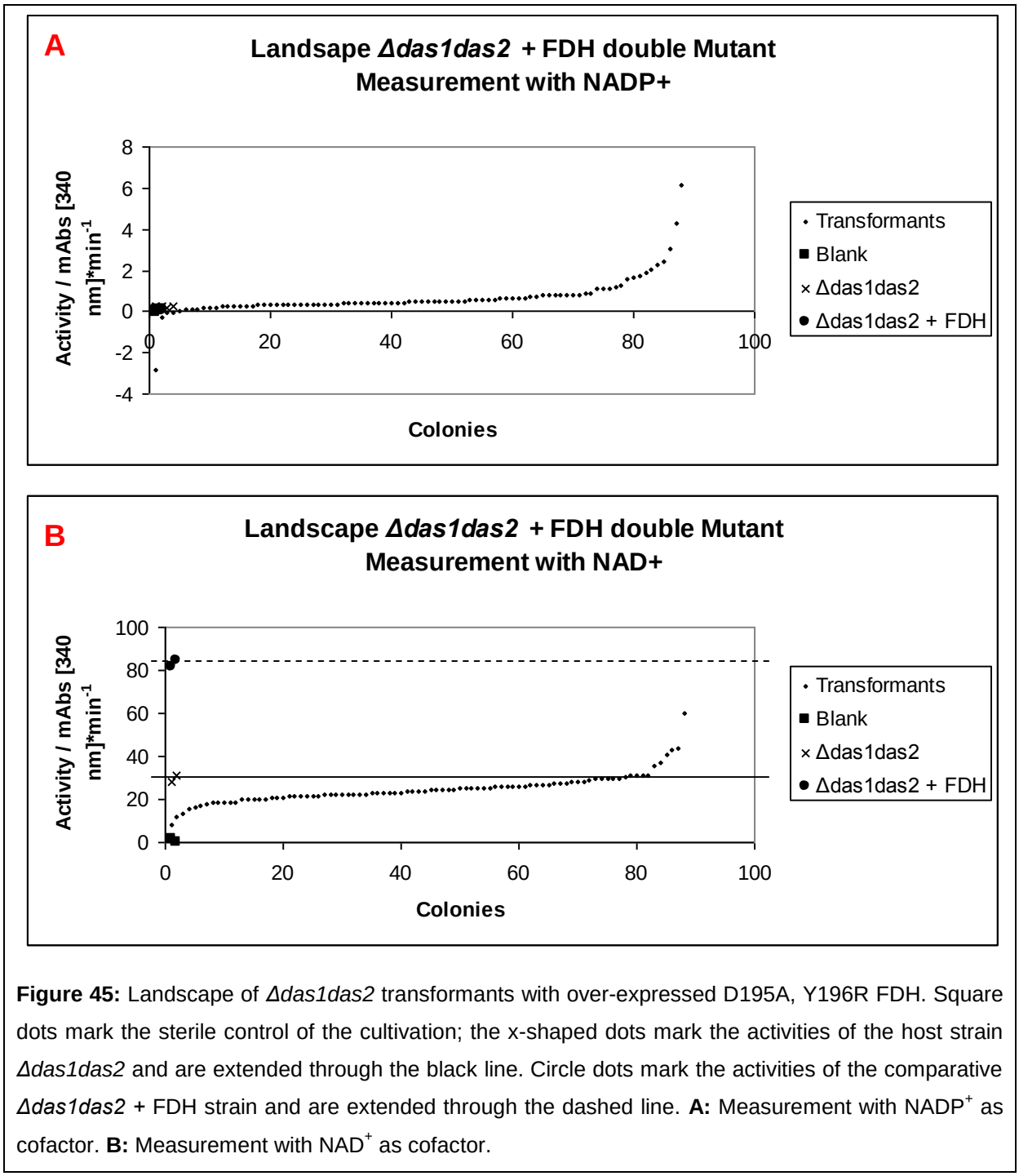

Figure 45: Landscape of *Δdas1das2* transformants with over-expressed D195A, Y196R FDH. Square dots mark the sterile control of the cultivation; the x-shaped dots mark the activities of the host strain *Δdas1das2* and are extended through the black line. Circle dots mark the activities of the comparative *Δdas1das2* + FDH strain and are extended through the dashed line. **A:** Measurement with $NADP^+$ as cofactor. **B:** Measurement with NAD^+ as cofactor.

The screening assay with NADP+ led to mediocre results. Although there are transformants with a significant enhancement on NADP+ acceptance relative to the host strain., the results are not in the same range as if they were done under normal circumstances (e.g. usage of NAD+).

Interestingly, the mutation on these specific amino acids has a tremendous effect on the FDH activities with NAD+. Almost all transformants perform worse in the screening than the correspondent host strain. Only a few outliner had enhanced activities, but then again, without reaching the same level as the over-expression of wildtype *P. pastoris* FDH.

6.3.2 Site-saturated mutagenesis of FDH

The transformation rate was lower as expected. Therefore, only 352 instead of the 3600 transformants could be measured for enhanced $NADP^+$ activity.

Following figures show the results of the activity assays.

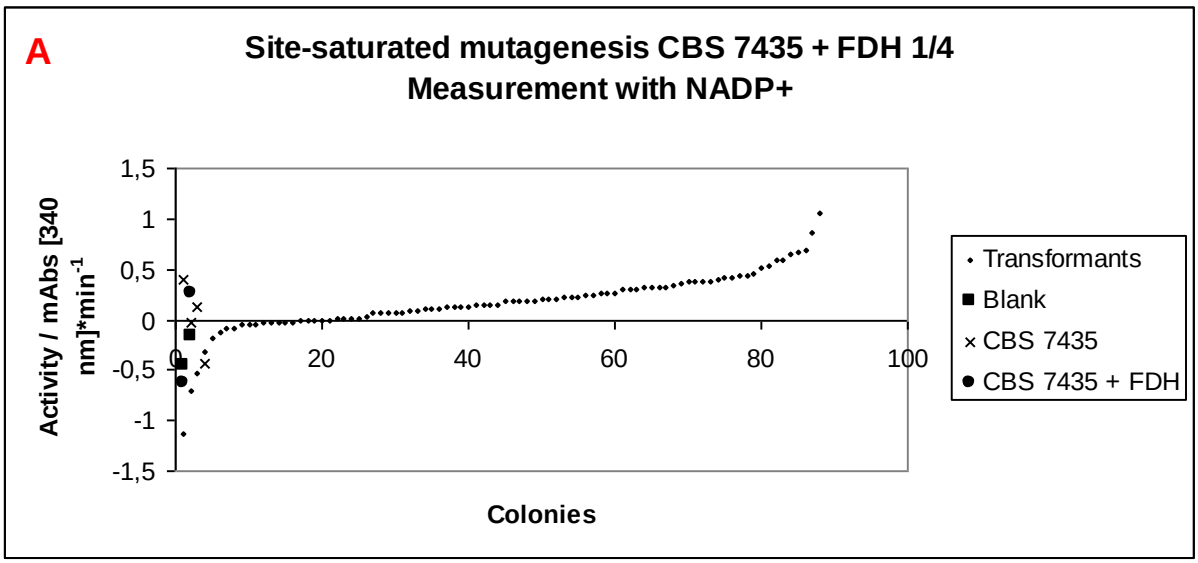

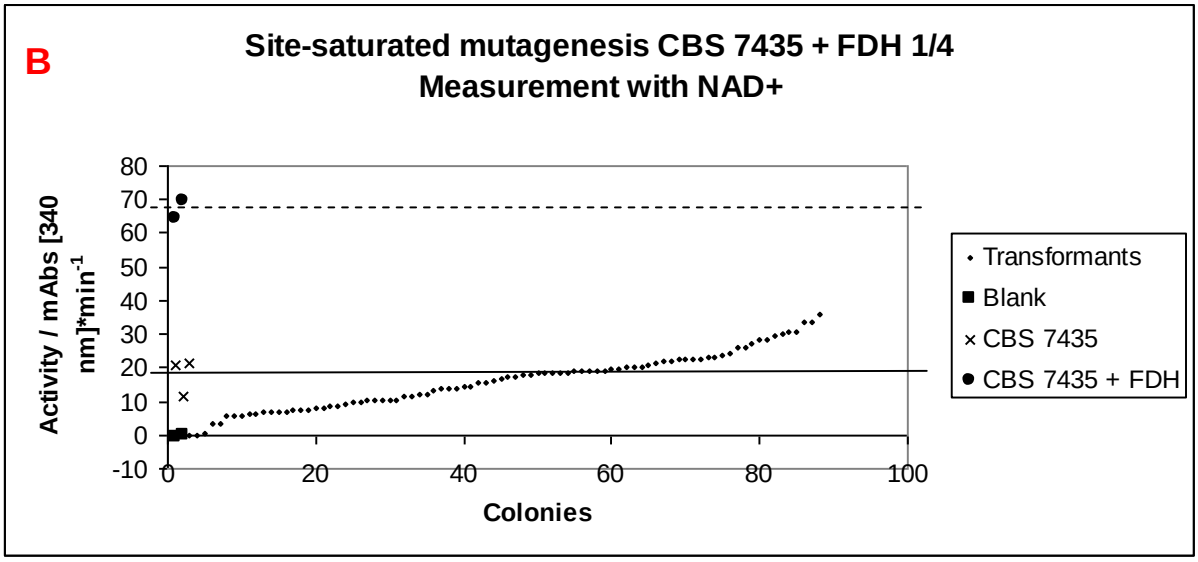

Figure 46: Landscape of CBS 7435 transformants with site-saturated mutagenesis on position 195 and 196 of *P. pastoris* FDH. Square dots mark the sterile control of the cultivation; the x-shaped dots mark the activities of the host strain CBS 7435 and are extended through the black line. Circle dots mark the activities of the comparative CBS 7435 + FDH strain and are extended through the dashed line. Figure 1 out of 4. **A:** Measurement with $NADP^+$ as cofactor. **B:** Measurement with NAD^+ as cofactor.

The measurement with NADP+ showed a slight enhancement compared to the host strain. However, all transformants range in about the standard derivation of the host strain activities and therefore this enhancement is not statistically firm.
Measurement with NAD+ led to the same results as discussed above with the (semi-) rational approach. The activities of all transformants are beneath the host strain.

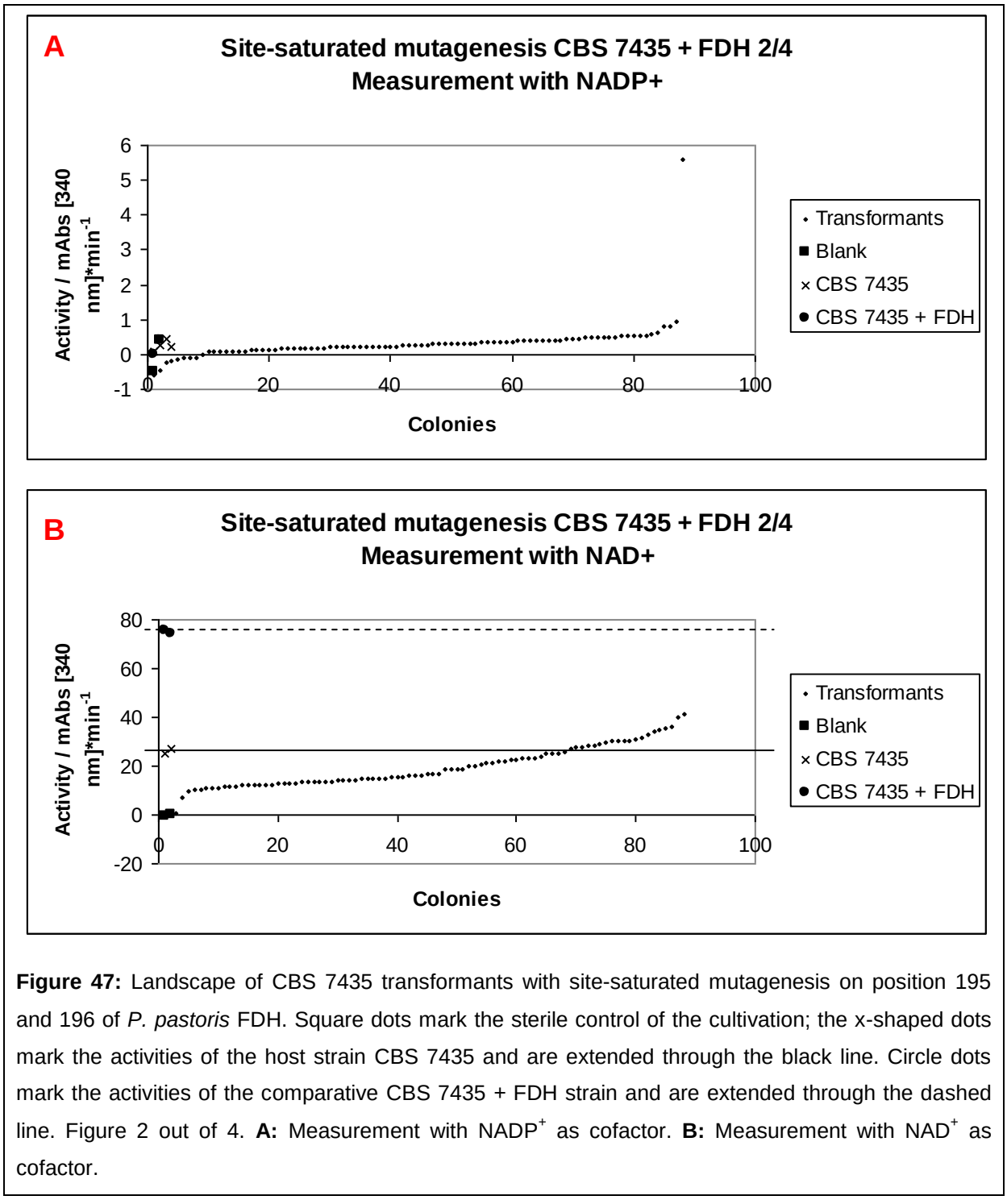

Figure 47: Landscape of CBS 7435 transformants with site-saturated mutagenesis on position 195 and 196 of *P. pastoris* FDH. Square dots mark the sterile control of the cultivation; the x-shaped dots mark the activities of the host strain CBS 7435 and are extended through the black line. Circle dots mark the activities of the comparative CBS 7435 + FDH strain and are extended through the dashed line. Figure 2 out of 4. **A:** Measurement with $NADP^+$ as cofactor. **B:** Measurement with NAD^+ as cofactor.

The measurement with NADP+ showed one transformant with a significant enhanced FDH activity compared to the host strain CBS 7435. It has yet to be established, if this transformant is an outlier or if the enhanced activity is reproducible.
Measurement with NAD+ led to the same results as discussed above with the (semi-) rational approach. The activities of all transformants are beneath the host strain.

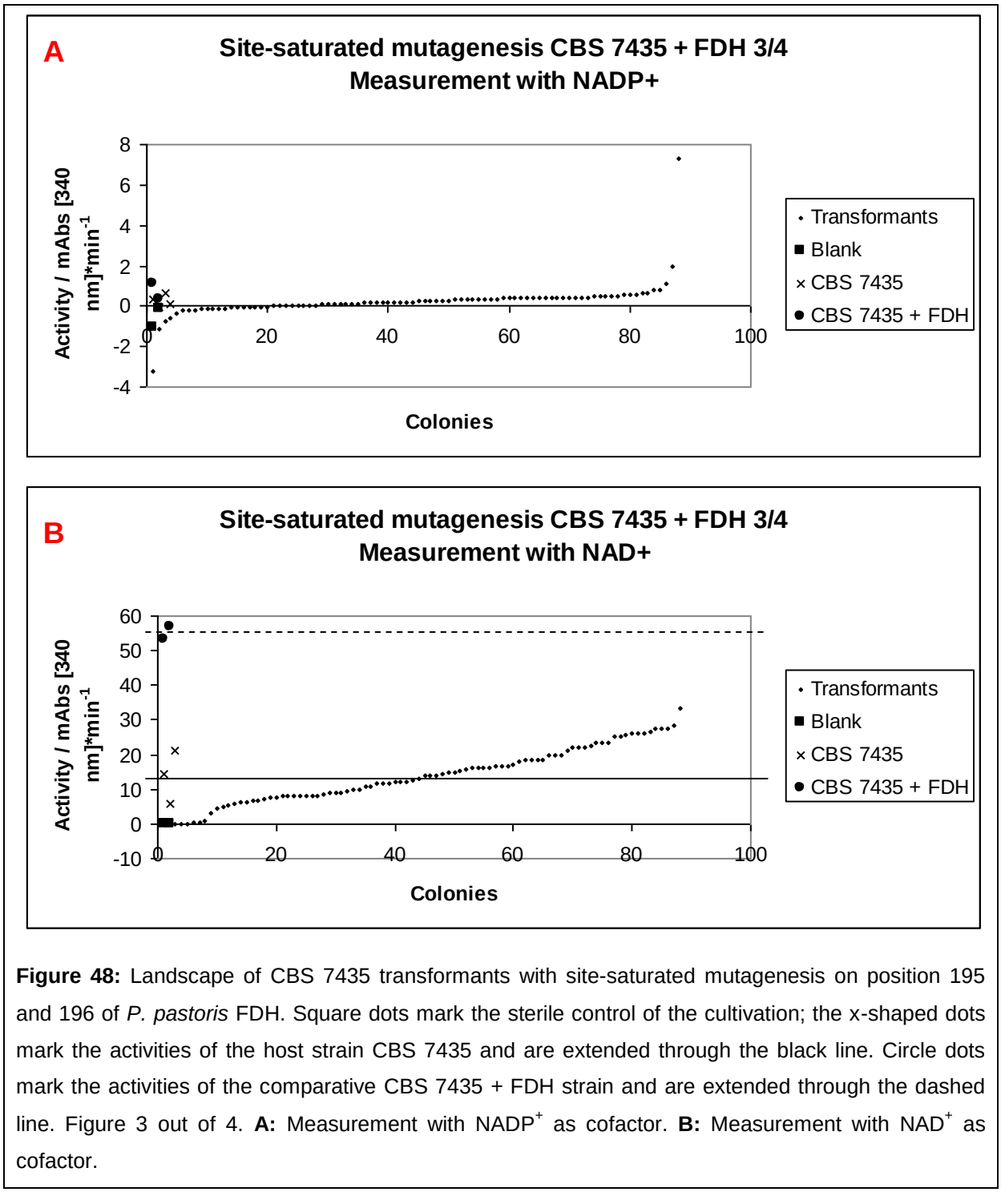

Figure 48: Landscape of CBS 7435 transformants with site-saturated mutagenesis on position 195 and 196 of *P. pastoris* FDH. Square dots mark the sterile control of the cultivation; the x-shaped dots mark the activities of the host strain CBS 7435 and are extended through the black line. Circle dots mark the activities of the comparative CBS 7435 + FDH strain and are extended through the dashed line. Figure 3 out of 4. **A:** Measurement with $NADP^+$ as cofactor. **B:** Measurement with NAD^+ as cofactor.

The measurement with NADP+ showed at least one transformant with a significant enhanced FDH activity compared to the host strain CBS 7435. It has yet to be established, if this transformant is an outlier or if the enhanced activity is reproducible.
Measurement with NAD+ led to the same results as discussed above with the (semi-) rational approach. The activities of all transformants are beneath the host strain.

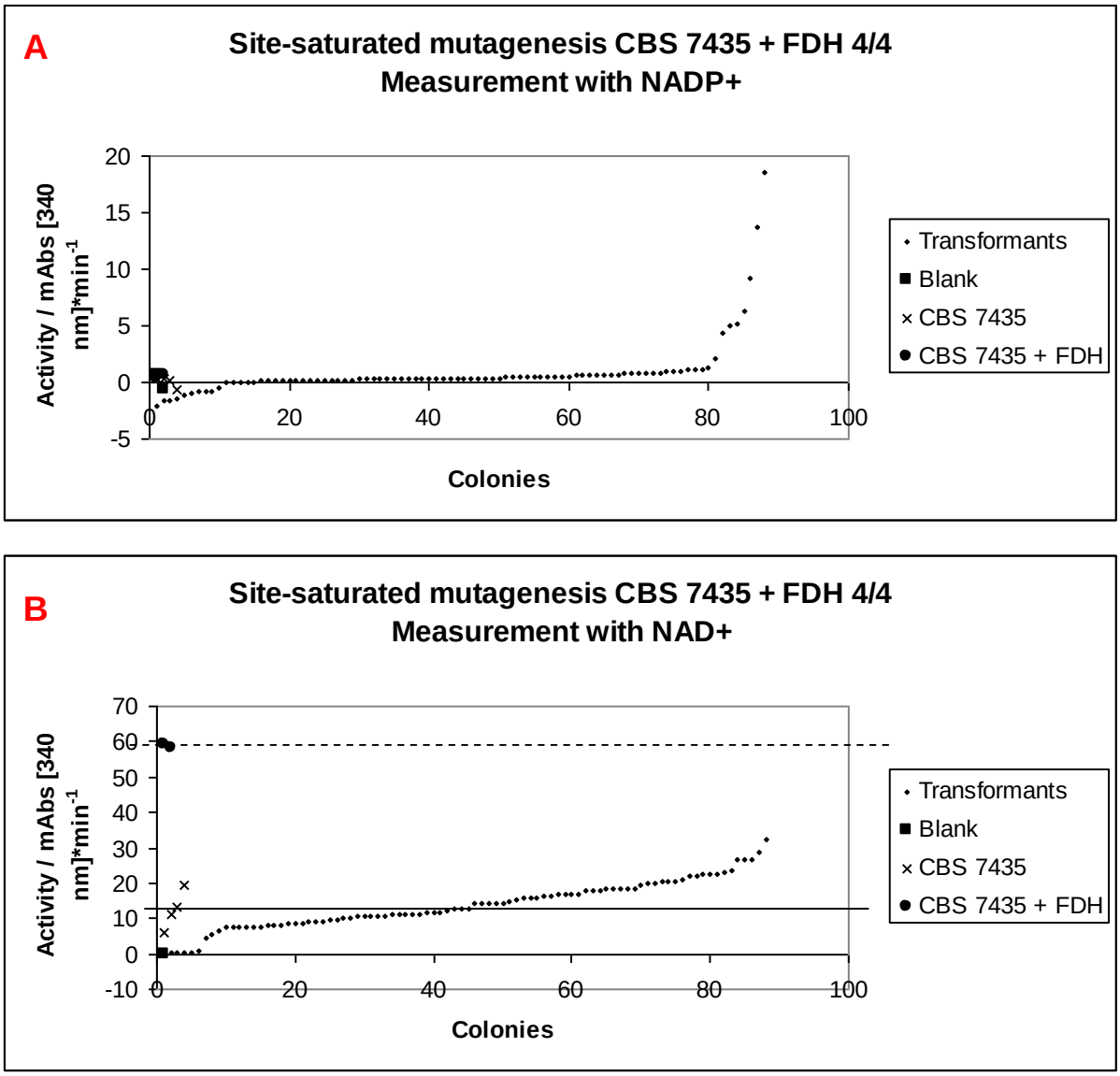

Figure 49: Landscape of CBS 7435 transformants with site-saturated mutagenesis on position 195 and 196 of *P. pastoris* FDH. Square dots mark the sterile control of the cultivation; the x-shaped dots mark the activities of the host strain CBS 7435 and are extended through the black line. Circle dots mark the activities of the comparative CBS 7435 + FDH strain and are extended through the dashed line. Figure 4 out of 4. **A:** Measurement with $NADP^+$ as cofactor. **B:** Measurement with NAD^+ as cofactor.

The measurement with NADP+ showed a few transformants with significant enhanced FDH activities compared to the host strain CBS 7435. It has yet to be established, if these transformants are outlier or if the enhanced activities are reproducible.

Measurement with NAD+ led to the same results as discussed above with the (semi-) rational approach. The activities of all transformants are beneath the host strain.

6.3.3Final discussion

FDH double mutant

The mutations of position 195 and 195 resulted in a screening of transformants with more or less active clones.

The decrease of FDH activity under normal conditions with NAD+ as cofactor indicated, that the mutation on 195, 196 indeed had an effect on the enzyme. It is, however, questionable, if the effect is positive or not. Taken the relative measurements, there is a significant enhancement of NADP+ acceptance in the engineered enzyme. By means of the absolute values, the activities seem still to be very low.

Site-saturated mutagenesis

For a statistically firm end result, no less than 3600 transformants should be measured under the prospective of 2 random mutated triplets within the DNA sequence. However for initial experiments to show the proof of concept that this method might deliver the desired engineered enzyme the 352 transformants – about 10% of targeted number – were cultivated and measured for enhanced $NADP^+$ activity.

Even with this low number of transformants, the first enhancements could already be obtained. Especially in the 4^{th} DWP assayed in this study, there seemed to be some strains with enhanced abilities. However no rescreens or lager experiments under tightly controlled conditions have been performed to reproduce or verify these initial positive hits.

Future perspectives

The screening experiments of the site-saturated mutagenesis experiments showed at least the possibilities of this system. Another experiment with statistical firm scale could help to identify and find transformants with enhanced NADP+ dependency.

Since the work by Kirsten Schroer [35] showed, that FLD, not FDH, has the greatest impact on the conversion rate of the product on whole-cell level, maybe it should be questioned, if FDH should be the targeted model enzyme of choice. Formaldehyde would be a cheap substrate too, in a working *P. pastoris* environment the over-expression of FLD showed no negative (e.g. toxic) effects on the yeast, and due to the whole-cell catalysis, the stability issue has to be revisited under another point of view.

7 Conclusion

7.1 BDH strains

Pichia pastoris as a platform for whole-cell biotransformations is nowadays a well known system. Therefore, a large set of different applications of conversions employing oxidoreductases is already established.
The enhanced cofactor regeneration strains produced in this diploma thesis allow the platform to work more efficiently and faster than before. Due to higher conversion rates and the irreversible reaction at the end of the NADH regeneration pathway, the strains have a higher performance as well as the possibilities to use cheap substrates for reduction of NAD+.

By using these newly produced strains in whole-cell biotransformations, higher reaction rates should be possible.

7.2 XR and XR-M strains

Similar to results of the studies with the BDH strains, the strains with xylose reductase activity also show improved capatilities of cofactor regeneration and therefore theoretical improved reaction rates on whole-cell level.

Unfortunately, first experiments with xylose as substrate for whole-cell biotransformations showed almost no activity in fermentations on shake flask level. Although enzyme activity is present as demonstrated by studies with the crude extract of the cell lysis. This fact maybe indicates a bottleneck in the transportation mechanisms of the substrate. On the other side the level of reductase expression in these engineered strains is not known.

7.3 Cofactor dependency

The first analyzed data on the topic of cofactor dependency showed conflicting results.

The approach of a double mutant of FDH according to previous studies available in literature showed no improvement whatsoever. A further sequencing of the mutant could determine, if the mutations are in order and in the right spot. Variations on a sequence level could be the explanation for the lack of improvements.

The results of the site-saturated mutagenesis approach (the semi-rational approach) are more promising. First screening showed slightly-to-moderate improvements on some strains. Further work on this strategy could give the desired results.

8 Outlook

The significant improvements in the whole-cell biotransformations of the BDH strains showed the potential of the MUT pathway enhancements.
The work presented in this thesis focused on the over-expression of the *P. pastoris* endogenous FLD and FDH enzymes, therefore future studies could implement regenerative enzymes from different sources, especially since previous work on this topic showed, that the endogenous MUT enzymes may not be the most efficient ones known [48, 51, 52]. On the other hand native sequences might provide advantages in respect to their expression. Therefore directed evolution of these enzymes for higher activity is an interesting alternative.

On the topic of combining an enhanced cofactor recycling with the NADPH dependent oxidase XR and XR-M, the positive screening results could not backed up by the first biotransformations. More detailed research on the transport mechanisms in *P. pastoris* may be a reasonable approach for a better understanding of this problem.

The results of different engineering approaches of *P. pastoris* FDH showed the potential of this system. However, a number of wider experiments have to be designed to assure the statistically firm conclusion of another site-saturated mutagenesis approach.

9 Appendix

9.1 Sequence of genes

9.1.1 *E. coli / P. pastoris* shuttle vector 3,2-8 Kan

AGATCCAATTCCCGCTTTGACTGCCTGAAATCTCCATCGCCTACAATGATGACATTTGGATTTGGTTGACTCATG
TTGGTATTGTGAAATAGACGCAGATCGGGAACACTGAAAAATACACAGTTATTATTCAGATCTAACATCCAAAGA
CGAAAGGTTGAATGAAACCTTTTTGCCATCCGACATCCACAGGTCCATTCTCACACATAAGTGCCAAACGCAACA
GGAGGGGATACACTAGCAGCAGACCGTTGCAAACGCAGGACCTCCACTCCTCTTCTCCTCAACACCCACTTTTGC
CATCGAAAAACCAGCCCAGTTATTGGGCTTGATTGGAGCTCGCTCATTCCAATTCCTTCTATTAGGCTACTAACA
CCATGACTTTATTAGCCTGTCTATCCTGGCCCCCCTGGCGAGGTTCATGTTTGTTTATTTCCGAATGCAACAAGC
TCCGCATTACACCCGAACATCACTCCAGATGAGGGCTTTCTGAGTGTGGGGTCAAATAGTTTCATGTTCCCCAAA
TGGCCCAAAACTGACAGTTTAAACGCTGTCTTGGAACCTAATATGACAAAAGCGTGATCTCATCCAAGATGAACT
AAGTTTGGTTCGTTGAAATGCTAACGGCCAGTTGGTCAAAAAGAAACTTCCAAAAGTCGGCATACCGTTTGTCTT
GTTTGGTATTGATTGACGAATGCTCAAAAATAATCTCATTAATGCTTAGCGCAGTCTCTCTATCGCTTCTGAACC
CCGGTGCACCTGTGCCGAAACGCAAATGGGGAAACACCCGCTTTTTGGATGATTATGCATTGTCTCCACATTGTA
TGCTTCCAAGATTCTGGTGGGAATACTGCTGATAGCCTAACGTTCATGATCAAAATTTAACTGTTCTAACCCCTA
CTTGACAGCAATATATAAACAGAAGGAAGCTGCCCTGTCTTAAACCTTTTTTTTTATCATCATTATTAGCTTACT
TTCATAATTGCGACTGGTTCCAATTGACAAGCTTTTGATTTTAACGACTTTTAACGACAACTTGAGAAGATCAAA
AAACAACTAATTATTGAAAGAATTCACTAGTGGCGCGCCGCGGCCGCTCAAGAGGATGTCAGAATGCCATTTGCC
TGAGAGATGCAGGCTTCATTTTTGATACTTTTTTATTTGTAACCTATATAGTATAGGATTTTTTTTGTCATTTTG
TTTCTTCTCGTACGAGCTTGCTCCTGATCAGCCTATCTCGCAGCAGATGAATATCTTGTGGTAGGGGTTTGGGAA
AATCATTCGAGTTTGATGTTTTTCTTGGTATTTCCCACTCCTCTTCAGAGTACAGAAGATTAAGTGAGACCTTCG
TTTGTGCGGATCCTTCAGTAATGTCTTGTTTCTTTTGTTGCAGTGGTGAGCCATTTTGACTTCGTGAAAGTTTCT
TTAGAATAGTTGTTTCCAGAGGCCAAACATTCCACCCGTAGTAAAGTGCAAGCGTAGGAAGACCAAGACTGGCAT
AAATCAGGTATAAGTGTCGAGCACTGGCAGGTGATCTTCTGAAAGTTTCTACTAGCAGATAAGATCCAGTAGTCA
TGCATATGGCAACAATGTACCGTGTGGATCTAAGAACGCGTCCTACTAACCTTCGCATTCGTTGGTCCAGTTTGT
TGTTATCGATCAACGTGACAAGGTTGTCGATTCCGCGTAAGCATGCATACCCAAGGACGCCTGTTGCAATTCCAA
GTGAGCCAGTTCCAACAATCTTTGTAATATTAGAGCACTTCATTGTGTTGCGCTTGAAAGTAAAATGCGAACAAA
TTAAGAGATAATCTCGAAACCGCGACTTCAAACGCCAATATGATGTGCGGCACACAATAAGCGTTCATATCCGCT
GGGTGACTTTCTCGCTTTAAAAAATTATCCGAAAAAATTTTCTTCCCTTCTCTTCCAAATATCGTCTCCACAAAT
CTAGAGTGTTGACACTTTATACTTCCGGCTCGTATAATACGACAAGGTGTAAGGAGGACTAAACCATGGGTAAGG
AAAAGACTCACGTTTCGAGGCCGCGATTAAATTCCAACATGGATGCTGATTTATATGGGTATAAATGGGCTCGCG
ATAATGTCGGGCAATCAGGTGCGACAATCTATCGATTGTATGGGAAGCCCGATGCGCCAGAGTTGTTTCTGAAAC
ATGGCAAAGGTAGCGTTGCCAATGATGTTACAGATGAGATGGTCAGACTAAACTGGCTGACGGAATTTATGCCTC
TTCCGACCATCAAGCATTTTATCCGTACTCCTGATGATGCATGGTTACTCACCACTGCGATCCCCGGCAAAACAG
CATTCCAGGTATTAGAAGAATATCCTGATTCAGGTGAAAATATTGTTGATGCGCTGGCAGTGTTCCTGCGCCGGT
TGCATTCGATTCCTGTTTGTAATTGTCCTTTTAACAGCGATCGCGTATTTCGTCTCGCTCAGGCGCAATCACGAA
TGAATAACGGTTTGGTTGATGCGAGTGATTTTGATGACGAGCGTAATGGCTGGCCTGTTGAACAAGTCTGGAAAG
AAATGCATAAGCTTTTGCCATTCTCACCGGATTCAGTCGTCACTCATGGTGATTTCTCACTTGATAACCTTATTT
TTGACGAGGGGAAATTAATAGGTTGTATTGATGTTGGACGAGTCGGAATCGCAGACCGATACCAGGATCTTGCCA
TCCTATGGAACTGCCTCGGTGAGTTTTCTCCTTCATTACAGAAACGGCTTTTTCAAAAATATGGTATTGATAATC
CTGATATGAATAAATTGCAGTTTCATTTGATGCTCGATGAGTTTTTCTAACCTAGGACACCTTACGATTATTTAG
AGAGTATTTATTAGTTTTATTGTATGTATACGGATGTTTTATTATCTATTTATGCCCTTATATTCTGTAACTATC
CAAAAGTCCTATCTTATCAAGCCAGCAATCTATGTCCGCGAACGTCAACTAAAAATAAGCTTTTTATGCTCTTCT
CTCTTTTTTTCCCTTCGGTATAATTATACCTTGCATCCACAGATTCTCCTGCCAAATTTTGCATAATCCTTTACA
ACATGGCTATATGGGAGCACTTAGCGCCCTCCAAAACCCATATTGCCTACGCATGTATAGGTGTTTTTTCCACAA
TATTTTCTCTGTGCTCTCTTTTTATTAAAGAGAAGCTCTATATCGGAGAAGCTTCTGTGGCCGTTATATTCGGCC
TTATCGTGGGACCACATTGCCTGAATTGGTTTGCCCCGGAAGATTGGGGAAACTTGGATCTGATTACCTTAGCTG
CAGGTACCACTGAGCGTCAGACCCCGTAGAAAAGATCAAAGGATCTTCTTGAGATCCTTTTTTTCTGCGCGTAAT
CTGCTGCTTGCAAACAAAAAAACCACCGCTACCAGCGGTGGTTTGTTTGCCGGATCAAGAGCTACCAACTCTTTT
TCCGAAGGTAACTGGCTTCAGCAGAGCGCAGATACCAAATACTGTCCTTCTAGTGTAGCCGTAGTTAGGCCACCA
CTTCAAGAACTCTGTAGCACCGCCTACATACCTCGCTCTGCTAATCCTGTTACCAGTGGCTGCTGCCAGTGGCGA
TAAGTCGTGTCTTACCGGGTTGGACTCAAGACGATAGTTACCGGATAAGGCGCAGCGGTCGGGCTGAACGGGGGG
TTCGTGCACACAGCCCAGCTTGGAGCGAACGACCTACACCGAACTGAGATACCTACAGCGTGAGCTATGAGAAAG
CGCCACGCTTCCCGAAGGGAGAAAGGCGGACAGGTATCCGGTAAGCGGCAGGGTCGGAACAGGAGAGCGCACGAG
GGAGCTTCCAGGGGGAAACGCCTGGTATCTTTATAGTCCTGTCGGGTTTCGCCACCTCTGACTTGAGCGTCGATT

TTTGTGATGCTCGTCAGGGGGGCGGAGCCTATGGAAAAACGCCAGCAACGCGGCCTTTTTACGGTTCCTGGCCTT
TTGCTGGCCTTTTGCTCACATGTTCTTTCCTGCGGTACCC

9.1.2*E. coli / P. pastoris* shuttle vector T2

AGATCCAATTCCCGCTTTGACTGCCTGAAATCTCCATCGCCTACAATGATGACATTTGGATTTGGTTGACTCATG
TTGGTATTGTGAAATAGACGCAGATCGGGAACACTGAAAAATACACAGTTATTATTCAGATCTAACATCCAAAGA
CGAAAGGTTGAATGAAACCTTTTTGCCATCCGACATCCACAGGTCCATTCTCACACATAAGTGCCAAACGCAACA
GGAGGGGATACACTAGCAGCAGACCGTTGCAAACGCAGGACCTCCACTCCTCTTCTCCTCAACACCCACTTTTGC
CATCGAAAAACCAGCCCAGTTATTGGGCTTGATTGGAGCTCGCTCATTCCAATTCCTTCTATTAGGCTACTAACA
CCATGACTTTATTAGCCTGTCTATCCTGGCCCCCCTGGCGAGGTTCATGTTTGTTTATTTCCGAATGCAACAAGC
TCCGCATTACACCCGAACATCACTCCAGATGAGGGCTTTCTGAGTGTGGGGTCAAATAGTTTCATGTTCCCCAAA
TGGCCCAAAACTGACAGTTTAAACGCTGTCTTGGAACCTAATATGACAAAAGCGTGATCTCATCCAAGATGAACT
AAGTTTGGTTCGTTGAAATGCTAACGGCCAGTTGGTCAAAAAGAAACTTCCAAAAGTCGGCATACCGTTTGTCTT
GTTTGGTATTGATTGACGAATGCTCAAAAATAATCTCATTAATGCTTAGCGCAGTCTCTCTATCGCTTCTGAACC
CCGGTGCACCTGTGCCGAAACGCAAATGGGGAAACACCCGCTTTTTGGATGATTATGCATTGTCTCCACATTGTA
TGCTTCCAAGATTCTGGTGGGAATACTGCTGATAGCCTAACGTTCATGATCAAAATTTAACTGTTCTAACCCCTA
CTTGACAGCAATATATAAACAGAAGGAAGCTGCCCTGTCTTAAACCTTTTTTTTTATCATCATTATTAGCTTACT
TTCATAATTGCGACTGGTTCCAATTGACAAGCTTTTGATTTTAACGACTTTTAACGACAACTTGAGAAGATCAAA
AAACAACTAATTATTGAAAGAATTCACTAGTGGCGCGCCGCGGCCGCTCAAGAGGATGTCAGAATGCCATTTGCC
TGAGAGATGCAGGCTTCATTTTTGATACTTTTTTATTTGTAACCTATATAGTATAGGATTTTTTTTGTCATTTTG
TTTCTTCTCGTACGAGCTTGCTCCTGATCAGCCTATCTCGCAGCAGATGAATATCTTGTGGTAGGGGTTTGGGAA
AATCATTCGAGTTTGATGTTTTTCTTGGTATTTCCCACTCCTCTTCAGAGTACAGAAGATTAAGTGAGACCTTCG
TTTGTGCGGATCCTTCAGTAATGTCTTGTTTCTTTTGTTGCAGTGGTGAGCCATTTTGACTTCGTGAAAGTTTCT
TTAGAATAGTTGTTTCCAGAGGCCAAACATTCCACCCGTAGTAAAGTGCAAGCGTAGGAAGACCAAGACTGGCAT
AAATCAGGTATAAGTGTCGAGCACTGGCAGGTGATCTTCTGAAAGTTTCTACTAGCAGATAAGATCCAGTAGTCA
TGCATATGGCAACAATGTACCGTGTGGATCTAAGAACGCGTCCTACTAACCTTCGCATTCGTTGGTCCAGTTTGT
TGTTATCGATCAACGTGACAAGGTTGTCGATTCCGCGTAAGCATGCATACCCAAGGACGCCTGTTGCAATTCCAA
GTGAGCCAGTTCCAACAATCTTTGTAATATTAGAGCACTTCATTGTGTTGCGCTTGAAAGTAAAATGCGAACAAA
TTAAGAGATAATCTCGAAACCGCGACTTCAAACGCCAATATGATGTGCGGCACACAATAAGCGTTCATATCCGCT
GGGTGACTTTCTCGCTTTAAAAAATTATCCGAAAAAATTTTCTTCCCTTCTCTTCCAAATATCGTCTCCACAAAT
CTAGAGTGTTGACACTTTATACTTCCGGCTCGTATAATACGACAAGGTGTAAGGAGGACTAAACCATGGCTAAAC
TCACCTCTGCTGTTCCAGTCCTGACTGCTCGTGATGTTGCTGGTGCTGTTGAGTTCTGGACTGATAGACTCGGTT
TCTCCCGTGACTTCGTAGAGGACGACTTTGCCGGTGTTGTACGTGACGACGTTACCCTGTTCATCTCCGCAGTTC
AGGACCAGGTTGTGCCAGACAACACTCTGGCATGGGTATGGGTTCGTGGTCTGGACGAACTGTACGCTGAGTGGT
CTGAGGTCGTGTCTACCAACTTCCGTGATGCATCTGGTCCAGCTATGACCGAGATCGGTGAACAGCCCTGGGGTC
GTGAGTTTGCACTGCGTGATCCAGCTGGTAACTGCGTGCATTTCGTCGCAGAAGAGCAGGACTAACAATTGACAC
CTTACGATTATTTAGAGAGTATTTATTAGTTTTATTGTATGTATACGGATGTTTTATTATCTATTTATGCCCTTA
TATTCTGTAACTATCCAAAAGTCCTATCTTATCAAGCCAGCAATCTATGTCCGCGAACGTCAACTAAAAATAAGC
TTTTTATGCTCTTCTCTCTTTTTTTCCCTTCGGTATAATTATACCTTGCATCCACAGATTCTCCTGCCAAATTTT
GCATAATCCTTTACAACATGGCTATATGGGAGCACTTAGCGCCCTCCAAAACCCATATTGCCTACGCATGTATAG
GTGTTTTTTCCACAATATTTTCTCTGTGCTCTCTTTTTATTAAAGAGAAGCTCTATATCGGAGAAGCTTCTGTGG
CCGTTATATTCGGCCTTATCGTGGGACCACATTGCCTGAATTGGTTTGCCCCGGAAGATTGGGGAAACTTGGATC
TGATTACCTTAGCTGCAGGTACCACTGAGCGTCAGACCCCGTAGAAAAGATCAAAGGATCTTCTTGAGATCCTTT
TTTTCTGCGCGTAATCTGCTGCTTGCAAACAAAAAAACCACCGCTACCAGCGGTGGTTTGTTTGCCGGATCAAGA
GCTACCAACTCTTTTTCCGAAGGTAACTGGCTTCAGCAGAGCGCAGATACCAAATACTGTCCTTCTAGTGTAGCC
GTAGTTAGGCCACCACTTCAAGAACTCTGTAGCACCGCCTACATACCTCGCTCTGCTAATCCTGTTACCAGTGGC
TGCTGCCAGTGGCGATAAGTCGTGTCTTACCGGGTTGGACTCAAGACGATAGTTACCGGATAAGGCGCAGCGGTC
GGGCTGAACGGGGGGTTCGTGCACACAGCCCAGCTTGGAGCGAACGACCTACACCGAACTGAGATACCTACAGCG
TGAGCTATGAGAAAGCGCCACGCTTCCCGAAGGGAGAAAGGCGGACAGGTATCCGGTAAGCGGCAGGGTCGGAAC
AGGAGAGCGCACGAGGGAGCTTCCAGGGGGAAACGCCTGGTATCTTTATAGTCCTGTCGGGTTTCGCCACCTCTG
ACTTGAGCGTCGATTTTTGTGATGCTCGTCAGGGGGGCGGAGCCTATGGAAAAACGCCAGCAACGCGGCCTTTTT
ACGGTTCCTGGCCTTTTGCTGGCCTTTTGCTCACATGTTCTTTCCTGCGGTACCC

9.1.3*S. cerevisiae* BDH

>gi|296142477|ref|NM_001178202.1| Saccharomyces cerevisiae S288c (2R,3R)-2,3-butanediol dehydrogenase (BDH1), mRNA

```
ATGAGAGCTTTGGCATATTTCAAGAAGGGTGATATTCACTTCACTAATGATATCCCTAGGCCAGAAATCC
AAACCGACGATGAGGTTATTATCGACGTCTCTTGGTGTGGGATTTGTGGCTCGGATCTTCACGAGTACTT
GGATGGTCCAATCTTCATGCCTAAAGATGGAGAGTGCCATAAATTATCCAACGCTGCTTTACCTCTGGCA
ATGGGCCATGAGATGTCAGGAATTGTTTCCAAGGTTGGTCCTAAAGTGACAAAGGTGAAGGTTGGCGACC
ACGTGGTCGTTGATGCTGCCAGCAGTTGTGCGGACCTGCATTGCTGGCCACACTCCAAATTTTACAATTC
CAAACCATGTGATGCTTGTCAGAGGGGCAGTGAAAATCTATGTACCCACGCCGGTTTTGTAGGACTAGGT
GTGATCAGTGGTGGCTTTGCTGAACAAGTCGTAGTCTCTCAACATCACATTATCCCGGTTCCAAAGGAAA
TTCCTCTAGATGTGGCTGCTTTAGTTGAGCCTCTTTCTGTCACCTGGCATGCTGTTAAGATTTCTGGTTT
CAAAAAAGGCAGTTCAGCCTTGGTTCTTGGTGCAGGTCCCATTGGGTTGTGTACCATTTTGGTACTTAAG
GGAATGGGGGCTAGTAAAATTGTAGTGTCTGAAATTGCAGAGAGAAGAATAGAAATGGCCAAGAAACTGG
GCGTTGAGGTGTTCAATCCCTCCAAGCACGGTCATAAATCTATAGAGATACTACGTGGTTTGACCAAGAG
CCATGATGGGTTTGATTACAGTTATGATTGTTCTGGTATTCAAGTTACTTTCGAAACCTCTTTGAAGGCA
TTAACATTCAAGGGGACAGCCACCAACATTGCAGTTTGGGGTCCAAAACCTGTCCCATTCCAACCAATGG
ATGTGACTCTCCAAGAGAAAGTTATGACTGGTTCGATCGGCTATGTTGTCGAAGCCTTCGAAGAAGTTGT
TCGTGCCATCCACAACGGAGACATCGCCATGGAAGATTGTAAGCAACTAATCACTGGTAAGCAAAGGATT
GAGGACGGTTGGGAAAAGGGATTCCAAGAGTTGATGGATCACAAGGAATCCAACGTTAAGATTCTATTGA
CGCCTAACAATCACGGTGAAATGAAGTAA
```

9.1.4*C. tenuis* xylose reductase

>gi|3289018:601-1569 Candida tenuis xylose reductase (xylr) gene, complete cds

```
ATGAGCGCAAGTATCCCAGACATCAAATTGAGCTCCGGCCACTTAATGCCTTCCATCGGTTTCGGCTGTT
GGAAGCTCGCCAACGCTACCGCCGGTGAACAAGTCTACCAAGCCATCAAGGCCGGTTACAGATTGTTCGA
CGGTGCCGAGGACTACGGTAACGAAAAGGAAGTCGGTGACGGTGTCAAGAGAGCCATCGACGAAGGTCTT
GTCAAGAGAGAAGAGATCTTCCTCACCTCCAAGTTGTGGAACAACTACCACGACCCAAAGAACGTCGAGA
CCGCCTTGAACAAAACCCTCGCCGACCTTAAGGTTGACTACGTTGACTTGTTCTTGATCCATTTCCCAAT
TGCCTTCAAGTTCGTCCCAATCGAGGAGAAGTACCCACCAGGATTCTACTGTGGTGACGGTAACAACTTC
GTCTACGAAGACGTTCCAATCTTGGAGACCTGGAAGGCCCTCGAGAAGTTGGTTGCTGCCGGTAAGATTA
AGTCCATCGGTGTCTCTAACTTCCCAGGTGCTTTGCTCTTGGACTTGCTCAGAGGTGCTACCATCAAGCC
AGCTGTCTTGCAAGTTGAGCACCACCCATACTTGCAACAACCAAAGTTGATCGAGTTCGCTCAAAAGGCC
GGTGTTACCATCACCGCCTACTCTTCTTTCGGTCCTCAATCTTTCGTTGAGATGAACCAAGGTAGAGCTT
TGAACACCCCAACCTTGTTCGCACACGACACCATCAAGGCTATTGCTGCCAAGTACAACAAGACCCCAGC
TGAGGTTTTATTGAGATGGGCCGCCCAAAGAGGTATCGCTGTCATTCCAAAGTCTAACCTCCCAGAGAGA
TTAGTCCAAAACAGAAGTTTCAACACCTTCGACTTGACCAAGGAGGACTTCGAGGAAATCGCCAAGTTGG
ACATCGGCTTGAGATTCAACGACCCATGGGACTGGGACAACATTCCAATCTTCGTTTAA
```

9.1.5*P. pastoris* AOX1

>gi|2104960:470-2461 Pichia pastoris strain NRRL Y-11430 alcohol oxidase (AOX1) gene, complete cds

```
ATGGCTATCCCCGAAGAGTTTGATATCCTAGTTCTAGGTGGTGGATCCAGTGGATCCTGTATTGCCGGAA
GATTGGCAAACTTGGACCACTCCTTGAAAGTTGGTCTTATCGAAGCAGGTGAGAACAACCTCAACAACCC
ATGGGTCTACCTTCCAGGTATTTACCCAAGAAACATGAAGTTGGACTCCAAGACTGCTTCCTTCTACACT
TCTAACCCATCTCCTCACTTGAATGGTAGAAGAGCCATTGTTCCATGTGCTAACGTCTTGGGTGGTGGTT
CTTCTATCAACTTCATGATGTACACCAGAGGTTCTGCTTCTGATTACGATGACTTCCAAGCCGAGGGCTG
GAAAACCAAGGACTTGCTTCCATTGATGAAAAAGACTGAGACCTACCAAAGAGCTTGCAACAACCCTGAC
ATTCACGGTTTCGAAGGTCCAATCAAGGTTTCTTTCGGTAACTACACCTACCCAGTTTGCCAGGACTTCT
TGAGGGCTTCTGAGTCCCAAGGTATTCCATACGTTGACGACTTGGAAGACTTGGTTACTGCTCACGGTGC
TGAACACTGGTTGAAGTGGATCAACAGAGACACTGGTCGTCGTTCCGACTCTGCTCATGCATTTGTCCAC
TCTACTATGAGAAACCACGACAACTTGTACTTGATCTGTAACACGAAGGTCGACAAAATTATTGTCGAAG
ACGGAAGAGCTGCTGCTGTTAGAACCGTTCCAAGCAAGCCTTTGAACCCAAAGAAGCCAAGTCACAAGAT
CTACCGTGCTAGAAAGCAAATCGTTTTGTCTTGTGGTACCATCTCCTCTCCATTGGTTTTGCAAAGATCC
```

GGTTTTGGTGACCCAATCAAGTTGAGAGCCGCTGGTGTTAAGCCTTTGGTCAACTTGCCAGGTGTCGGAA
GAAACTTCCAAGACCACTACTGTTTCTTCAGTCCTTACAGAATCAAGCCTCAGTACGAGTCTTTCGATGA
CTTCGTCCGTGGTGATGCTGAGATTCAAAAGAGAGTCTTTGACCAATGGTACGCCAATGGTACTGGTCCT
CTTGCCACTAACGGTATCGAAGCTGGTGTCAAGATCAGACCAACACCAGAAGAACTCTCTCAAATGGACG
AATCCTTCCAGGAGGGTTACAGAGAATACTTCGAAGACAAGCCAGACAAGCCAGTTATGCACTACTCCAT
CATTGCTGGTTTCTTCGGTGACCACACCAAGATTCCTCCTGGAAAGTACATGACTATGTTCCACTTCTTG
GAATACCCATTCTCCAGAGGTTCCATTCACATTACCTCCCCAGACCCATACGCAGCTCCAGACTTCGACC
CAGGTTTCATGAACGATGAAAGAGACATGGCTCCTATGGTTTGGGCTTACAAGAAGTCTAGAGAAACCGC
TAGAAGAATGGACCACTTTGCCGGTGAGGTCACTTCTCACCACCCTCTGTTCCCATACTCATCCGAGGCC
AGAGCCTTGGAAATGGATTTGGAGACCTCTAATGCCTACGGTGGACCTTTGAACTTGTCTGCTGGTCTTG
CTCACGGTTCTTGGACTCAACCTTTGAAGAAGCCAACTGCAAAGAACGAAGGCCACGTTACTTCGAACCA
GGTCGAGCTTCATCCAGACATCGAGTACGATGAGGAGGATGACAAGGCCATTGAGAACTACATTCGTGAG
CACACTGAGACCACATGGCACTGTCTGGGAACCTGTTCCATCGGTCCAAGAGAAGGTTCCAAGATCGTCA
AATGGGGTGGTGTTTTGGACCACAGATCCAACGTTTACGGAGTCAAGGGCTTGAAGGTTGGTGACTTGTC
CGTGTGCCCAGACAATGTTGGTTGTAACACCTACACCACCGCTCTTTTGATCGGTGAAAAGACTGCCACT
TTGGTTGGAGAAGATTTAGGATACTCTGGTGAGGCCTTAGACATGACTGTTCCTCAGTTCAAGTTGGGCA
CTTACGAGAAGACCGGTCTTGCTAGATTCTAA

9.1.6*P. pastoris* FLD

>(gi|3599998:598-615, 730-1851) Pichia pastoris formaldehyde dehydrogenase (FLD1) gene, complete cds
ATGTCTACCGAAGGTCAAATCATCAAATGTAAGGCAGCTGTTGCCTGGGAGGCAGGAAAGGATCTCTCTA
TTGAGGAGATTGAGGTTCTTCCTCCAAGAGCCCATGAAGTTAGAGTGAAAGTGGAATTCACTGGTGTATG
CCACACTGATGCTTACACGCTTTCTGGTGCAGATGCAGAGGGAAGTTTCCCTGTTGTGTTCGGCCATGAA
GGTGCTGGTGTTGTCGAGTCAGTTGGAGAAGGTGTTGAGTCCGTGAAGGTTGGGGATTCTGTAGTGCTTC
TGTACACTCCTGAGTGCAGAGAGTGCAAGTTCTGTCTGTCTGGTAAGACGAACCTCTGTGGTAAAATCAG
AGCCACCCAGGGTAAAGGTTTGTTACCAGACGGGACTTCTCGTTTCCGTTGTAAGGGCAAGGATTTGTTT
CACTATATGGGATGTTCTTCCTTTTCTCAATACACTGTGGTGGCTGACATCTCAGTGGTTAAAGTCCAAG
ACGAAGCTCCTAAGGACAAGACATGTCTGTTGGGTTGTGGTGTTACCACAGGGTACGGTGCTGCTATCAA
CACTGCTAAGATCTCTAAGGGTGACAAGATCGGTGTGTTTGGTGCTGGATGTATTGGATTATCTGTCATC
CAAGGTGCAGTTTCCAAAGGTGCAAGCGAGATTATTGTAATTGACATCAATGATTCAAAGAAGGCATGGG
CGGACCAATTTGGTGCAACTAAGTTTGTCAATCCTACAACCTTACCAGAAGGTACCAATATTGTTGACTA
CTTGATTGATATCACTGACGGAGGCTTTGACTATACCTTCGACTGTACCGGTAATGTTCAAGTAATGAGA
AATGCACTTGAATCTTGCCACAAGGGTTGGGGTGAGTCGATCATCATCGGTGTCGCTGCTGCTGGTAAAG
AAATCTCTACCCGTCCTTTCCAGTTGGTTACTGGCAGAGTCTGGAGAGGATGCGCCTTTGGAGGTATCAA
GGGACGTACTCAAATGCCATCTTTGGTTCAGGACTATCTTGATGGTAAGATTAAAGTTGACGAGTTTATC
ACACACAGACATGACCTGGACAACATCAACAAAGCATTTCATGACATGCATGCTGGAAACTGTATTCGTG
CTGTGATTACTATGCACTAA

9.1.7*P. pastoris* FDH

>gi|227908542|dbj|AB472090.1| Pichia pastoris FDH1 gene for NAD-dependent formate dehydrogenase, complete cds
ATGAAAATCGTTCTCGTTTTGTACTCCGCTGGTAAGCACGCCGCCGATGAACCAAAGTTGTATGGTTGTA
TCGAAAATGAATTGGGTATTAGACAATGGCTTGAGAAGGGCGGCCATGAATTGGTTACTACATCAGACAA
AGAGGGTGAAAACTCTGAGTTAGAAAAGCACATTCCTGACGCTGATGTGATTATTTCCACTCCATTCCAT
CCAGCCTACATCACGAAGGAGAGAATCCAAAAAGCCAAGAAGCTGAAGTTGTTGGTCGTTGCTGGTGTCG
GTTCCGACCACATTGACTTGGACTACATTGAACAAAATGGCCTAGATATTTCGGTCCTAGAGGTTACTGG
TTCCAACGTTGTTTCAGTGGCTGAGCATGTCGTTATGACTATATTGAACTTGGTGAGAAACTTTGTTCCA
GCTCACGAGCAAATTGTTAACCACGGCTGGGACGTTGCTGCCATCGCCAAGGACGCCTACGATATCGAAG
GTAAGACCATCGCAACAATTGGTGCTGGAAGAATTGGTTACAGAGTCTTAGAGAGACTTGTGGCTTTCAA
CCCTAAGGAATTGTTGTACTACGACTACCAAGGTCTTCCAAAAGAGGCCGAGGAAAAAGTTGGTGCCAGA
AGAGTCGACACTGTCGAGGAGCTGGTTGCTCAAGCCGATGTTGTTACCGTCAATGCCCCACTGCACGCAG
GTACTAAGGGTTTAGTTAACAAGGAGCTTCTGTCCAAGTTCAAGAAGGGTGCTTGGTTGGTTAACACAGC
CAGAGGTGCCATCTGCAATGCTCAAGATGTCGCTGATGCCGTTGCATCTGGTCAATTGAGAGGTTACGGT
GGTGACGTCTGGTTCCCTCAGCCAGCTCCAAAGGACCATCCATGGAGAGATATGAGAAACAAGTACGGAT
ACGGAAACGCCATGACTCCTCATTACTCAGGTACCACTTTGGACGCCCAGGTCAGATATGCCGAAGGTAC
CAAGAACATCTTGAACTCATTCCTTACCAAGAAGTTTGACTACAGACCTCAAGATGTCATTCTTTTGAAC

GGTAAGTACAAGACCAAGGCTTATGGTAATGACAAAAAGGTCGCATAA

9.1.8*P. pastoris* FLD+FDH cassette

ACCACTAGTATGAAAATCGTTCTCGTTTTGTACTCCGCTGGTAAGCACGCCGCCGATGAACCAAAGTTGTATGGT
TGTATCGAAAATGAATTGGGTATTAGACAATGGCTTGAGAAGGGCGGCCATGAATTGGTTACTACATCAGACAAA
GAGGGTGAAAACTCTGAGTTAGAAAAGCACATTCCTGACGCTGATGTGATTATTTCCACTCCATTCCATCCAGCC
TACATCACGAAGGAGAGAATCCAAAAAGCCAAGAAGCTGAAGTTGTTGGTCGTTGCTGGTGTCGGTTCCGACCAC
ATTGACTTGGACTACATTGAACAAAATGGCCTAGATATTTCGGTCCTAGAGGTTACTGGTTCCAACGTTGTTTCA
GTGGCTGAGCATGTCGTTATGACTATATTGAACTTGGTGAGAAACTTTGTTCCAGCTCACGAGCAAATTGTTAAC
CCCGGCTGGGACGTTGCTGCCATCGCCAAGGACGCCTACGATATTGAAGGTAAGACCATCGCAACAATTGGTGCT
GGAAGAATTGGTTACAGAGTCTTAGAGAGACTTGTGGCTTTCAACCCTAAGGAATTGTTGTACTACGACTACCAA
GGTCTTCCAAAAGAGGCCGAGGAAAAAGTTGGTGCCAGAAGAGTCGACACTGTCGAGGAGCTGGTTGCTCAAGCC
GATGTTGTTACCGTCAATGCCCCACTGCACGCAGGTACTAAGGGTTTAGTTAACAAGGAGCTTCTGTCCAAGTTC
AAGAAGGGTGCTTGGTTGGTTAACACAGCCAGAGGTGCCATCTGCAATGCTCAAGATGTCGCTGATGCCGTTGCA
TCTGGTCAATTGAGAGGTTACGGTGGTGACGTCTGGTTCCCTCAGCCAGCTCCAAAGGACCATCCATGGAGAGAT
ATGAGAAACAAGTACGGATACGGAAACGCCATGACTCCTCATTACTCAGGTACCACTTTGGACGCCCAGGTCAGA
TATGCCGAAGGTACCAAGAACATCTTGAACTCATTCCTTACCAAGAAGTTTGACTACAGACCTCAAGATGTCATT
CTTTTGAACGGTAAGTACAAGACCAAGGCTTATGGTAATGACAAAAAGGTCGCATAAATCAAGAGGATGTCAGAA
TGCCATTTGCCTGAGAGATGCAGGCTTCATTTTTGATACTTTTTTATTTGTAACCTATATAGTATAGGATTTTTT
TTGTCATTTTGTTTCTTCTCGTACGAGCTTGCTCCTGATCAGCCTATCTCGCAGCAGATGAATATCTTGTGGTAG
GGGTTTGGGAAAATCATTCGAGTTTGATGTTTTTCTTGGTATTTCCCACTCCTCTTCAGAGTACAGAAGATTAAG
TGAGACCTTCGTTTGTGCAACATCCAAAGACGAAAGGTTGAATGAAACCTTTTTGCCATCCGACATCCACAGGTC
CATTCTCACACATAAGTGCCAAACGCAACAGGAGGGGATACACTAGCAGCAGACCGTTGCAAACGCAGGACCTCC
ACTCCTCTTCTCCTCAACACCCACTTTTGCCATCGAAAAACCAGCCCAGTTATTGGGCTTGATTGGAGCTCGCTC
ATTCCAATTCCTTCTATTAGGCTACTAACACCATGACTTTATTAGCCTGTCTATCCTGGCCCCCCTGGCGAGGTT
CATGTTTGTTTATTTCCGAATGCAACAAGCTCCGCATTACACCCGAACATCACTCCAGATGAGGGCTTTCTGAGT
GTGGGGTCAAATAGTTTCATGTTCCCCAAATGGCCCAAAACTGACAGTTTAAACGCTGTCTTGGAACCTAATATG
ACAAAAGCGTGATCTCATCCAAGATGAACTAAGTTTGGTTCGTTGAAATGCTAACGGCCAGTTGGTCAAAAAGAA
ACTTCCAAAAGTCGGCATACCGTTTGTCTTGTTTGGTATTGATTGACGAATGCTCAAAAATAATCTCATTAATGC
TTAGCGCAGTCTCTCTATCGCTTCTGAACCCCGGTGCACCTGTGCCGAAACGCAAATGGGGAAACACCCGCTTTT
TGGATGATTATGCATTGTCTCCACATTGTATGCTTCCAAGATTCTGGTGGGAATACTGCTGATAGCCTAACGTTC
ATGATCAAAATTTAACTGTTCTAACCCCTACTTGACAGCAATATATAAACAGAAGGAAGCTGCCCTGTCTTAAAC
CTTTTTTTTTATCATCATTATTAGCTTACTTTCATAATTGCGACTGGTTCCAATTGACAAGCTTTTGATTTTAAC
GACTTTTAACGACAACTTGAGAAGATCAAAAAACAACTAATTATTGAAAATGTCTACCGAAGGTCAAGTAAGTTC
AATCAAAGTAATTGTTTGGGAGGGAAGAAGATTGTTTTATTGCGAACCTTTCAATATCTTACCCGACTAAATAAC
CATTACAGTGAATTTTTTACTAACTATATAGATCATCAAATGTAAGGCAGCTGTTGCCTGGGAGGCAGGAAAGGA
TCTCTCTATTGAGGAGATTGAGGTTCTTCCTCCAAGAGCCCATGAAGTTAGAGTGAAAGTGGAATTCACTGGTGT
ATGCCACACTGATGCTTACACGCTTTCTGGTGCAGATGCAGAGGGAAGTTTCCCTGTTGTGTTCGGCCATGAAGG
TGCTGGTGTTGTCGAGTCAGTTGGAGAAGGTGTTGAGTCCGTGAAGGTTGGGGATTCTGTAGTGCTTCTGTACAC
TCCTGAGTGCAGAGAGTGCAAGTTCTGTCTGTCTGGTAAGACGAACCTCTGTGGTAAAATCAGAGCCACCCAGGG
TAAAGGTTTGTTACCAGACGGGACTTCTCGTTTCCGTTGTAAGGGCAAGGATTTGTTTCACTATATGGGATGTTC
TTCCTTTTCTCAATACACTGTGGTGGCTGACATCTCAGTGGTTAAAGTCCAAGACGAAGCTCCTAAGGACAAGAC
ATGTCTGTTGGGTTGTGGTGTTACCACAGGGTACGGTGCTGCTATCAACACTGCTAAAATCTCTAAGGGTGACAA
GATCGGTGTGTTTGGTGCTGGATGTATTGGATTATCTGTCATCCAAGGTGCAGTTTCCAAAGGTGCAAGCGAGAT
TATTGTAATTGACATCAATGATTCAAAGAAGGCATGGGCGGACCAATTTGGTGCAACTAAGTTTGTCAATCCTAC
AACCTTACCAGAAGGTACCAATATTGTTGACTACTTGATTGATATCACTGACGGAGGCTTTGACTATACCTTCGA
CTGTACCGGTAATGTTCAAGTAATGAGAAATGCACTTGAATCTTGCCACAAGGGTTGGGGTGAGTCGATCATCAT
CGGTGTCGCTGCTGCTGGTAAAGAAATCTCTACCCGTCCTTTCCAGTTGGTTACTGGCAGAGTCTGGAGAGGATG
CGCCTTTGGAGGTATCAAGGGACGTACTCAAATGCCATCTTTGGTTCAGGACTATCTTGATGGTAAGATTAAAGT
TGACGAGTTTATCACACACAGACATGACCTGGACAACATCAACAAAGCATTTCATGACATGCATGCTGGAAACTG
TATTCGTGCTGTGATTACTATGCACTAAGCGGCCGCCCA

9.2 Strains generated during this thesis

Table 33: Strains generated during this thesis

Host strain	Employed oxidoreductase	Co-expression of
CBS 7435	BDH	AOX1
		FLD
		FDH
		FLD+FDH
	XR	FLD
		FDH
		FLD+FDH
	XR-M	FLD
		FDH
		FLD+FDH
Das1das2	BDH	AOX1
		FLD
		FDH
		FLD+FDH
	XR	FLD
		FDH
		FLD+FDH
	XR-M	FLD
		FDH
		FLD+FDH
CBS 7435	none	FDH*

*engineered double mutant

Backups of all produced strains were made with glycerol stocks and stored in the -80°C Freezer in the Boxes “Klaus Luef Diplomarbeit – Xylose reductase strains” and “Klaus Luef Diplomarbeit – BDH strains”

9.3 Index of tables

TABLE 1: *P. PASTORIS* PHENOTYPES CONCERNING THE MUT PATHWAY 4
TABLE 2 *P. PASTORIS* MEDIA. STOCK SOLUTIONS FOR *P. PASTORIS* MEDIA; ALL SOLUTIONS EXCEPT 500XB WERE AUTOCLAVED AT 121°C FOR 20 MINUTES (500X B WAS FILTER STERILISED) 16
TABLE 3: RESTRICTION ENZYMES (FERMENTAS) 18
TABLE 4: COMPOSITION OF *AOX1* ACTIVITY ASSAY 26
TABLE 5: COMPOSITION OF FDH PHOTOMETRIC ASSAY 27
TABLE 6: COMPOSITION OF FLD PHOTOMETRIC ASSAY 27
TABLE 7: ASSAY FOR NADPH SCREENING OF XYLOSE REDUCTASE 28
TABLE 8: ASSAY FOR NADH SCREENING OF XYLOSE REDUCTASE MUTANT 28
TABLE 9: PRIMERES USED 28
TABLE 10: CONSTRUCTION OF *P. PASTORIS* STRAINS FOR A ENHANCED NADH COFACTOR REGENERATION 33
TABLE 11: STANDARD COMPOSITION OF PCR USING THE EXAMPLE OF FLD 34
TABLE 12: STANDARD TEMPERATURE PROGRAM USED FOR PCR 34
TABLE 13: USED TEMPLATES AND PRIMERS IN OE-PCR 37
TABLE 14: STANDARD COMPOSITION OF OE-PCR (1^{ST} STEP) 38
TABLE 15: STANDARD PROGRAM USED FOR OE-PCR IN THERMOCYCLERS 38
TABLE 16: STANDARD COMPOSITION OF OE-PCR (2^{ND} STEP) 39
TABLE 17: RE-SCREEN RESULTS OF *P. PASTORIS* CBS 7435 STRAINS. 45
TABLE 18: RE-SCREEN RESULTS OF *P. PASTORIS ΔDAS1DAS2* STRAINS. 49
TABLE 19: SUMMARY OF BEST STRAINS AFTER RE-SCREEN. 51
TABLE 20: SUMMARY OF BEST STRAINS AFTER RE-SCREEN. 52
TABLE 21: CONSTRUCTION OF *P. PASTORIS* STRAINS FOR FURTHER CO-EXPRESSION 55
TABLE 22: CONSTRUCTION OF *P. PASTORIS* CO-EXPRESSION STRAINS FOR ENHANCED NAD(P)H REGENERATION 56
TABLE 23: STANDARD COMPOSITION OF PCR OF XR 57
TABLE 24: STANDARD PCR PROGRAM USED IN THERMOCYCLERS 57
TABLE 25: USED TEMPLATES AND PRIMERS IN OE-PCR 58
TABLE 26: STANDARD COMPOSITION OF OE-PCR (1^{ST} STEP) 58
TABLE 27: STANDARD PROGRAM USED FOR OE-PCR IN THERMOCYCLERS 59
TABLE 28: STANDARD COMPOSITION OF OE-PCR (2^{ND} STEP) 59
TABLE 29: CONSTRUCTED *P. PASTORIS* STRAINS 87
TABLE 30: STANDARD COMPOSITION OF TWO-STEP PCR 88
TABLE 31: PROGRAM USED IN THE 1^{ST} STEP OF TWO-STEP PCR 88
TABLE 32: PROGRAM USED IN THE 2^{ND} STEP OF TWO-STEP PCR 89
TABLE 33: STRAINS GENERATED DURING THIS THESIS 110

9.4 Index of figures

FIGURE 1: DETAIL OF THE *P. PASTORIS* MEOH UTILIZATION PATHWAY (MUT). 1: ALCOHOL OXIDASE 1 AND 2 (AOX1/2). 2: FORMALDEHYDE DEHYDROGENASE (FLD). 3: FORMATE DEHYDROGENASE (FDH). 4: CATALASE. 5: DIHYDROXYACETONE SYNTHASE 1 AND 2 (DAS1/2). GSH: GLUTAHION, DHA: DIHYDROXYACETONE, GAP: GLYCERALDEHYDES 3-PHOSPHATE. THE REACTION MARKED BY THE DOTTED RED LINE SHOWS THE GENERAL CONVERSION OF AN OXIDOREDUCTASE. FIGURE ADAPTED FROM KIRSTEN SCHROER [35]. 3

FIGURE 2: REACTION CATALYZED BY *P. PASTORIS* AOX1/2. METHANOL IS OXIDIZED TO FORMALDEHYDE UNDER THE PRODUCTION OF TOXIC COMPOUND H_2O_2. 4

FIGURE 3: REACTION CATALYZED BY *P. PASTORIS FLD.* AFTER SEPARATION OF THE GLUTATHIONE INTERMEDIATE, FORMALDEHYDE IS OXIDIZED TO FORMATE AND CONSUMES ONE EQUIVALENT OF COFACTOR NAD^+. 5

FIGURE 4: REACTION CATALYZED BY *P. PASTORIS FDH.* FORMATE IS IRREVERSIBLE CONVERTED TO CO_2 AND CONSUMES ONE EQUIVALENT OF NAD^+ IN THE PROCESS. 6

FIGURE 5: THE LUCKY FOUR FACTS OF THE METHYLOTROPHIC YEAST *P. PASTORIS* AS A PLATFORM FOR WHOLE-CELL BIOCATALYSIS. FIGURE ADOPTED FROM A. GLIEDER. 8

FIGURE 6: THE REACTION CATALYZED BY *S. CEREVISIAE* BDH. BUTANONE IS CONVERTED VIA BDH TO A MIX OF *MESO*-2,3-BUTANEDIOL AND *2R,3R*-BUTANEDIOL. 11

FIGURE 7: THE REACTION CATALYZED BY *C. TENIUS* XR. D-XYLOSE IS CONVERTED TO XYLITOL AND CONSUMES ONE EQUIVALENT OF NADPH IN THE PROCESS. 11

FIGURE 8 PJET 1.2/BLUNT VECTOR: *BLA*: B-LACTAMASE GENE CONFERRING AMPICILLIN RESISTANCE; REP (PMB1): REPLICON FOR PLASMID REPLICATION IN *E. COLI*; PLACUV5: MODIFIED LAC PROMOTER FOR IPTG INDEPENDENT *ECO47IR* GENE EXPRESSION; *ECO47IR*: LETHAL GENE FOR POSITIVE SELECTION OF TRANSFORMANTS BEARING AN INSERT; MCS: MULTIPLE CLONING SITE CONTAINING DIFFERENT RESTRICTION SITES; T7 PROMOTER: T7 RNA POLYMERASE PROMOTER FOR *IN VITRO* TRANSCRIPTION OF THE CLONED INSERT (GENEJET™ PCR CLONING KIT, FERMENTAS INC., GLEN BURNIE MA, USA). 20

FIGURE 9 KAN 3,2-8 SHUTTLE VECTOR: PUC ORI: ORIGIN OF REPLICATION FOR *E. COLI*; 5'AOX PROM: 5' EXTENSION OF THE STANDARD *AOX1* PROMOTER; AOX SYN: SYNTHETIC *AOX1* PROMOTER REGION; AOX1 TT: SYNTHETIC *AOX1* TRANSCRIPTION TERMINATION SEQUENZE; P(ILV5-KURZ): *P. PASTORIS* IL5V (ACETOHYDROXYACID REDUCTOISOMERASE) PROMOTER; EM72: SYNTHETIC BACTERIAL PROMOTER EM72; KANMX6: GENE FOR KANAMYCIN/GENETICIN RESISTANCE; AOD TT: *P. PASTORIS* AOD (ALTERNATIVE OXIDASE) TRANSCRIPTION TERMINATON SITE; VECTOR PROVIDED BY BEATE PSCHEIDT. 21

FIGURE 10 T2 SHUTTLE VECTOR: PUC ORI: ORIGIN OF REPLICATION FOR *E. COLI*; 5'AOX PROM: 5' EXTENSION OF THE STANDARD *AOX1* PROMOTER; AOX SYN: SYNTHETIC *AOX1* PROMOTER REGION; AOX1 TT: SYNTHETIC *AOX1* TRANSCRIPTION TERMINATION

SEQUENZE; P(ILV5-KURZ): *P. PASTORIS* IL5V (ACETOHYDROXYACID REDUCTOISOMERASE) PROMOTER; EM72: SYNTHETIC BACTERIAL PROMOTER EM72; ZEOCIN: GENE FOR ZEOCIN™ RESISTANCE; AOD TT: *P. PASTORIS* AOD (ALTERNATIVE OXIDASE) TRANSCRIPTION TERMINATON SITE; VECTOR PROVIDED BY BEATE PSCHEIDT 22

FIGURE 11: SCHEMATIC VIEW OF *P. PASTORIS* METHANOL UTILIZATION PATHWAY ADAPTED FROM KIRSTEN SCHROER [35]. 1: ALCOHOL OXIDASE 1 AND 2 (AOX1/2). 2: FORMALDEHYDE DEHYDROGENASE (FLD). 3: FORMATE DEHYDROGENASE (FDH). 4: CATALASE. 5: DIHYDROXYACETONE SYNTHASE 1 AND 2 (DAS 1/2). 6: DIHYDROXYACETONE KINASE. 7: TRIOSPHOSPHATE ISOMERASE. 8: FRUCTOSE 1,6-BIPHOSPHATE ALDOLASE. 9: FRUCTOSE 1,6-BIPHOSPHATASE. 10: BUTANEDIOL DEHYDROGENASE. DELETION OF DIHYDROXYACETONE SYNTHASE, THE METHANOL DISSIMILATION PATHWAY LEADS TO A REINFORCED NADH FORMATION 30

FIGURE 12: GENE SEQUENCE OF *P. PASTORIS* FDH FOUND IN US 7087418 32

FIGURE 13: SCHEMATIC VIEW OF THE WORKING STEPS LEADING TO A COMPLETE *FLD* AND *FDH* PLASMID 36

FIGURE 14: SCHEMATIC VIEW OF A 96-WELL DEEP WELL PLATE. TRANSFORMANT, HOST STRAIN *ΔDAS1DAS2* + BDH HOST STRAIN CBS 7435 + BDH; CORRESPONDING WILDTYPE CBS 7435, STERILE CONTROL. 40

FIGURE 15: RESULTS OF AOX1 ASSAY. SCREENSHOT FROM SOFTMAX PRO 4.8. *P. PASTORIS ΔDAS1DAS2* + BDH, *P. PASTORIS* CBS 7435 + BDH, *P. PASTORIS* CBS 7435, STERILE CONTROL. 41

FIGURE 16: LANDSCAPE OF *P. PASTORIS* CBS 7435 TRANSFORMANTS WITH OVER-EXPRESSED BDH AND FLD. SQUARE DOTS MARK THE STERILE CONTROLS OF THE CULTIVATIONS. THE X-SHAPED DOTS MARK THE FLD ACTIVITIES OF THE HOST STRAIN *P. PASTORIS* CBS 7435 + BDH. 42

FIGURE 17: LANDSCAPE OF *P. PASTORIS* CBS 7435 TRANSFORMANTS WITH OVER-EXPRESSED BDH AND FDH. SQUARE DOTS MARK THE STERILE CONTROLS OF THE CULTIVATIONS. THE X-SHAPED DOTS MARK THE FDH ACTIVITIES OF THE HOST STRAIN *P. PASTORIS* CBS 7435 + BDH 43

FIGURE 18: LANDSCAPE OF *P. PASTORIS* CBS 7435 TRANSFORMANTS WITH OVER-EXPRESSED BDH, FLD AND FDH. SQUARE DOTS MARK THE STERILE CONTROLS OF THE CULTIVATIONS. THE X-SHAPED DOTS MARK THE CORRESPONDENT ACTIVITIES OF THE HOST STRAIN *P. PASTORIS* CBS 7435 + BDH AND ARE EXTENDED THROUGH THE BLACK LINE. **A:** MEASUREMENT OF FDH ACTIVITY. **B:** MEASUREMENT OF FLD ACTIVITY 44

FIGURE 19: LANDSCAPE OF *P. PASTORIS ΔDAS1DAS2* TRANSFORMANTS WITH OVER-EXPRESSED BDH AND FLD. GROWN SQUARE DOTS MARK THE STERILE CONTROLS OF THE CULTIVATIONS. THE X-SHAPED DOTS MARK THE FLD ACTIVITIES OF THE HOST STRAIN *P. PASTORIS ΔDAS1DAS2* + BDH. 46

FIGURE 20: LANDSCAPE OF *P. PASTORIS ΔDAS1DAS2* TRANSFORMANTS WITH OVER-EXPRESSED BDH AND FDH. SQUARE DOTS MARK THE STERILE CONTROLS OF THE CULTIVATIONS.

THE X-SHAPED DOTS MARK THE FDH ACTIVITIES OF THE HOST STRAIN *P. PASTORIS ΔDAS1DAS2* + BDH AND ARE EXTENDED THROUGH THE BLACK LINE. 47
FIGURE 21: LANDSCAPE OF *P. PASTORIS ΔDAS1DAS2* TRANSFORMANTS WITH OVER-EXPRESSED BDH AND FLD. SQUARE DOTS MARK THE STERILE CONTROLS OF THE CULTIVATIONS. THE X-SHAPED DOTS MARK THE ACTIVITIES OF THE HOST STRAIN *P. PASTORIS ΔDAS1DAS2* + BDH. A: MEASUREMENT OF FLD ACTIVITY. B: MEASUREMENT OF FDH ACTIVITY. 48
FIGURE 22: CATALYZED REACTION OF XYLOSE REDUCTASE 54
FIGURE 23: SCHEMATIC VIEW OF A 96-WELL DEEP WELL PLATE. TRANSFORMANT, HOST STRAIN *ΔDAS1DAS2* + XR(-M) HOST STRAIN CBS 7435 + XR(-M); CORRESPONDENT WILDTYPE, STERILE CONTROL. 61
FIGURE 24: LANDSCAPE OF *P. PASTORIS* CBS 7435 TRANSFORMANTS WITH OVER-EXPRESSED FLD. SQUARE DOTS MARK THE STERILE CONTROL OF THE CULTIVATION. THE X-SHAPED DOTS MARK THE FLD ACTIVITY OF THE WILD TYPE STRAIN *P. PASTORIS* CBS 7435 AND ARE VISUALIZED THROUGH THE EXTENDED BLACK LINE. 62
FIGURE 25: LANDSCAPE OF *P. PASTORIS* CBS 7435 TRANSFORMANTS WITH OVER-EXPRESSED FDH. SQUARE DOTS MARK THE STERILE CONTROL OF THE CULTIVATION. THE X-SHAPED DOTS MARK THE FDH ACTIVITY OF THE WILD TYPE STRAIN *P. PASTORIS* CBS 7435 AND ARE VISUALIZED THROUGH THE EXTENDED BLACK LINE. 63
FIGURE 26: LANDSCAPES OF *P. PASTORIS* CBS 7435 TRANSFORMANTS WITH OVER-EXPRESSED FLD AND FDH. SQUARE DOTS MARK THE STERILE CONTROLS OF THE CULTIVATIONS. THE X-SHAPED DOTS MARK THE ACTIVITIES OF THE WILD TYPE STRAIN *P. PASTORIS* CBS 7435 AND ARE VISUALIZED THROUGH THE EXTENDED BLACK LINES. A: MEASUREMENT OF FLD ACTIVITY. B: MEASUREMENT OF FDH ACTIVITY. 64
FIGURE 27: LANDSCAPES OF *P. PASTORIS* CBS 7435 TRANSFORMANTS WITH OVER-EXPRESSED XR AND FLD. SQUARE DOTS MARK THE STERILE CONTROLS OF THE CULTIVATIONS. THE X-SHAPED DOTS MARK THE ACTIVITIES OF THE WILD TYPE STRAIN *P. PASTORIS* CBS 7435 AND ARE VISUALIZED THROUGH THE EXTENDED BLACK LINES. A: MEASUREMENT OF XR ACTIVITY WITH NADPH. B: MEASUREMENT OF FLD ACTIVITY. 65
FIGURE 28: LANDSCAPES OF *P. PASTORIS* CBS 7435 TRANSFORMANTS WITH OVER-EXPRESSED XR AND FDH. SQUARE DOTS MARK THE STERILE CONTROLS OF THE CULTIVATIONS. THE X-SHAPED DOTS MARK THE ACTIVITIES OF THE WILD TYPE STRAIN *P. PASTORIS* CBS 7435 AND ARE VISUALIZED THROUGH THE EXTENDED BLACK LINES. A: MEASUREMENT OF XR ACTIVITY WITH NADPH. B: MEASUREMENT OF FDH ACTIVITY. 66
FIGURE 29: LANDSCAPES OF *P. PASTORIS* CBS 7435 TRANSFORMANTS WITH OVER-EXPRESSED XR, FLD AND FDH. SQUARE DOTS MARK THE STERILE CONTROLS OF THE CULTIVATIONS. THE X-SHAPED DOTS MARK THE ACTIVITIES OF THE WILD TYPE STRAIN *P. PASTORIS* CBS 7435 AND ARE VISUALIZED THROUGH THE EXTENDED BLACK LINES. A: MEASUREMENT OF XR ACTIVITY WITH NADPH. B: MEASUREMENT OF FLD ACTIVITY. C: MEASUREMENT OF FDH ACTIVITY. 68
FIGURE 30: LANDSCAPES OF *P. PASTORIS* CBS 7435 TRANSFORMANTS WITH OVER-EXPRESSED XR-M AND FLD. SQUARE DOTS MARK THE STERILE CONTROLS OF THE CULTIVATIONS.

THE X-SHAPED DOTS MARK THE ACTIVITIES OF THE WILD TYPE STRAIN *P. PASTORIS* CBS 7435 AND ARE VISUALIZED THROUGH THE EXTENDED BLACK LINES. A: MEASUREMENT OF XR-M ACTIVITY WITH NADH. B: MEASUREMENT OF FLD ACTIVITY. 69

FIGURE 31: LANDSCAPES OF *P. PASTORIS* CBS 7435 TRANSFORMANTS WITH OVER-EXPRESSED XR-M AND FDH. SQUARE DOTS MARK THE STERILE CONTROLS OF THE CULTIVATIONS. THE X-SHAPED DOTS MARK THE ACTIVITIES OF THE WILD TYPE STRAIN *P. PASTORIS* CBS 7435 AND ARE VISUALIZED THROUGH THE EXTENDED BLACK LINES. A: MEASUREMENT OF XR-M ACTIVITY WITH NADH. B: MEASUREMENT OF FDH ACTIVITY. 70

FIGURE 32: LANDSCAPES OF *P. PASTORIS* CBS 7435 TRANSFORMANTS WITH OVER-EXPRESSED XR-M, FLD AND FDH. SQUARE DOTS MARK THE STERILE CONTROLS OF THE CULTIVATIONS. THE X-SHAPED DOTS MARK THE ACTIVITIES OF THE WILD TYPE STRAIN *P. PASTORIS* CBS 7435 AND ARE VISUALIZED THROUGH THE EXTENDED BLACK LINES. A: MEASUREMENT OF XR-M ACTIVITY WITH NADPH AS COFACTOR. B: MEASUREMENT OF XR-M ACTIVITY WITH NADH AS COFACTOR. C: MEASUREMENT OF FLD ACTIVITY. D: MEASUREMENT OF FDH ACTIVITY. 72

FIGURE 33: LANDSCAPE OF *P. PASTORIS ΔDAS1DAS2* TRANSFORMANTS WITH OVER-EXPRESSED XR. SQUARE DOTS MARK THE STERILE CONTROL OF THE CULTIVATION. THE X-SHAPED DOTS MARK THE ACTIVITY OF THE HOST STRAIN *P. PASTORIS ΔDAS1DAS2* AND ARE VISUALIZED THROUGH THE EXTENDED BLACK LINE. 73

FIGURE 34: LANDSCAPES OF *P. PASTORIS ΔDAS1DAS2* TRANSFORMANTS WITH OVER-EXPRESSED XR AND FLD. SQUARE DOTS MARK THE STERILE CONTROLS OF THE CULTIVATION. THE X-SHAPED DOTS MARK THE ACTIVITIES OF THE HOST STRAIN *P. PASTORIS ΔDAS1DAS2* AND ARE VISUALIZED THROUGH THE EXTENDED BLACK LINES. A: MEASUREMENT OF XR ACTIVITY. B: MEASUREMENT OF FLD ACTIVITY. 74

FIGURE 35: LANDSCAPES OF *P. PASTORIS ΔDAS1DAS2* TRANSFORMANTS WITH OVER-EXPRESSED XR AND FDH. SQUARE DOTS MARK THE STERILE CONTROLS OF THE CULTIVATION. THE X-SHAPED DOTS MARK THE ACTIVITIES OF THE HOST STRAIN *P. PASTORIS ΔDAS1DAS2* AND ARE VISUALIZED THROUGH THE EXTENDED BLACK LINES. A: MEASUREMENT OF XR ACTIVITY. B: MEASUREMENT OF FDH ACTIVITY. 75

FIGURE 36: LANDSCAPES OF *P. PASTORIS ΔDAS1DAS2* TRANSFORMANTS WITH OVER-EXPRESSED XR, FLD AND FDH. SQUARE DOTS MARK THE STERILE CONTROLS OF THE CULTIVATION. THE X-SHAPED DOTS MARK THE ACTIVITIES OF THE HOST STRAIN *P. PASTORIS ΔDAS1DAS2* AND ARE VISUALIZED THROUGH THE EXTENDED BLACK LINES. A: MEASUREMENT OF XR ACTIVITY WITH NADPH. B: MEASUREMENT OF FLD ACTIVITY. C: MEASUREMENT OF FDH ACTIVITY. 77

FIGURE 37: LANDSCAPE OF *P. PASTORIS ΔDAS1DAS2* TRANSFORMANTS WITH OVER-EXPRESSED XR-M. SQUARE DOTS MARK THE STERILE CONTROL OF THE CULTIVATION. THE X-SHAPED DOTS MARK THE XR-M ACTIVITY OF THE HOST STRAIN *P. PASTORIS ΔDAS1DAS2* AND ARE VISUALIZED THROUGH THE EXTENDED BLACK LINE. 78

FIGURE 38: LANDSCAPES OF *P. PASTORIS ΔDAS1DAS2* TRANSFORMANTS WITH OVER-EXPRESSED XR-M AND FLD. SQUARE DOTS MARK THE STERILE CONTROLS OF THE

CULTIVATION. THE X-SHAPED DOTS MARK THE ACTIVITIES OF THE HOST STRAIN *P. PASTORIS ΔDAS1DAS2* AND ARE VISUALIZED THROUGH THE EXTENDED BLACK LINES. A: MEASUREMENT OF XR-M ACTIVITY WITH NADH. B: MEASUREMENT OF FLD ACTIVITY. 79

FIGURE 39: LANDSCAPES OF *P. PASTORIS ΔDAS1DAS2* TRANSFORMANTS WITH OVER-EXPRESSED XR-M AND FDH. SQUARE DOTS MARK THE STERILE CONTROLS OF THE CULTIVATION. THE X-SHAPED DOTS MARK THE ACTIVITIES OF THE HOST STRAIN *P. PASTORIS ΔDAS1DAS2* AND ARE VISUALIZED THROUGH THE EXTENDED BLACK LINES. A: MEASUREMENT OF XR-M ACTIVITY WITH NADH. B: MEASUREMENT OF FDH ACTIVITY. 80

FIGURE 40: LANDSCAPES OF *P. PASTORIS ΔDAS1DAS2* TRANSFORMANTS WITH OVER-EXPRESSED XR-M, FLD AND FDH. SQUARE DOTS MARK THE STERILE CONTROLS OF THE CULTIVATION. THE X-SHAPED DOTS MARK THE ACTIVITIES OF THE HOST STRAIN *P. PASTORIS ΔDAS1DAS2* AND ARE VISUALIZED THROUGH THE EXTENDED BLACK LINES. A: MEASUREMENT OF XR-M ACTIVITY WITH NADH. B: MEASUREMENT OF FDH ACTIVITY. C: MEASUREMENT OF FLD ACTIVITY. 82

FIGURE 41 A: SCHEMATIC VIEW OF A TYPICAL ROSSMAN FOLD B: SURFACE OF *P.PASTORIS* FDH. MARKED IN GREEN (C-ATOMS) AND RED (O-ATOMS) ARE THE SIDECHAINES OF RESIDUE D195 AND Y196. C: MAGNIFICATION OF NAD^+ (MARKED IN RED) BINDING SITE IN *P. PASTORIS* FDH 86

FIGURE 42: SCHEMATIC VIEW OF THE LINEAR EXPRESSION CASSETTE OF FDH 90

FIGURE 43: SIMPLIFIED CONSTRUCTION SCHEME OF THE LINEAR FDH EXPRESSION CASSETTE 91

FIGURE 44: SCHEMATIC VIEW OF A 96-WELL DEEP WELL PLATE. BLUE FIELDS INDICATE A TRANSFORMANT, YELLOW AND ORANGE FIELDS INDICATE ONE OR TWO HOST STRAINS. IN THE GREEN FIELDS, THE CORRESPONDENT WILDTYPE WAS CULTIVATED, WHILE THE GREY FIELDS WERE STERILITY CONTROL WELLS ONLY FILLED WITH MEDIUM. 92

FIGURE 45: LANDSCAPE OF *ΔDAS1DAS2* TRANSFORMANTS WITH OVER-EXPRESSED D195A, Y196R FDH. SQUARE DOTS MARK THE STERILE CONTROL OF THE CULTIVATION; THE X-SHAPED DOTS MARK THE ACTIVITIES OF THE HOST STRAIN *ΔDAS1DAS2* AND ARE EXTENDED THROUGH THE BLACK LINE. CIRCLE DOTS MARK THE ACTIVITIES OF THE COMPARATIVE *ΔDAS1DAS2* + FDH STRAIN AND ARE EXTENDED THROUGH THE DASHED LINE. A: MEASUREMENT WITH $NADP^+$ AS COFACTOR. B: MEASUREMENT WITH NAD^+ AS COFACTOR. 93

FIGURE 46: LANDSCAPE OF CBS 7435 TRANSFORMANTS WITH SITE-SATURATED MUTAGENESIS ON POSITION 195 AND 196 OF *P. PASTORIS* FDH. SQUARE DOTS MARK THE STERILE CONTROL OF THE CULTIVATION; THE X-SHAPED DOTS MARK THE ACTIVITIES OF THE HOST STRAIN CBS 7435 AND ARE EXTENDED THROUGH THE BLACK LINE. CIRCLE DOTS MARK THE ACTIVITIES OF THE COMPARATIVE CBS 7435 + FDH STRAIN AND ARE EXTENDED THROUGH THE DASHED LINE. FIGURE 1 OUT OF 4. A: MEASUREMENT WITH $NADP^+$ AS COFACTOR. B: MEASUREMENT WITH NAD^+ AS COFACTOR. 95

FIGURE 47: LANDSCAPE OF CBS 7435 TRANSFORMANTS WITH SITE-SATURATED MUTAGENESIS ON POSITION 195 AND 196 OF *P. PASTORIS* FDH. SQUARE DOTS MARK THE STERILE

CONTROL OF THE CULTIVATION; THE X-SHAPED DOTS MARK THE ACTIVITIES OF THE HOST STRAIN CBS 7435 AND ARE EXTENDED THROUGH THE BLACK LINE. CIRCLE DOTS MARK THE ACTIVITIES OF THE COMPARATIVE CBS 7435 + FDH STRAIN AND ARE EXTENDED THROUGH THE DASHED LINE. FIGURE 2 OUT OF 4. A: MEASUREMENT WITH $NADP^+$ AS COFACTOR. B: MEASUREMENT WITH NAD^+ AS COFACTOR. 96

FIGURE 48: LANDSCAPE OF CBS 7435 TRANSFORMANTS WITH SITE-SATURATED MUTAGENESIS ON POSITION 195 AND 196 OF *P. PASTORIS* FDH. SQUARE DOTS MARK THE STERILE CONTROL OF THE CULTIVATION; THE X-SHAPED DOTS MARK THE ACTIVITIES OF THE HOST STRAIN CBS 7435 AND ARE EXTENDED THROUGH THE BLACK LINE. CIRCLE DOTS MARK THE ACTIVITIES OF THE COMPARATIVE CBS 7435 + FDH STRAIN AND ARE EXTENDED THROUGH THE DASHED LINE. FIGURE 3 OUT OF 4. A: MEASUREMENT WITH $NADP^+$ AS COFACTOR. B: MEASUREMENT WITH NAD^+ AS COFACTOR. 97

FIGURE 49: LANDSCAPE OF CBS 7435 TRANSFORMANTS WITH SITE-SATURATED MUTAGENESIS ON POSITION 195 AND 196 OF *P. PASTORIS* FDH. SQUARE DOTS MARK THE STERILE CONTROL OF THE CULTIVATION; THE X-SHAPED DOTS MARK THE ACTIVITIES OF THE HOST STRAIN CBS 7435 AND ARE EXTENDED THROUGH THE BLACK LINE. CIRCLE DOTS MARK THE ACTIVITIES OF THE COMPARATIVE CBS 7435 + FDH STRAIN AND ARE EXTENDED THROUGH THE DASHED LINE. FIGURE 4 OUT OF 4. A: MEASUREMENT WITH $NADP^+$ AS COFACTOR. B: MEASUREMENT WITH NAD^+ AS COFACTOR. 99

10 Literature

1. Rozzell, J.D., *Commercial scale biocatalysis: myths and realities.* Bioorg Med Chem, 1999. **7**(10): p. 2253-61.
2. Schmid, A., et al., *Industrial biocatalysis today and tomorrow.* Nature, 2001. **409**(6817): p. 258-68.
3. Schoemaker, H.E., D. Mink, and M.G. Wubbolts, *Dispelling the myths--biocatalysis in industrial synthesis.* Science, 2003. **299**(5613): p. 1694-7.
4. Pollard, D.J. and J.M. Woodley, *Biocatalysis for pharmaceutical intermediates: the future is now.* Trends Biotechnol, 2007. **25**(2): p. 66-73.
5. Macauley-Patrick, S., et al., *Heterologous protein production using the Pichia pastoris expression system.* Yeast, 2005. **22**(4): p. 249-70.
6. Resina, D., et al., *Developing high cell density fed-batch cultivation strategies for heterologous protein production in Pichia pastoris using the nitrogen source-regulated FLD1 Promoter.* Biotechnol Bioeng, 2005. **91**(6): p. 760-7.
7. Pscheidt, B. and A. Glieder, *Yeast cell factories for fine chemical and API production.* Microb Cell Fact, 2008. **7**: p. 25.
8. Cos, O., et al., *Operational strategies, monitoring and control of heterologous protein production in the methylotrophic yeast Pichia pastoris under different promoters: a review.* Microb Cell Fact, 2006. **5**: p. 17.
9. Cereghino, J.L. and J.M. Cregg, *Heterologous protein expression in the methylotrophic yeast Pichia pastoris.* FEMS Microbiol Rev, 2000. **24**(1): p. 45-66.
10. De Schutter, K., et al., *Genome sequence of the recombinant protein production host Pichia pastoris.* Nat Biotechnol, 2009. **27**(6): p. 561-6.
11. Hartner, F.S. and A. Glieder, *Regulation of methanol utilisation pathway genes in yeasts.* Microb Cell Fact, 2006. **5**: p. 39.
12. Cregg, J.M., et al., *Functional characterization of the two alcohol oxidase genes from the yeast Pichia pastoris.* Mol Cell Biol, 1989. **9**(3): p. 1316-23.
13. Koutz, P., et al., *Structural comparison of the Pichia pastoris alcohol oxidase genes.* Yeast, 1989. **5**(3): p. 167-77.
14. Szamecz, B., et al., *Identification of four alcohol oxidases from methylotrophic yeasts.* Yeast, 2005. **22**(8): p. 669-76.
15. Cregg, J.M., et al., *Recombinant protein expression in Pichia pastoris.* Mol Biotechnol, 2000. **16**(1): p. 23-52.
16. Lee, B., et al., *Physiological role of the glutathione-dependent formaldehyde dehydrogenase in the methylotrophic yeast Candida boidinii.* Microbiology, 2002. **148**(Pt 9): p. 2697-704.
17. Nakagawa, T., et al., *Molecular characterization of the glutathione-dependent formaldehyde dehydrogenase gene FLD1 from the methylotrophic yeast Pichia methanolica.* Yeast, 2004. **21**(5): p. 445-53.
18. Shen, S., et al., *A strong nitrogen source-regulated promoter for controlled expression of foreign genes in the yeast Pichia pastoris.* Gene, 1998. **216**(1): p. 93-102.
19. Baerends, R.J., et al., *Molecular characterization of the Hansenula polymorpha FLD1 gene encoding formaldehyde dehydrogenase.* Yeast, 2002. **19**(1): p. 37-42.

20. Serov, A.E., et al., *Engineering of coenzyme specificity of formate dehydrogenase from Saccharomyces cerevisiae.* Biochem J, 2002. **367**(Pt 3): p. 841-7.
21. Tishkov, V.I., et al., *Pilot scale production and isolation of recombinant NAD+- and NADP+-specific formate dehydrogenases.* Biotechnol Bioeng, 1999. **64**(2): p. 187-93.
22. Tishkov, V.I. and V.O. Popov, *Catalytic mechanism and application of formate dehydrogenase.* Biochemistry (Mosc), 2004. **69**(11): p. 1252-67.
23. Goldberg, S.L., *Pichia pastoris formate dehydrogenase and uses therefor.* Patent No.: US 7,087,418 B2, 2006.
24. Sakai, Y., et al., *Regulation and physiological role of the DAS1 gene, encoding dihydroxyacetone synthase, in the methylotrophic yeast Candida boidinii.* J Bacteriol, 1998. **180**(22): p. 5885-90.
25. Gutmann, A., *A kit for accelerated enzyme expression and development in Pichia pastoris.* Diploma thesis, 2009.
26. Carugo, O. and P. Argos, *NADP-dependent enzymes. II: Evolution of the mono- and dinucleotide binding domains.* Proteins, 1997. **28**(1): p. 29-40.
27. Popov, V., *NAD+-dependent formate dehydrogenase. From a model enzyme to a versatile biocatalyst.* Protein Structures: Kaleidoscope of Structural Properties and Functions, 2003: p. 441-473.
28. Andreadeli, A., et al., *Structure-guided alteration of coenzyme specificity of formate dehydrogenase by saturation mutagenesis to enable efficient utilization of NADP+.* Febs J, 2008. **275**(15): p. 3859-69.
29. van der Donk, W.A. and H. Zhao, *Recent developments in pyridine nucleotide regeneration.* Curr Opin Biotechnol, 2003. **14**(4): p. 421-6.
30. Klyushnichenko, V., V. Tishkov, and M.R. Kula, *Rapid SDS-Gel capillary electrophoresis for the analysis of recombinant NADP(+)-dependent formate dehydrogenase during expression in Escherichia coli cells and its purification.* J Biotechnol, 1997. **58**(3): p. 187-95.
31. Labrou, N.E., D.J. Rigden, and Y.D. Clonis, *Characterization of the NAD+ binding site of Candida boidinii formate dehydrogenase by affinity labelling and site-directed mutagenesis.* Eur J Biochem, 2000. **267**(22): p. 6657-64.
32. Tishkov, V.I. and V.O. Popov, *Protein engineering of formate dehydrogenase.* Biomol Eng, 2006. **23**(2-3): p. 89-110.
33. Ehsani, M., et al., *Reversal of coenzyme specificity of 2,3-butanediol dehydrogenase from Saccharomyces cerevisae and in vivo functional analysis.* Biotechnol Bioeng, 2009. **104**(2): p. 381-9.
34. Faber, K. and W. Kroutil, *New enzymes for biotransformations.* Curr Opin Chem Biol, 2005. **9**(2): p. 181-7.
35. Schroer, K., et al., *Engineering the Pichia pastoris methanol oxidation pathway for improved NADH regeneration during whole-cell biotransformation.* Metab Eng, 2010. **12**(1): p. 8-17.
36. Goldberg, K., et al., *Biocatalytic ketone reduction--a powerful tool for the production of chiral alcohols--part I: processes with isolated enzymes.* Appl Microbiol Biotechnol, 2007. **76**(2): p. 237-48.
37. Goldberg, K., et al., *Biocatalytic ketone reduction--a powerful tool for the production of chiral alcohols-part II: whole-cell reductions.* Appl Microbiol Biotechnol, 2007. **76**(2): p. 249-55.
38. Dominguez, J.M., et al., *Ethanol production from xylose with the yeast Pichia stipitis and simultaneous product recovery by gas stripping using a gas-lift*

loop fermentor with attached side-arm (GLSA). Biotechnol Bioeng, 2000. **67**(3): p. 336-43.
39. Franzen, C.J., G. Liden, and C. Niklasson, *A new method for studying microaerobic fermentations. II. An experimental investigation of xylose fermentation.* Biotechnol Bioeng, 1994. **44**(4): p. 429-35.
40. McMillan, J.D., *Bioethanol production: Status and prospects.* Renewable Energy, 1997. **10**(2-3): p. 295-302.
41. Olah, G.A., *Beyond oil and gas: the methanol economy.* Angew Chem Int Ed Engl, 2005. **44**(18): p. 2636-9.
42. Petschacher, B., et al., *The coenzyme specificity of Candida tenuis xylose reductase (AKR2B5) explored by site-directed mutagenesis and X-ray crystallography.* Biochem J, 2005. **385**(Pt 1): p. 75-83.
43. Petschacher, B. and B. Nidetzky, *Engineering Candida tenuis Xylose reductase for improved utilization of NADH: antagonistic effects of multiple side chain replacements and performance of site-directed mutants under simulated in vivo conditions.* Appl Environ Microbiol, 2005. **71**(10): p. 6390-3.
44. Petschacher, B. and B. Nidetzky, *Altering the coenzyme preference of xylose reductase to favor utilization of NADH enhances ethanol yield from xylose in a metabolically engineered strain of Saccharomyces cerevisiae.* Microb Cell Fact, 2008. **7**: p. 9.
45. Lin-Cereghino, J., et al., *Condensed protocol for competent cell preparation and transformation of the methylotrophic yeast Pichia pastoris.* Biotechniques, 2005. **38**(1): p. 44, 46, 48.
46. Weis, R., et al., *Reliable high-throughput screening with Pichia pastoris by limiting yeast cell death phenomena.* FEMS Yeast Res, 2004. **5**(2): p. 179-89.
47. Jungo, C., et al., *Quantitative characterization of the regulation of the synthesis of alcohol oxidase and of the expression of recombinant avidin in a Pichia pastoris Mut+ strain.* Enzyme and Microbial Technology, 2006. **39**(4): p. 936-944.
48. Allais, J.J., *Oxidation of Methanol by the Yeast, Pichia pastoris, Purification and Properties of the Formaldeyde Dehydrogenase.* Agric. Biol. Chem., 1983. **47**(7): p. 1509-1516.
49. Andreesen, J.R. and L.G. Ljungdahl, *Nicotinamide adenine dinucleotide phosphate-dependent formate dehydrogenase from Clostridium thermoaceticum: purification and properties.* J Bacteriol, 1974. **120**(1): p. 6-14.
50. NCBI, *http://www.ncbi.nlm.nih.gov/.*
51. Brisdelli, F., et al., *Kinetic properties of native and mutagenized isoforms of mitochondrial alcohol dehydrogenase III purified from Kluyveromyces lactis.* Biochimie, 2004. **86**(9-10): p. 705-12.
52. Fernandez, M.R., et al., *Class III alcohol dehydrogenase from Saccharomyces cerevisiae: structural and enzymatic features differ toward the human/mammalian forms in a manner consistent with functional needs in formaldehyde detoxication.* FEBS Lett, 1995. **370**(1-2): p. 23-6.
53. Patel, R.N., C.T. Hou, and P. Derelanko, *Microbial oxidation of methanol: purification and properties of formaldehyde dehydrogenase from a Pichia sp. NRRL-Y-11328.* Arch Biochem Biophys, 1983. **221**(1): p. 135-42.